

# **Dissertation**

submitted to the

Combined Faculties for the Natural Sciences and for Mathematics  
of the Ruperto-Carola University of Heidelberg, Germany

for the degree of

**Doctor of Natural Sciences**

presented by

Diplom-Biologin Corinna D. Berger  
born in Heidelberg, Germany

Oral-examination:.....

**Regulation of Morphogenetic Cell Behavior by  
*Xenopus* Paraxial Protocadherin**

Referees:

Prof. Dr. Herbert Steinbeisser

Prof. Dr. Jörg Großhans

## Table of Contents

<b>1</b>	<b>Summary</b>	<b>1</b>
<b>2</b>	<b>Introduction</b>	<b>3</b>
2.1	Gastrulation	3
2.2	Convergent extension movements	4
2.3	Tissue separation	6
2.4	Regulators of convergent extension and tissue separation	7
2.4.1	Wnt-pathways	7
2.4.2	Cadherins	11
2.5	Aim of this study	19
<b>3</b>	<b>Results</b>	<b>20</b>
3.1	PAPC has signaling properties	20
3.1.1	Rho activity in the dorsal mesoderm depends on PAPC function	20
3.1.2	PAPC and Spry interact independently of FGF-signaling	23
3.1.3	PAPC does not signal by recruiting dsh-GFP to the cell membrane	27
3.1.4	PAPCc is localized to the nucleus and to the cell membrane	28
3.1.5	Loss of PAPC leads to a change in cell shape and loss of cell polarity	31
3.2	PAPC modulates cell adhesion	34
3.2.1	PAPC mediates cell sorting in reaggregation assays	34
3.2.2	PAPC causes internalization of C-Cadherin in animal cap cells	37
3.2.3	PAPC and C-Cadherin colocalize	38
3.2.4	PAPC is internalized with C-Cadherin-eGFP	39
3.2.5	PAPC and Fz7 mediate the relocalization of C-Cadherin from the membrane to the cytoplasm	40
3.2.6	Rab5a, a marker of early endosomes, colocalizes with C-Cadherin	41
3.3	Interaction partners of PAPC	44
3.3.1	Bimolecular fluorescence complementation	44
3.3.2	Tissue separation	52
3.3.3	Functional consequence of the interaction between PAPC, Fz7 and C-Cadherin	53
<b>4</b>	<b>Discussion</b>	<b>56</b>
4.1	PAPC physically interacts with C-Cadherin	57
4.1.1	Localization of interaction	58
4.2	Binding between PAPC and C-Cadherin reduces cell adhesion	58

---

4.2.1	Endocytosis and cell adhesion _____	58
4.2.2	Tissue versus single cells _____	59
<b>4.3</b>	<b>Regulators of cell adhesion _____</b>	<b>60</b>
<b>4.4</b>	<b>Tissue separation _____</b>	<b>62</b>
<b>4.5</b>	<b>Model of dynamic cell adhesion _____</b>	<b>63</b>
<b>4.6</b>	<b>Additional roles of PAPC _____</b>	<b>65</b>
4.6.1	Signal transduction _____	65
4.6.2	Gene transcription _____	66
<b>4.7</b>	<b>PAPC functions can be mapped to its protein domains _____</b>	<b>68</b>
<b>5</b>	<b><i>Material</i> _____</b>	<b>71</b>
5.1	Chemicals _____	71
5.2	Buffers _____	71
5.3	Oligonucleotides _____	72
5.4	Plasmids _____	73
5.5	Proteins, enzymes, inhibitors, and markers _____	75
5.6	Antibodies _____	75
5.7	Bacteria and cells _____	75
5.8	Kits _____	75
5.9	Other material _____	76
5.10	Microscopes and equipment _____	76
5.11	Computer programs _____	76
<b>6</b>	<b><i>Methods</i> _____</b>	<b>77</b>
<b>6.1</b>	<b>DNA/RNA-methods _____</b>	<b>77</b>
6.1.1	Isolation of nucleic acids _____	77
6.1.2	PCR _____	77
6.1.3	Cloning _____	78
6.1.4	Sequencing _____	78
6.1.5	Cap-mRNA _____	79
<b>6.2</b>	<b>Biochemical and immunological methods _____</b>	<b>79</b>
6.2.1	Protein extraction from cell culture cells _____	79

---

6.2.2	Protein extraction from embryos _____	79
6.2.3	SDS-PAGE and Western blot _____	79
6.2.4	Immunostainings of cell culture cells _____	79
6.2.5	Immunostainings of animal caps _____	80
6.2.6	RBD-GFP staining _____	80
<b>6.3</b>	<b>Bacteria and cell culture methods _____</b>	<b>80</b>
6.3.1	Chemical transformation of bacteria _____	80
6.3.2	Electroporation of bacteria _____	80
6.3.3	Maintaining cell lines _____	81
6.3.4	Transfection of cultured cells _____	81
6.3.5	bFGF treatment of cultured cells _____	81
6.3.6	FACS _____	81
<b>6.4</b>	<b>Embryological methods _____</b>	<b>81</b>
6.4.1	Embryo culture and manipulations _____	81
6.4.2	Cell dispersion assay _____	81
6.4.3	Dissociation and reaggregation assay _____	82
6.4.4	Reaggregation assay _____	82
6.4.5	Dorsal marginal zone (DMZ) explants _____	82
6.4.6	Tissue separation _____	83
6.4.7	Cryosections _____	83
<b>6.5</b>	<b>Microscopy _____</b>	<b>83</b>
<b>7</b>	<b>References _____</b>	<b>84</b>
	<b>Abbreviations _____</b>	<b>i</b>
	<b>Figures _____</b>	<b>ii</b>
	<b>Tables _____</b>	<b>iii</b>
	<b>Acknowledgements _____</b>	<b>iv</b>

## 1 Summary

Gastrulation is one of the most important processes during embryogenesis and must therefore be strictly controlled. A central regulator of this complex morphogenetic process is Paraxial Protocadherin (PAPC). PAPC function is necessary for convergent extension movements and tissue separation. It promotes  $\beta$ -catenin-independent Wnt-signaling and modulates C-Cadherin-mediated cell adhesion.

In this work I explored the role of PAPC in convergent extension and tissue separation. I could show using loss of function approaches that PAPC is necessary for the elongated cell shape and the bipolarity of mesodermal cells. Furthermore the activation of endogenous Rho, which can be visualized by a novel *in situ* staining method, depends on PAPC in the dorsal marginal zone. PAPC promotes the activation of Rho by antagonizing Spry, an inhibitor of  $\beta$ -catenin-independent Wnt-signaling, by binding to it. The interaction between PAPC and Spry is independent of FGF signaling, but the two putative phosphorylation sites at serines 741 and 955 in the cytoplasmic domain of PAPC are essential for it. The expression of the PAPC cytoplasmic domain alone but not of the point mutant PAPC-S741A/S955A, which is unable to bind to Spry, can rescue Rho activation after PAPC loss of function. In addition the cytoplasmic domain of PAPC can enter the nucleus, where it might mediate transcription.

Using bimolecular fluorescence complementation I could show that PAPC interacts with C-Cadherin and the receptor Frizzled 7 (Fz7). In gain of function experiments PAPC decreases cell adhesion by binding to C-Cadherin. For this function only the extracellular and transmembrane domains of PAPC are necessary. Although PAPC induces endocytosis of C-Cadherin/PAPC-complexes in intact tissues, this effect does not contribute to the downregulation of cell adhesion. PAPC interacts with Fz7 via their extracellular domains. PAPC and Fz7 do not act as ligand and receptor across cell membranes; both proteins must be inside the same cell in order to induce ectopic tissue separation in the ectoderm. Furthermore the interaction between PAPC and Fz7 can be modulated by coexpression of C-Cadherin or Wnt11, a ligand of Fz7.

## Zusammenfassung

Die Gastrulation ist einer der wichtigsten Vorgänge während der Embryonalentwicklung und wird daher streng geregelt. Ein zentraler Teil der Steuerung dieses komplexen morphogenetischen Prozesses ist Paraxiales Protocadherin (PAPC). Die Funktion von PAPC ist erforderlich für die konvergente Extension und das Gewebetrennungsverhalten. PAPC fördert den  $\beta$ -Catenin-unabhängigen Wnt-Signalweg und moduliert die von C-Cadherin vermittelte Zelladhäsion.

Im Rahmen dieser Arbeit wurde die Rolle von PAPC während der konvergenten Extension und des Gewebetrennungsverhaltens untersucht. Mit Hilfe von „loss of function“-Experimenten konnte gezeigt werden, dass PAPC für die elongierte Form und Polarität von Mesodermzellen notwendig ist. Die Aktivierung der kleinen GTPase Rho, die mittels einer neuen Färbemethode *in situ* gezeigt werden kann, hängt in der dorsalen Marginalzone von PAPC ab. PAPC fördert die Aktivierung von Rho, indem es Spry, einen Inhibitor des  $\beta$ -Catenin-unabhängigen Wnt-Signalwegs, bindet und neutralisiert. Die Bindung zwischen PAPC und Spry ist unabhängig von FGF-Signalen, braucht jedoch die mutmaßlich phosphorylierten Serine 741 und 955 der zytoplasmatischen Domäne von PAPC. Die Expression der zytoplasmatischen Domäne, nicht jedoch die der Mutante PAPC-S741A/S955A, konnte die Rho-Aktivierung nach Verlust von PAPC wiederherstellen. Schließlich kann die zytoplasmatische Domäne von PAPC in den Zellkern gelangen, wo sie möglicherweise Gentranskription reguliert.

Mittels bimolekularer Fluoreszenzkomplementierung konnte gezeigt werden, dass PAPC an C-Cadherin und den Rezeptor Frizzled 7 (Fz7) bindet. Überexprimiertes PAPC vermindert die von C-Cadherin vermittelte Zelladhäsion, indem es an C-Cadherin bindet. Für diesen Vorgang werden nur die extrazelluläre und die Transmembrandomäne von PAPC benötigt. Obwohl PAPC in intakten Geweben die Endozytose von PAPC/C-Cadherin-Komplexen auslöst, hat diese keinen Einfluss auf die Zelladhäsion. PAPC bindet über die jeweiligen extrazellulären Domänen an Fz7. PAPC und Fz7 wirken nicht wie Rezeptor und Ligand über Zellgrenzen hinweg, sondern beide Proteine müssen in der gleichen Zelle vorhanden sein, um ektopisches Gewebetrennungsverhalten im Ektoderm hervorzurufen. Zudem kann die Bindung zwischen PAPC und Fz7 durch die Koexpression von C-Cadherin oder Wnt11, einem Liganden von Fz7, reguliert werden.

## 2 Introduction

*"Should one wish to learn the methods of a conjurer, he might vainly watch the latter's customary repertoire, and, so long as everything went smoothly, might never obtain a clue to the mysterious performance, baffled by the precision of the manipulations and the complexity of the apparatus; if, however, a single error were made in any part or if a single deviation from the customary method should force the manipulator along an unaccustomed path, it would give the investigator an opportunity to obtain a part or the whole of the secret. Thus ... it seems likely that through the study of the abnormal or unusual, some insight may be obtained into that mystery of mysteries, the development of an organism."* H. H. Wilder, 1908.

### 2.1 Gastrulation

Gastrulation is a period during the early development of animals, when major cell and tissue movements remodel an initially unstructured group of cells. A hierarchy of genetic control mechanisms, involving cell signaling and transcriptional regulation, set up the embryonic axes and specify the territories of the future germ layers. Cells in these territories modulate their cytoskeleton and their adhesive behavior, resulting in shape changes and movement (Leptin, 2005). In the course of gastrulation, the precursors of the three germ layers, the endoderm, mesoderm and ectoderm, are repositioned from the surface of the blastula, such that at the end of gastrulation the mesoderm is placed between the internal endoderm and the superficial ectoderm. Moreover, gastrulation molds the germ layers into a body rudiment with anteroposterior and dorsoventral asymmetries (Solnica-Krezel, 2006).

In *Xenopus* four kinds of cell movements drive gastrulation: invagination, involution, convergent extension (CE) and epiboly (Solnica-Krezel, 2005). At the dorsal marginal zone, cells constrict apically to become bottle cells and form an invagination. The cells of the mesoderm begin to involute into the embryo at this site of invagination, which is then called the dorsal lip or blastopore (Fig.1). The involuting cells migrate along the inside of the blastocoel toward the animal cap. Cells from the lateral marginal zone migrate toward the dorsal midline and intercalate with the cells there. This intercalation narrows (convergence) and lengthens (extension) the anterior-

posterior aspect of the embryo. Meanwhile the cells of the animal cap undergo epiboly and spread toward the vegetal pole to cover the entire embryo (Solnica-Krezel, 2005).

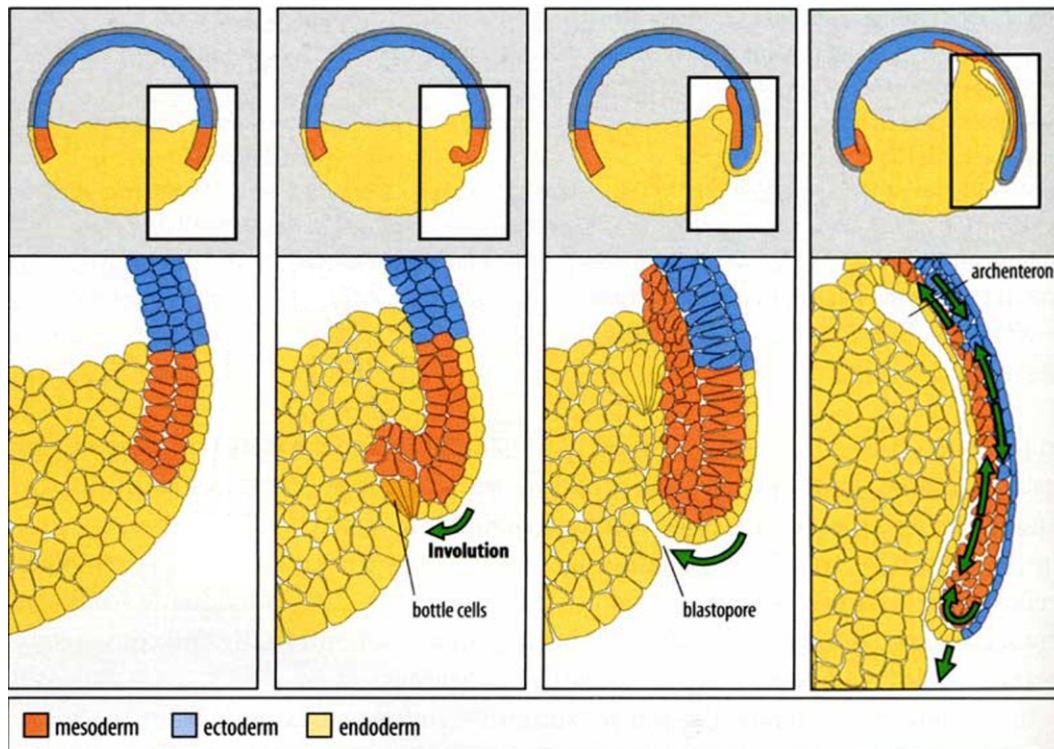


**Fig.1. Schematic drawing of early *Xenopus* gastrulation.** Gastrulation starts on the dorsal side of the embryo by apical constriction of the bottle cells, followed by involution of the mesoderm. The mesendoderm moves up against the blastocoel roof thereby forming the archenteron. Green arrows depict the cell movement as a result of epiboly and convergent extension. Picture adapted from Wolpert (2006).

## 2.2 Convergent extension movements

The closure of the blastopore and the elongation of the anterior-posterior body axis are accomplished largely by convergence and extension (Keller, 1986). CE involves two types of cell intercalation. First, several layers of deep cells intercalate along the radius of the embryo (**radial intercalation**) to produce fewer layers of greater length; and then the deep cells intercalate mediolaterally (**mediolateral intercalation**) to produce a narrower and longer array (Wilson and Keller, 1991; Shih and Keller, 1992) (Fig.2, A). Radial intercalation predominates in the first half of gastrulation and mediolateral intercalation predominates in the second half of gastrulation and through neurulation in both the dorsal mesodermal tissue and in the prospective posterior

neural tissue (spinal cord and hindbrain). During mesodermal mediolateral cell intercalation, protrusive activity becomes polarized with large lamelliform protrusions at the medial and lateral ends of the cells and small filiform protrusions at their anterior and posterior surfaces (Fig.2, B). The medial and lateral protrusions exert traction on adjacent cells, and generate tension in the mediolateral axis. The cells become mediolaterally elongated, oriented parallel to one another, and move between one another (Shih and Keller, 1992).

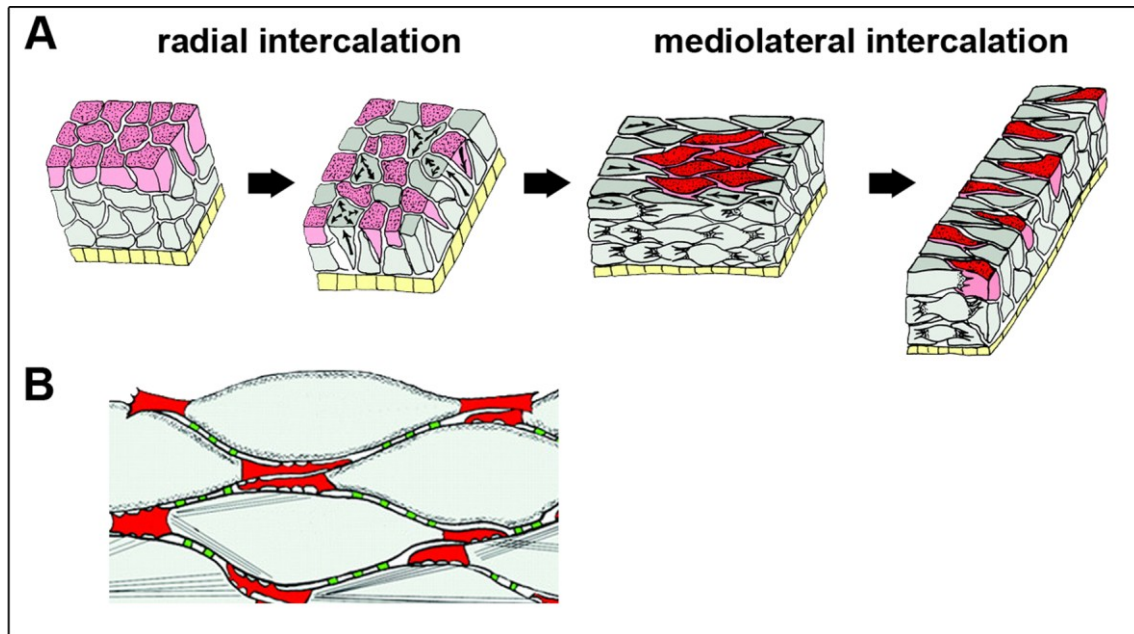


**Fig.2. Cellular behavior during gastrulation.** (A) During early gastrulation the mesoderm extends by radial intercalation of cells, a process in which several cell layers merge to become one. From midgastrulation onwards the mediolateral intercalation of cells elongates the embryonic axis. (B) During convergent extension mediolateral lamelliform protrusions (red) attach to neighboring cells and exert traction. The small filiform protrusions (green) are dynamic structures which stiffen the tissue but also allow sliding of cells past each other. Picture adapted from Keller (2002).

The mesodermal and neural tissues that converge and extend in the embryo also do so when explanted in a culture dish, which shows that these movements are independent of other tissues, independent of an external substrate, and driven by internal forces (Keller and Danilchik, 1988). Cell intercalation is a subtle but powerful mechanism; locally, cells move only short distances as they wedge between one another, but the collective effect of this behavior is a rapid change in tissue shape.

Convergent extension by cell intercalation is a common if not universal mechanism of shaping large features of metazoan embryos. It occurs during gastrulation and axis elongation of ascidians (Munro and Odell, 2002), teleost fish (Glickman et al., 2003),

birds (Lawson and Schoenwolf, 2001), and mammals (Sausedo and Schoenwolf, 1994), and during *Drosophila* germ band extension (Irvine and Wieschaus, 1994) and echinoderm gut elongation (Hardin, 1989).

### 2.3 Tissue separation

Boundaries between cell populations often occur in morphologically homogeneous tissues, in which they form barriers to cell mixing and are of great developmental importance. It was proposed that differential cell affinities play a critical role in forming such tissue boundaries. During development, most tissue boundaries become eventually morphologically apparent as folds or clefts, which often become the extracellular matrix filled spaces known to physically separate most mature tissues (Tepass et al., 2002).

During *Xenopus* gastrulation, the involuting mesendodermal cells are brought into contact with the multilayered blastocoel roof (BCR). The two tissues do not fuse, but remain separated by a morphological structure called Brachet's cleft (Wacker et al., 2000). The anterior cleft separates ectoderm and anterior mesendoderm, while the posterior part arises between ectoderm and involuted trunk mesoderm. The maintenance of a stable interface is a precondition for the movement of these tissues past each other. Several observations suggest that achieving this tissue separation is not a trivial problem. First, BCR cells and translocating mesoderm cells are in direct contact. The BCR is covered by a network of fibronectin fibrils, but the BCR matrix is not dense enough to physically separate the BCR cell layer from the translocating mesoderm, as, e.g., a basal lamina would do (Nakatsuji and Johnson, 1983). Second, cadherins that mediate cohesion of the early embryo, EP/C- and XB/U-cadherin, are expressed in both the mesendoderm and the BCR cells (Choi et al., 1990; Angres et al., 1991; Ginsberg et al., 1991; Heasman et al., 1994b; Kühl and Wedlich, 1996). Nevertheless, the two cell populations do not mix. Tissue separation behavior develops in the tissues apposed to the blastocoel roof in a time-dependent manner (Wacker et al., 2000). It spreads temporally during gastrulation from the vegetal cell mass into the anterior and then posterior mesoderm, roughly in parallel to internalization movements (Fig.3).

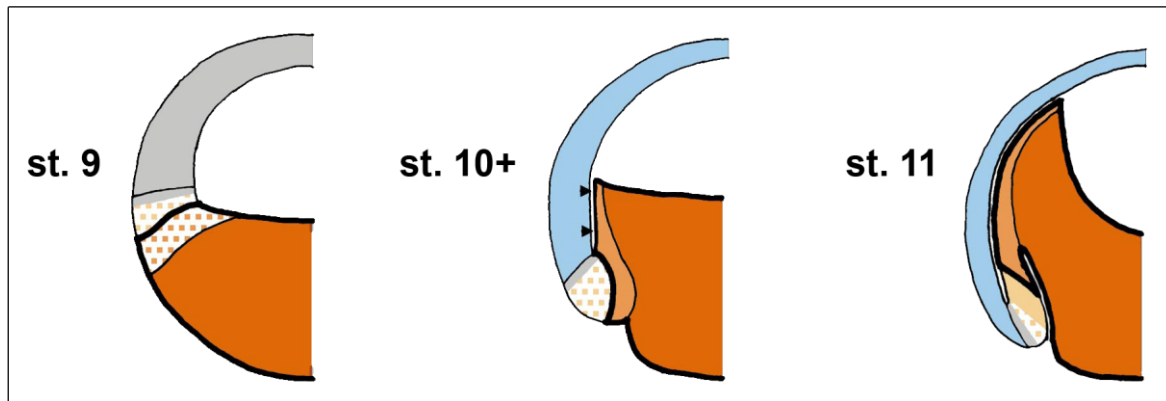


**Fig.3. Temporal development of tissue separation during gastrulation.** Dorsal part of an embryo at late blastula (st.9), early gastrula (st.10+), and midgastrula (st.11) stages. Regions of indiscriminate behavior are shown in gray, differential repulsion behavior by the future ectoderm in blue, separation behavior in orange, with lighter shading indicating later expression of behavior. Prospective regions of separation behavior are dotted in orange. Arrowheads indicate Brachet's cleft. Picture adapted from Wacker et al. (2000).

## 2.4 Regulators of convergent extension and tissue separation

### 2.4.1 Wnt-pathways

Wnt signaling controls a wide array of embryonic and adult processes ranging from gastrulation to aging. Members of the Wnt family are defined by their sequence homology to the *Drosophila* segment polarity gene *wingless* (*Wg*) and the mouse gene *Wnt-1*. Wnts can activate different intracellular signaling pathways by interacting with Frizzled (Fz) receptors. The best known Wnt pathway is the **Wnt/ $\beta$ -catenin-pathway**, also referred to as the canonical Wnt-pathway. Activation of this pathway is characterized by its regulation of gene transcription through  $\beta$ -catenin and TCF (Fig.4, A) and results in axis duplication in *X. laevis* as well as transformation of C57mg mammary epithelial cells. Wnt genes that elicit these effects comprise the Wnt-1 class. The earliest role of the  $\beta$ -catenin pathway in frog embryos is the breaking of embryonic symmetry to establish the dorsal blastula organizer, or the Nieuwkoop center. Accumulation of  $\beta$ -catenin in nuclei of the dorsal blastula activates expression of a suite of genes to establish the Spemann–Mangold gastrula organizer, which controls both cell fates and CE movements during gastrulation. The requirement of  $\beta$ -catenin signaling for dorsal axis formation has been shown in a variety of different loss of function approaches in *Xenopus*. Two exclusive target genes for the Wnt/ $\beta$ -catenin pathway have been identified in *Xenopus*, the homeobox

transcription factor *siamois* and the TGF- $\beta$  family member *Xenopus nodal-related 3* (*Xnr-3*). The function of *siamois* has been shown to be required for dorsal axis formation and *Xnr-3* has been shown to initiate morphogenetic movements (Kühl, 2002; Heisenberg and Solnica-Krezel, 2008).

The  **$\beta$ -catenin-independent Wnt-pathways** regulate cell movement and polarization, which are important for gastrulation movements and neural tube closure, without affecting cell fate (Moon et al., 1993; Ungar et al., 1995; Sokol, 1996; Djiane et al., 2000; Medina et al., 2000). Recent studies revealed that these events are controlled by a system similar to the **Planar Cell Polarity (PCP)** pathway initially described in *Drosophila*. There PCP controls the apico-basolateral polarization of epithelial cells as well as the polarization of cells within the plane of the tissue. Mutations of PCP genes cause disorganization of cuticular structures and/or the compound eye (Klein and Mlodzik, 2005). Based on these phenotypes, *D. melanogaster* researchers discovered an evolutionarily conserved set of genes that control the establishment of planar polarity not only in flies but also in vertebrates (Seifert and Mlodzik, 2007). In vertebrates, the definition of what constitutes a PCP process is not entirely clear. One rough operational definition is that PCP is any process that affects cell polarity within an epithelial plane and involves one or more of the core PCP genes (as defined by the PCP phenotype of the *Drosophila* homolog). At present, the developmental processes that meet these criteria are convergent extension, neural tube closure, eyelid closure, hair bundle orientation in inner ear sensory cells, and hair follicle orientation in the skin (Wang and Nathans, 2007).

One major difference between the vertebrate and *Drosophila* Wnt/PCP pathway is that the vertebrate noncanonical pathway clearly involves Wnt ligands, such as Silberblick (Wnt11) and Pipetail (Wnt5), whereas no Wnt ligand is known to be involved in *Drosophila* PCP signaling. In vertebrates, the Wnt genes that can activate the non-canonical pathways are referred to as the Wnt-5A class. They do not elicit axis duplication in *Xenopus* nor do they transform C57mg cells. However, they block the activity of the Wnt-1 class of Wnt genes and influence cell adhesion and cell movements. Three members of the Wnt gene family have been shown to belong to this class, Wnt-4, Wnt-5A, and Wnt-11. Of those, Wnt-5A and Wnt-11 are expressed maternally and during early development of *X. laevis* (Kühl, 2002; Veeman et al., 2003).

Vertebrate Wnt5a and Wnt11 initiate signaling via seven-pass transmembrane receptors of the Frizzled (Fz) family, which may activate trimeric G proteins and Dishevelled (dsh) (Fig.4, B). dsh is translocated to the cell membrane and phosphorylated; concomitantly dsh/effector complexes are assembled. dsh recruitment to the membrane by Fz is regulated by kinases including Par1 (partitioning-defective 1), CK1 $\epsilon$  (casein kinase 1 $\epsilon$ ), and PKC $\delta$  (protein kinase C $\delta$ ). Multiple pathways downstream of dsh regulate the actin cytoskeleton or cell adhesion by activating the small GTPases Rho and Rac (Eaton et al., 1996; Fanto et al., 2000; Habas et al., 2003; Tahinci and Symes, 2003). One pathway signals to Rho, and occurs through the molecule DAAM1 (Dishevelled associated activator of morphogenesis 1) (Habas et al., 2001). This Rho pathway leads to the activation of the Rho-associated kinase ROCK, which mediates cytoskeletal re-organization (Winter et al., 2001; Marlow et al., 2002; Kim and Han, 2005). Another pathway activates Rac, which in turns stimulates JNK (c-Jun N-terminal kinase) activity (Boutros et al., 1998; Yamanaka et al., 2002; Habas et al., 2003). In vertebrates exist also a number of PCP components which have not been implied in *Drosophila* PCP signaling. Among them are PAPC (Paraxial Protocadherin), Ror2 (receptor tyrosine kinase-like orphan receptor 2), Scrb1 (Scribble) and Ptk7 (protein tyrosine kinase 7) (Hikasa et al., 2002; Murdoch et al., 2003; Lu et al., 2004; Medina et al., 2004; Unterseher et al., 2004; Schambony and Wedlich, 2007; Wang et al., 2008).

Finally, there are also other  $\beta$ -catenin-independent Wnt pathways. The **Wnt/Ca<sup>2+</sup> pathway** may actually influence the function of both the Wnt/ $\beta$ -catenin and PCP pathways. Wnt/Fz signaling via dsh activates phospholipase C (PLC), leading to the generation of DAG and IP<sub>3</sub> which increases the Ca<sup>2+</sup> concentration in the cell. In *Xenopus* embryos, overexpression of Wnt5a or Wnt11 can activate the calcium-sensitive protein kinase C $\alpha$  (PKC $\alpha$ ) (Sheldahl et al., 1999) and calcium/calmodulin-dependent kinase II (CamKII) (Kuhl et al., 2000) (Fig.4, C). Wnt5a-Ca<sup>2+</sup>-CamKII signaling can also activate TGF- $\beta$  activated kinase 1 (TAK1) and nemo-like kinase (NLK), which inhibit TCF/ $\beta$ -catenin signaling (Ishitani et al., 1999). Upstream of dsh heterotrimeric G proteins are involved in signal transduction. Stimulation of calcium flux in zebrafish embryos by noncanonical Wnts and Frizzleds is sensitive to pertussis toxin (Slusarski et al., 1997), as is PKC and CamKII activation in *Xenopus* (Sheldahl et al., 1999; Kuhl et al., 2000).

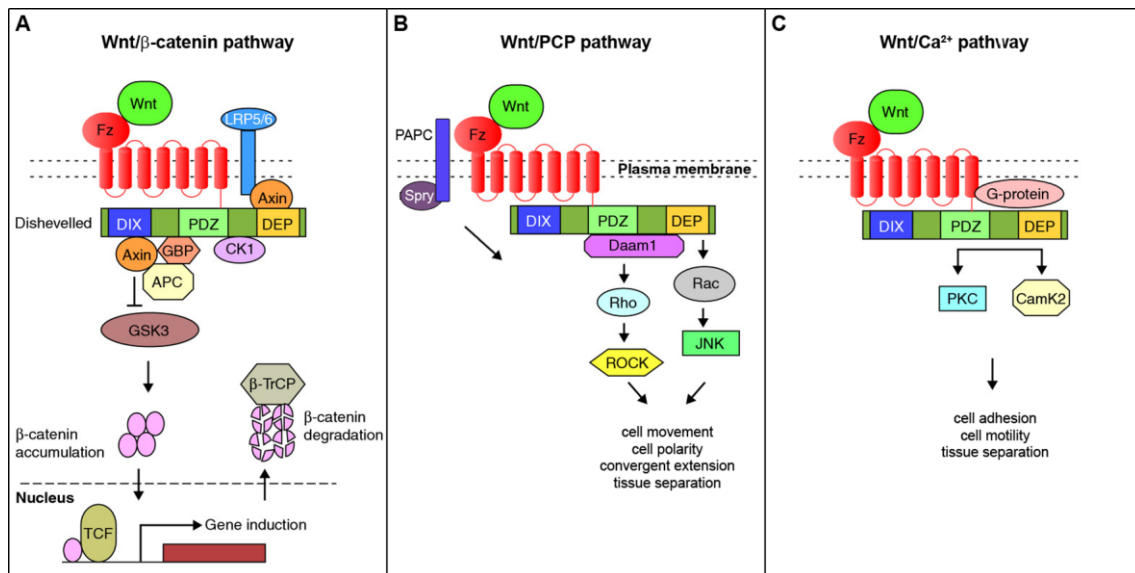


**Fig.4. Schematic representation of the Wnt signal transduction cascade.** (A) For the Wnt/ $\beta$ -catenin pathway, signaling through the Frizzled (Fz) and LRP5/6 receptor complex induces the stabilization of  $\beta$ -catenin via Dishevelled (dsh) and a number of factors including Axin, glycogen synthase kinase 3 (GSK3) and casein kinase 1 (CK1).  $\beta$ -catenin translocates into the nucleus where it complexes with members of the LEF/TCF family of transcription factors to mediate transcriptional induction of target genes.  $\beta$ -catenin is then exported from the nucleus and degraded via the proteosomal machinery. (B) For Wnt/PCP signaling, Wnt signal is transduced through Fz independent of LRP5/6. This pathway mediates cytoskeletal changes through activation of the small GTPases Rho and Rac via dsh. PAPC promotes Wnt/PCP signaling by inhibiting the negative regulator Spry. (C) For the Wnt/ $\text{Ca}^{2+}$  pathway, Wnt signaling via Fz mediates activation of heterotrimeric G-proteins, which engage dsh, phospholipase C (PLC, not shown), calcium-calmodulin kinase 2 (CamK2) and protein kinase C (PKC). This pathway also uses dsh to modulate cell adhesion and motility. For the PCP and  $\text{Ca}^{2+}$  pathways dsh is proposed to function at the membrane, whereas for canonical signaling dsh has been proposed to function in the cytoplasm or in the nucleus. Picture adapted from Habas and Dawid (2005).

Another function of  $\beta$ -catenin-independent Wnt-signaling through Fz7 and  $\text{PKC}\alpha$  is the establishment of tissue separation behavior in the dorsal mesoderm during gastrulation (Winklbauer et al., 2001). For this purpose, Fz7 must interact with the protocadherin PAPC. Activation of Rho signaling can partially substitute for PAPC in this process, while activation of JNK signaling cannot (Medina et al., 2004). dsh, however, which is upstream of Rho, JNK and  $\text{PKC}\alpha$  activation (Habas and Dawid, 2005), is not required for the establishment of tissue separation (Winklbauer et al., 2001). Complex behaviors, such as tissue separation and other morphogenetic movements, are therefore regulated by various parallel and partially overlapping signaling cascades of  $\beta$ -catenin-independent Wnt-signaling.

## 2.4.2 Cadherins

The adhesive properties of *Xenopus* gastrula cells that undergo convergent extension are more and more acknowledged to be essential for gastrulation (Hammerschmidt and Wedlich, 2008). This includes both cell-cell (Shih and Keller, 1992) and cell-matrix interaction (Winklbauer and Keller, 1996). The most prominent cell-cell adhesion molecules in gastrulation are the cadherins. Cadherins, which were initially identified in vertebrates, form a superfamily of transmembrane glycoproteins that are responsible for  $\text{Ca}^{2+}$ -dependent cell-cell adhesion (Halbleib and Nelson, 2006). Cadherins are defined as the proteins that contain multiple cadherin repeats in their extracellular domains (Suzuki, 2000). Depending on their conserved sequence motifs, the following Cadherin subfamilies can be distinguished: classical type I and type II cadherins, desmosomal cadherins, atypical cadherins, and protocadherins (Fig.5).

### 2.4.2.1 Classical cadherins

Many classical cadherins are associated with various forms of adherens junctions, which are close cell-cell contacts often associated with actin filaments at the cytoplasmic surface. Classical cadherins have five extracellular calcium-binding repeats (also called ectodomains or EC) in their extracellular domain. Binding between extracellular domains is thought to involve multiple *cis*-dimers of cadherin that form *trans*-oligomers between cadherins on opposing cell surfaces (Brieher et al., 1996; Chen et al., 2005). Binding between cadherin extracellular domains is weak, but strong cell-cell adhesion develops during lateral clustering of cadherins (Chen et al., 2005). The cytoplasmic domain of classical cadherins is highly conserved and binds directly to several cytoplasmic proteins including  $\beta$ -catenin and p120 catenin. This association links the cadherin protein to the cytoskeleton and is required for cell signaling. Without association with the catenins, the cadherins are non-adhesive. But it has become clear that the role of cadherins is not limited to mechanical adhesion between cells. Rather, cadherin function extends to multiple aspects of tissue morphogenesis, including cell recognition and sorting, boundary formation and maintenance, coordinated cell movements, and the induction and maintenance of structural and functional cell and tissue polarity (Halbleib and Nelson, 2006).

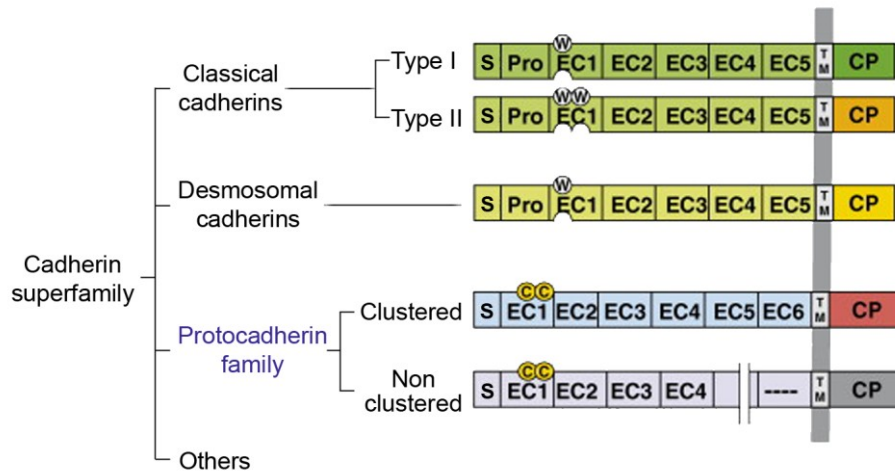


**Fig.5. Classification of the cadherin superfamily according to protein structure.** Classical type I cadherins have a conserved tryptophan (W2) in their EC1 domain and a hydrophobic pocket to accommodate W2 of a neighboring cadherin, which is crucial for homophilic adhesiveness. The prodomain (Pro) is removed to mediate functional adhesion. Type II cadherins have two conserved tryptophan residues (W2 and W4) and the hydrophobic pockets are correspondingly extensive. The cytoplasmic regions of classical cadherins have a catenin binding site which links it to the actin cytoskeleton. Desmosomal cadherins are similar to type I cadherins, but have distinctive cytoplasmic regions. Protocadherins neither have W2 nor a hydrophobic pocket but a characteristic disulfide-bonded loop (C-C) in the EC1 domain. Their cytoplasmic regions do not have a catenin binding site. The protocadherin family can be divided into two subgroups: clustered and nonclustered protocadherins based on their genomic organization. Clustered protocadherins have six EC domains. Nonclustered protocadherins have a variable number of EC domains. Proteins that contain an identifiable cadherin-like domain, e.g. the atypical cadherins, have been loosely referred to as “others”. CP, cytoplasmic domain; Pro, prodomain; S, signal peptide; TM, transmembrane domain. Picture adapted from Morishita and Yagi (2007).

Cadherin function is dynamic and regulated by developmental and cellular signals. Cadherin-mediated cell-cell adhesion is modulated by the phosphorylation of its intracellular binding partners or by changes in the level of cadherin on the cell surface (Duguay et al., 2003; Foty and Steinberg, 2005; Lilien and Balsamo, 2005). Cadherins are targets of ADAM10 (a disintegrin and metalloprotease domain 10) (Maretzky et al., 2005; Reiss et al., 2005) that cleaves the cadherin extracellular domain close to the transmembrane domain. The resulting extracellular fragment could further disrupt adhesion by competing with *trans* interactions between full-length cadherin complexes (Wheelock et al., 1987). The cytoplasmic domain of classical cadherins is also the target for proteolytic cleavage by the  $\gamma$ -secretase activity of Presenilin-1, which results in a loss of cell-cell adhesion (Marambaud et al.,

2002). Furthermore, constitutive endocytosis of a number of classical cadherins has been observed in cells that display apparently stable cell-cell contacts. Basal levels of cadherin internalization would be expected to support their metabolic turnover and perhaps contribute to local remodeling of contacts. Cadherin internalization may occur through different clathrin-dependent or -independent pathways (Yap et al., 2007).

Classical cadherins are indispensable for proper morphogenesis in sea urchin (Miller and McClay, 1997), zebrafish (Shimizu et al., 2005), and mouse embryos (Riethmacher et al., 1995). In *Xenopus* embryos, cadherins are required for blastomere adhesion, gastrulation movements, and tissue segregation. *Xenopus* cadherins are divided into two subclasses, the maternal and the zygotic cadherins, according to their temporal expression during embryogenesis. The maternal cadherins, XB/U- and EP/C-Cadherin, are stored as mRNA and proteins in the oocyte. The zygotic cadherins, E-, N- and F-Cadherin, are first expressed after midblastula transition. In the embryo, EP/C- and XB/U-Cadherin are distributed uniformly over the entire plasma membrane of all cells except for the outer surface. In contrast to maternal cadherins, zygotic cadherins show a tissue-specific distribution from the beginning of their expression. Specific members of the cadherin family can be allocated to the different cell behaviors during gastrulation; E-Cadherin is essential for the epiboly of the animal cap (Levine et al., 1994; Marsden and DeSimone, 2003), whereas EP/C- and XB/U-Cadherin promote convergent extension and most likely influence the active migration of the head mesoderm (Winklbauer et al., 1992; Lee and Gumbiner, 1995; Kuhl et al., 1996).

Inactivation of C-Cadherin, the primary mediator of adhesion in the *Xenopus* blastula, leads to both involution and convergent extension defects during gastrulation (Heasman et al., 1994a). Furthermore it was reported that EP/C-Cadherin-mediated cell adhesion is changed in response to mesoderm induction by activin (Brieher and Gumbiner, 1994). This modulation of cell-cell adhesion is not dependent on the amount of cadherin or on cadherin-catenin interaction. During involution of the mesoderm, the migrating cells change their adhesive properties. *In vitro* tissue separation assays show that before involution, the marginal cells integrate into the blastocoel roof, whereas involuted cells do not because they display tissue separation behavior. The molecular background of this change in cell behavior is still

unknown, but downregulation of C-Cadherin function seems to play a role in it (Wacker et al., 2000).

Proteolytic cleavage of cadherins has not, as yet, been shown to be relevant for gastrulation movements. Another way in which to regulate cadherin function is by internalization and trafficking of cadherins to and from the cell surface. Cadherin endocytosis was first shown to be required for gastrulation movements in studies of the GTPase Dynamin, a key regulator of clathrin-mediated endocytosis (Jarrett et al., 2002). A dominant-negative version of Dynamin applied to explanted *Xenopus* animal caps caused C-cadherin to accumulate at the cell membrane, while blocking the CE movements that are normally induced in the caps by activin (Jarrett et al., 2002). Two other proteins which are involved in Dynamin-dependent C-cadherin endocytosis are the type I transmembrane protein Fibronectin Leucine-rich Repeat Transmembrane 3 (FLRT3), and the small GTPase Rnd1 (Fig.6). FLRT3 and Rnd1 are both induced by activin in involuting mesodermal cells and form a complex required for the internalization of C-cadherin in Rab5-positive endosomes during *Xenopus* CE. By this mechanism, cells can undergo mediolateral intercalations and can slide past one another without sacrificing tissue integrity (Ogata et al., 2007). Similarly, the small GTPase Rab5c is required for E-cadherin endocytosis and for the dynamic regulation of cohesion during the anterior migration of prechordal plate cells in the zebrafish embryo (Ulrich et al., 2005). In this case, endocytosis depends on the non-canonical Wnt11 signal (Fig.6), consistent with the involvement of the PCP system in regulating E-cadherin recycling in the *Drosophila* wing (Classen et al., 2005). Still, it remains unclear how the endocytosis of cadherins is triggered (Hammerschmidt and Wedlich, 2008).

#### 2.4.2.2 Atypical cadherins

Atypical cadherins act to maintain polarity across tissues, regulate tissue size by controlling proliferation, and coordinate major morphogenetic movements in development (Halbleib and Nelson, 2006). Instead of five extracellular ECs characteristic of classical cadherins, atypical cadherins contain a variable number of EC repeats and other structural elements not present in other cadherins (Tepass et al., 2000). The large, atypical cadherins Dachsous (Ds) and Fat consist of 27 and 34 ECs, respectively (Mahoney et al., 1991; Clark et al., 1995). Flamingo (Fmi) is unique amongst the cadherins, as it is the only member with a seven-pass, rather than a

single, transmembrane domain and has a large extracellular sequence that includes nine ECs (Nakayama et al., 1998).

In *Drosophila* Ds, Fat, and Fmi are involved in the establishment of cell and tissue polarity. Ds/Fat and Fmi/Fz together with other core PCP proteins coordinate long range and local cell polarity (Strutt, 2008). Ds, which acts upstream of Fz (Yang et al., 2002), is expressed in a gradient across certain *Drosophila* tissues, but a gradient of Ds may not always be necessary for PCP (Simon, 2004). Ds binds Fat directly and negatively regulates its activity (Yang et al., 2002; Matakatsu and Blair, 2004). The extracellular domain of Ds is sufficient for its function in PCP, indicating that it may act as a ligand during PCP signaling (Matakatsu and Blair, 2006). Fat regulates PCP at least in part by binding the transcriptional corepressor Atrophin (Fanto et al., 2003). Intriguingly, it was recently shown that only the cytoplasmic tail of Fat is required for its effects on tissue growth and PCP (Matakatsu and Blair, 2006). Fmi functions downstream from Fz. Its expression precedes morphological changes associated with PCP, and Fmi localizes asymmetrically within tissues polarized by PCP signaling (Usui et al., 1999). Although Fmi homophilic adhesion has been demonstrated in vitro, its role in PCP appears to be independent of this property (Lu et al., 1999). The functional relationship of the Fat/Ds group to the Fz/Fmi PCP core group remains an open question. It has been thought that Fat/Ds acts upstream of Fz/PCP signaling, but more recently it has been suggested that the two signaling cassettes act in parallel and reinforce correct PCP establishment through their independent parallel inputs (Simons and Mlodzik, 2008).

In agreement with a role in PCP vertebrate Fmi mediates extension during zebrafish gastrulation (Formstone and Mason, 2005a) and is upregulated in the chick neural epithelium immediately prior to neural tube closure (Formstone and Mason, 2005b). The mouse Fmi ortholog Celsr1 localizes asymmetrically along the tissue plane in chick hair cells (Davies et al., 2005), and mutant Celsr1 disrupts stereocilia architecture in the inner ear (Curtin et al., 2003).

#### 2.4.2.3 Protocadherins

Protocadherins (Pcdhs) are a class of cadherins that are primarily expressed in the nervous system, but have additional important developmental expression patterns in nonneuronal tissues. With more than 70 members identified to date, they make up the largest subfamily of cadherins. Like classical cadherins, protocadherins are type I

transmembrane proteins. However, their extracellular domain has six to seven EC repeats that lack the conserved sequence elements present in classical cadherins. In general, protocadherins have weak adhesive properties in cell aggregation assays, and it is unclear whether they mediate homophilic or heterophilic adhesions. In addition, the cytoplasmic domain of protocadherins is structurally diverse, in contrast to the homology between classical cadherins, and less is known about cytoplasmic binding partners (Halbleib and Nelson, 2006).

Initially, protocadherins were thought to represent an ancient 'proto'-type of cadherin-like molecules. But none of the 15 and 17 cadherin superfamily members present in *Caenorhabditis elegans* and *Drosophila melanogaster* could be classified as a direct ortholog of vertebrate protocadherins (Hill et al., 2001). The mammalian protocadherin family can be roughly divided into two groups based on their genomic structure: clustered and nonclustered protocadherins (Fig.5). Clustered protocadherins consist of the Pcdh $\alpha$ ,  $\beta$  and  $\gamma$  family, each of which has a specific genomic organization clustered in a small genome locus. Nonclustered protocadherins can be divided into two subgroups: Pcdh $\delta$  and solitary protocadherins in the phylogenetic tree (Morishita and Yagi, 2007).

Analogous to the classical cadherins, protocadherin function can be regulated by proteolysis. Recent research demonstrated the specific cleavage of Pcdh $\alpha$  and Pcdh $\gamma$  proteins by ADAM10 and presenilin (Reiss et al., 2006; Bonn et al., 2007). In addition to modulating cell adhesion, proteolysis of Pcdh $\alpha$  and Pcdh $\gamma$  generates a cytoplasmic fragment that localizes to the nucleus (Haas et al., 2005; Bonn et al., 2007). There the Pcdh $\gamma$  cytoplasmic domain can activate the transcription of Pcdh $\gamma$  genes in an autoregulatory loop (Hambusch et al., 2005).

Functions of protocadherins have been examined in a variety of developmental systems. In *Xenopus* four protocadherins have been described so far: Paraxial Protocadherin (PAPC), Axial Protocadherin (AXPC), Neural Fold Protocadherin (NFPC), and Protocadherin in Neural crest and Somites (PCNS) (Bradley et al., 1998; Kim et al., 1998; Kuroda et al., 2002; Rangarajan et al., 2006). Of these, only PAPC has been shown to be involved in gastrulation movements. Since its discovery, PAPC has been implicated in various developmental processes, among them cell sorting, convergent extension, tissue separation and  $\beta$ -catenin-independent Wnt-signaling. The expression of *Xenopus* PAPC starts shortly before gastrulation in the

dorsal organizer and expands to a ring-like domain throughout the marginal zone. At neurulation stages, PAPC is expressed in the paraxial mesoderm but not in the future notochord. There AXPC is expressed in a complementary pattern. During somitogenesis PAPC is dynamically expressed in the presomitic mesoderm (Kim et al., 1998). In several assays PAPC-expressing cells were shown to sort out from AXPC-positive or uninjected cells (Kim et al., 1998). It was believed that the sorting was induced by homophilic binding properties of the extracellular domain of PAPC. However, a recent study demonstrated that PAPC mediates cell sorting by reducing C-Cadherin-mediated adhesion instead (Fig.6). Although the mechanism remains unresolved, it has been clearly shown that the intracellular domain is dispensable for this activity (Chen and Gumbiner, 2006).

Data from both gain and loss of function experiments revealed that PAPC promotes convergent extension and cell polarization/orientation during gastrulation movements without affecting cell fate (Kim et al., 1998; Medina et al., 2004; Unterseher et al., 2004). Consequently PAPC was shown to signal to downstream components of the Wnt/PCP pathway, which controls these morphogenetic processes. PAPC activates Rho and JNK, but inhibits Rac, without affecting Cdc42 activity (Fig.6) (Medina et al., 2004; Unterseher et al., 2004). PAPC is also necessary for the separation of involuting mesoderm cells from the ectoderm. Knockdown of PAPC abolishes the posterior part of Brachet's cleft, which is formed and maintained by tissue separation (Medina et al., 2004). Unexpectedly, PAPC could even induce tissue separation behavior in ectodermal cells without inducing mesoderm, when coexpressed with Fz7. For this function the extracellular interaction of PAPC and Fz7 is required, as well as the presence of the cytoplasmic domains of both proteins (Winklbauer et al., 2001; Medina et al., 2004).

The cytoplasmic domain of PAPC, which has been implicated in signal transduction but not in cell sorting, has been shown to interact with various intracellular proteins (Fig.6). Among them are ANR5 (Ankyrin Repeats domain protein 5) and Sprouty (Spry), both FGF target gene products. It is through these interacting proteins that PAPC influences the formation of cell protrusions, convergent extension and tissue separation. While ANR5 seems to be a positive regulator of Wnt/PCP signaling, Spry acts as an inhibitor whose function needs to be blocked in order to promote morphogenesis (Chung et al., 2007; Wang et al., 2008).

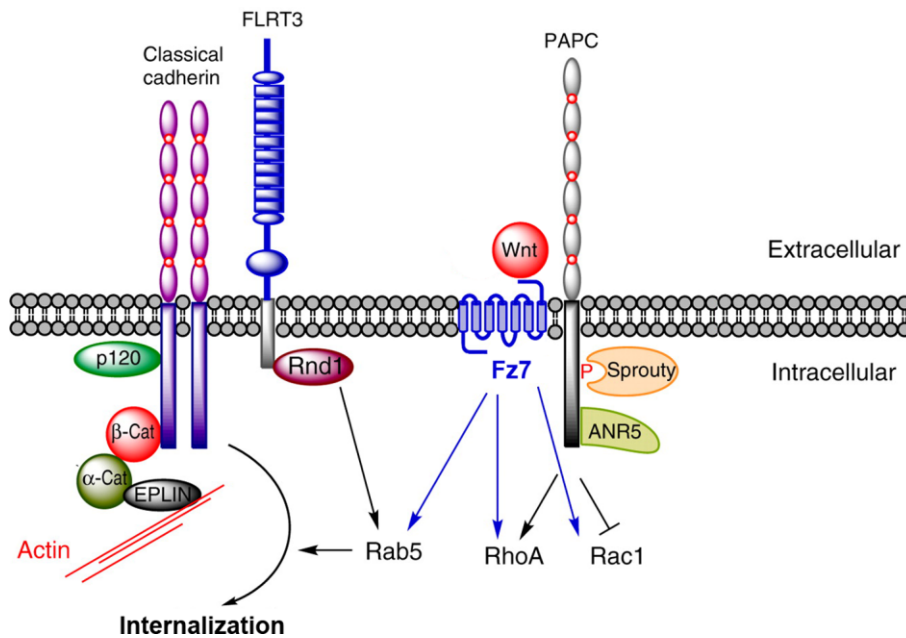


**Fig.6. Regulation of cell adhesion during gastrulation.** Classical cadherins, which mediate cell adhesion, are regulated by non-canonical Wnt signaling or by the small GTPase Rnd1. Rnd1 induces cadherin endocytosis in Rab5-positive vesicles by binding to the cytoplasmic domain of FLRT3. Paraxial Protocadherin (PAPC) regulates C-Cadherin-mediated adhesion via an unknown mechanism. The cytoplasmic tail of PAPC contains several binding sites for proteins that mediate intracellular signaling and interfere with non-canonical Wnt (PCP) signaling. Picture adapted from Hammerschmidt and Wedlich (2008).

The role of PAPC may be evolutionary conserved. Just as in *Xenopus*, the PAPC ortholog in zebrafish is expressed in the dorsal mesoderm but not in the midline. There it is required for mesodermal convergence movements (Yamamoto et al., 1998). In contrast the putative *mouse* ortholog, Pcdh8, while expressed in the primitive streak and the paraxial mesoderm, is not essential for gastrulation (Yamamoto et al., 2000). However, Pcdh8 may not represent the true PAPC ortholog, as sequence identity is relatively low (41%) (Frank and Kemler, 2002; Chen et al., 2007) and experimental data do not support an orthologous function.

## 2.5 Aim of this study

PAPC is involved in most aspects of cellular behavior during convergent extension and tissue separation. PAPC can modulate the activities of Wnt- and FGF-signaling components (Medina et al., 2004; Unterseher et al., 2004; Chung et al., 2007; Wang et al., 2008), and it also influences cell adhesion mediated by classical cadherins (Chen and Gumbiner, 2006). For some functions the extracellular domain seems to be indispensable, for others the intracellular domain (Medina et al., 2004; Chen and Gumbiner, 2006; Wang et al., 2008). Yet intriguingly little is known about what exactly PAPC does in order to promote gastrulation movements.

The aim of this study was therefore to:

- i. investigate the role of the different domains of PAPC in signaling and cell adhesion,
- ii. explore in depth the mechanisms by which PAPC exerts its signaling functions, particularly with regard to  $\beta$ -catenin-independent Wnt-signaling during gastrulation movements,
- iii. elucidate the effect of PAPC on C-Cadherin-mediated cell adhesion.

### 3 Results

#### 3.1 PAPC has signaling properties

##### 3.1.1 Rho activity in the dorsal mesoderm depends on PAPC function

PAPC is part of the non-canonical Wnt-signaling pathway and can modulate the activity of downstream effectors. Pull-down experiments have shown that PAPC activates JNK and RhoA, while it inhibits Rac1 (Medina et al., 2004; Unterseher et al., 2004). As these results had all been obtained by immunoprecipitating active Rho from embryo extracts, I wanted to investigate the effect of PAPC on active Rho *in situ*. Therefore I made use of a fusion protein of Rhotekin and GFP (RBD-GFP), which recognizes specifically active Rho (Goulimari et al., 2005). Incubation of stage 12 dorsal marginal zone (DMZ) explants with GFP led to a faint nonspecific staining, while RBD-GFP stained the cells at the cell membrane and the nucleus (Fig.7, B and C). The nuclear staining has been shown to be nonspecific in mouse embryonic fibroblast (MEF) cells (Goulimari et al., 2008). For manipulations of Rho signaling in DMZ explants I injected only the right side of the marginal zone so that the left side could serve as an internal control (Fig.7, A). When dominant negative RhoA (dnRhoA) was injected with histone 2B (H2B)-mRFP to mark the injected cells, the level of active Rho dropped dramatically. We observed that the cells in which Rho signaling was blocked were larger in size, often having two nuclei within the same cell (Fig.7, D and data not shown). This phenomenon could be due to the role of Rho in cytokinesis (Drechsel et al., 1997). In order to investigate whether the activation of Rho in the DMZ depended on PAPC, I knocked down PAPC by injecting morpholino oligonucleotides (MoPAPC) targeting the 5' UTR region of both alleles. Loss of function of PAPC resulted in a decrease in RhoA activation as judged by RBD-GFP staining. The injected cells were often bigger than the control cells but smaller than dnRhoA-injected cells (Fig.7, E). This effect depended on PAPC function because a PAPC construct lacking the Morpholino target sequence could rescue Rho activation when coexpressed with MoPAPC in the DMZ (Fig.7, F). In a recent study our lab could show that the intracellular domain, specifically amino acids 741 and 955, is indispensable for Rho activation (Wang et al., 2008). I could confirm these results *in situ* by injecting MoPAPC in combination with different truncated or mutated PAPC constructs into the marginal zone. The intracellular domain of PAPC, PAPCc, could rescue Rho activation partially (Fig.7, G).

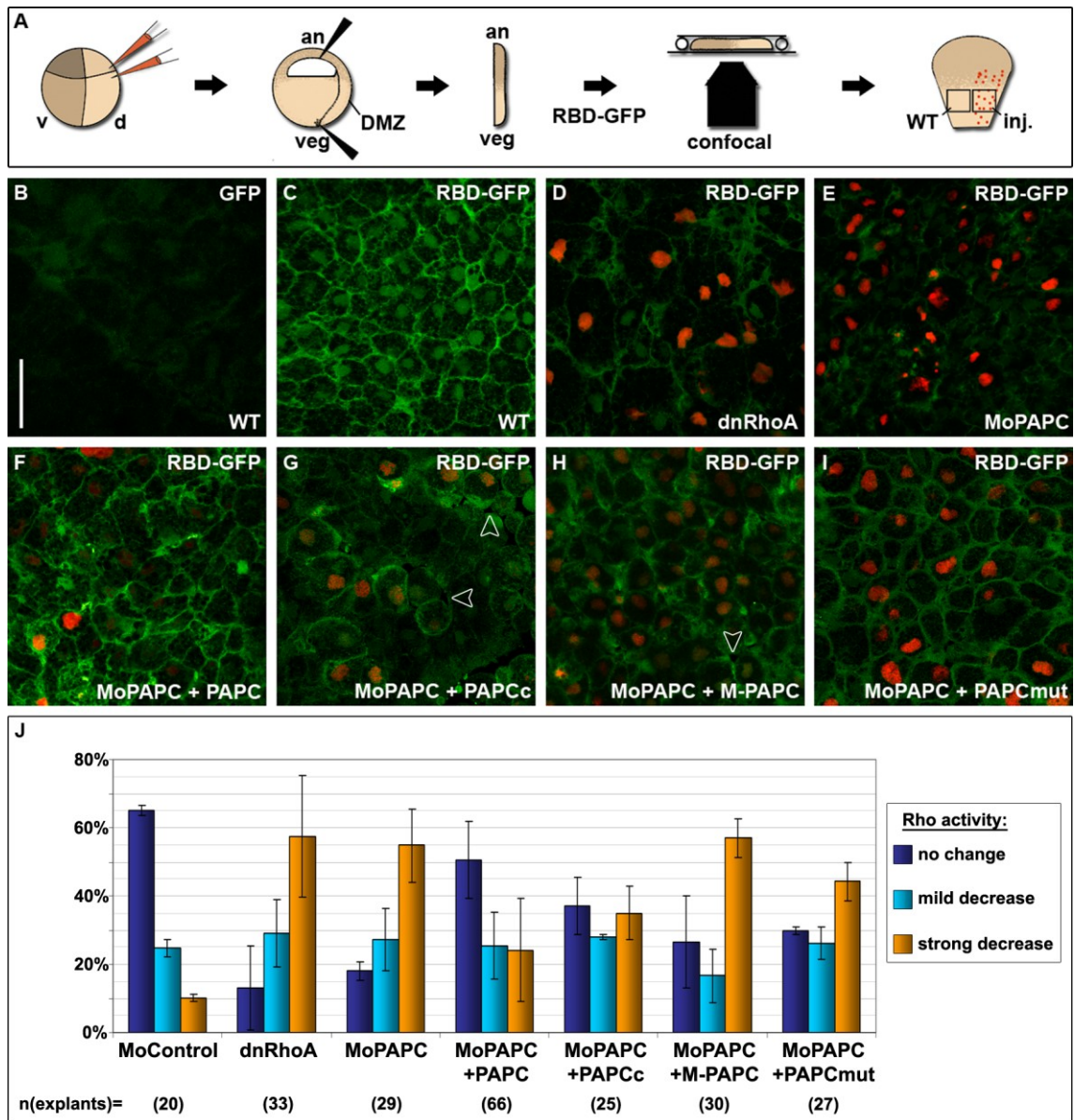


**Fig.7. The activation of Rho depends on P-42 in the DMZ.** (A) Schematic drawing of the experimental procedure. Embryos were injected into the right side of the DMZ with dnRhoA DNA (200pg), MoPAPC (40ng) alone or in combination with P-42, P-42c, M-P-42 or P-42mut mRNA (200pg each). Injected cells were marked by the expression of H2B-mRFP. The uninjected left side served as internal control. The DMZs were stained with RBD-GFP protein and analyzed by confocal microscopy. (B) Incubation of DMZs with GFP produced only a very faint background signal. (C) RBD-GFP recognized active Rho and stained cell membranes and the nuclei in DMZ explants. (D) Overexpression of dnRhoA inactivated Rho and resulted in increased cell size. (E) Knock-down of P-42 led to a loss of active Rho as shown by RBD-GFP staining. (F) Coinjection of P-42 together with MoPAPC could rescue Rho activation. (G) P-42c, the intracellular domain of P-42, could partially rescue the MoPAPC-induced loss of Rho activation. (H) A truncated form of P-42 without the cytoplasmic domain (M-P-42) was unable to rescue the MoPAPC-induced Rho phenotype. (I) P-42mut could not compensate the loss of P-42 with respect to Rho activation. (J) Quantification of experiments. Error bars represent standard deviation. Scale bar: 50 $\mu$ m. an, animal pole; d, dorsal; DMZ, dorsal marginal zone; inj, injected; v, ventral; veg, vegetal pole; WT, wild type.

In some cases Rho was activated above control level (data not shown) and frequently the cells presented a round cell shape with lost cell cohesion (Fig.7, G arrow heads). M-PAPC, which consists of the extracellular and the transmembrane domain as well as 17 intracellular amino acids, could not substitute for this PAPC function (Fig.7, H). Occasionally M-PAPC also induced round cells that were partly detached from the surrounding cells in DMZ explants (Fig.7, H arrow head). When amino acids 741 and 955 on the intracellular domain were mutated, giving rise to PAPCmut, Rho activity could not be rescued (Fig.7, I). These results show that Rho activation in the mesoderm depends on PAPC function and emphasize the importance of the intracellular domain for this process.

Since PAPC has been reported to be localized to the tips of elongating mesodermal cells (Unterseher et al., 2004), I expected to find activated Rho enriched at the tips as well. This was the case at embryonic stage 12 and became more pronounced at stage 15 (Fig.8, A and B, arrow heads). The localization of activated Rho at the tips of mesodermal cells reflected their movement towards the dorsal midline, since migratory MEF cells also accumulated activated Rho at the rear and at the leading edge (Goulimari et al., 2005).

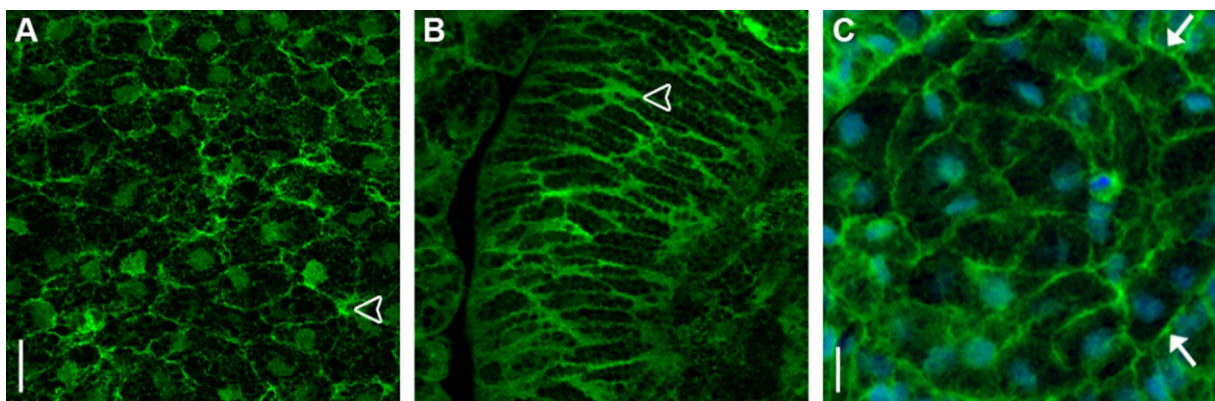


**Fig.8. Distribution of activated Rho in DMZ explants at gastrulation and neurulation stages.** (A, B) DMZ explants were stained with RBD-GFP and analyzed by confocal microscopy. (A) At stage 12 activated Rho is localized to the tips of mesoderm cells. (B) At stage 15 this localization becomes more pronounced. (C) Transverse cryosection of a DMZ at stage 22 stained with RBD-GFP and DAPI. The border between notochord and surrounding mesoderm is marked by arrows. Scale bar: 25 $\mu$ m.

At stage 22 cells of the notochord, which have already completed convergent extension, did not show any preferential localization of activated Rho (Fig.8, C). For quantitative analyses however the asymmetric distribution of activated Rho was not consistent enough at stage 12. While undergoing gastrulation movements, the cells

of the dorsal mesoderm elongated gradually. At stage 12, many cells did not show a clear polarization (Fig.15), making an analysis of the preferential localization of activated Rho difficult.

### 3.1.2 PAPC and Spry interact independently of FGF-signaling

Recently the mechanism how PAPC promotes Rho activation was discovered. In a yeast-two-hybrid screen for interaction partners of PAPCc, Spry was identified (Wang, 2007; Wang et al., 2008). Spry is an inhibitor of receptor tyrosine kinase signaling (Cabrita and Christofori, 2008). FGF induces the expression of Spry, which in turn acts as a negative feedback loop inhibitor at several levels of FGF signaling (Hacohen et al., 1998; Hanafusa et al., 2002; Cabrita and Christofori, 2008). In *Xenopus* Spry inhibits gastrulation movements by interfering with the PCP pathway, but MAPK signaling downstream of FGF is unaffected (Nutt et al., 2001; Sivak et al., 2005). This made Spry appear like an interesting candidate as signaling component downstream of PAPC.

The interaction between PAPC and Spry was confirmed by coimmunoprecipitation of overexpressed PAPCc and Spry from embryo extracts. When two point mutations were introduced into PAPCc at putative phosphorylation sites (giving rise to PAPCcmut), the interaction was abolished (Wang et al., 2008). If PAPC and Spry interact in the embryo, Spry should be recruited to the cell membrane, and indeed this was the case. When both PAPC and GFP-Spry were expressed in the animal pole GFP-Spry was localized to the cell membrane (Wang et al., 2008). In C2C12 cells, a mouse myoblast cell line, Spry has been shown to translocate to the cell membrane upon FGF treatment (Hanafusa et al., 2002). To investigate the connection between PAPC, Spry and FGF signaling, I turned to cell culture where the presence of signaling molecules can be better controlled than in the embryo. First I showed that FGF also induces the membrane recruitment of Spry in HEK293 cells, and that blocking FGF signaling with the inhibitor SU5402 abolishes this recruitment (Fig.9).

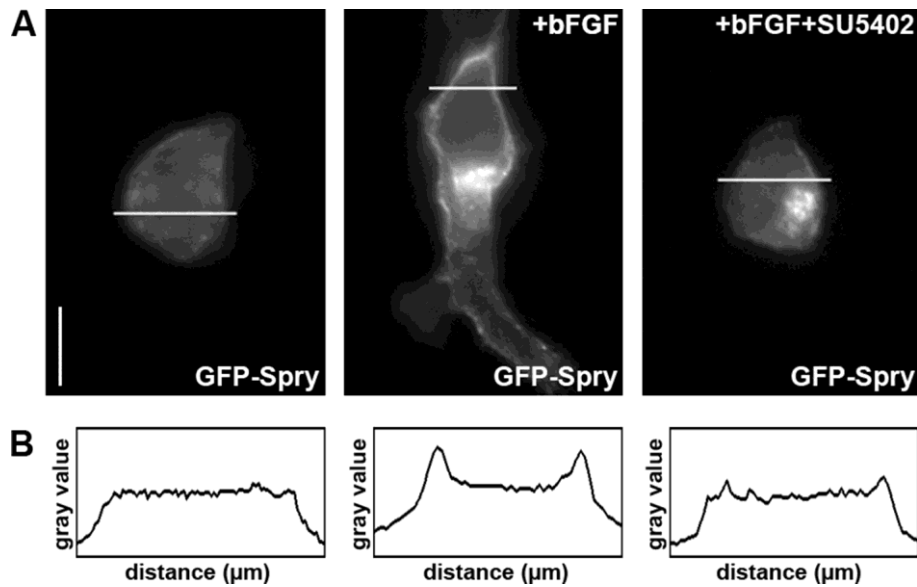


**Fig.9. bFGF-induced membrane recruitment of Spry can be inhibited by SU5402.** HEK293 cells were transfected with GFP-Spry and treated with bFGF in the absence or presence of SU5402, an inhibitor of the FGF-receptor. The cells were fixed and GFP-Spry localization was analyzed by fluorescent microscopy. (A) GFP-Spry is recruited to the cell membrane upon activation of the FGF pathway. This activation can be blocked by SU5402. (B) Fluorescent signal intensities were measured along the white lines in A. Scale bar: 10 $\mu$ m.

Next I could confirm the interaction between PAPC and Spry in HEK293 cells. GFP-Spry was recruited to the cell membrane when PAPC was cotransfected. In contrast PAPCmut did not cause membrane translocation of GFP-Spry although proteins were expressed at comparative levels and were localized to the cell membrane (Fig.10, A and B, and data not shown). These findings show that PAPC can bind Spry and emphasize the importance of the PAPC phosphorylation sites S741 and S955 for the interaction. But since the cells were cultured in medium containing fetal bovine serum, the presence of FGF could not be excluded in this setup. To address this point the experiment was repeated, but this time the cells were cultured in serum-free medium in the presence of the FGF inhibitor SU5402. Still, PAPC induced the membrane recruitment of GFP-Spry, and PAPCmut was unable to do so (Fig.10, C and D). These results show that PAPC can bind Spry and recruit it to the membrane independently of FGF signaling.

The expression of Spry inhibited  $\beta$ -catenin-independent Wnt signaling at different levels; Spry blocked Rho activation as well as the membrane recruitment of dsh and PKC $\delta$  in the embryo. These effects could be reversed by coexpression of PAPC, but not of PAPCmut (Wang et al., 2008). Therefore the binding of PAPC to Spry is sufficient for antagonizing Spry function during PCP signaling.

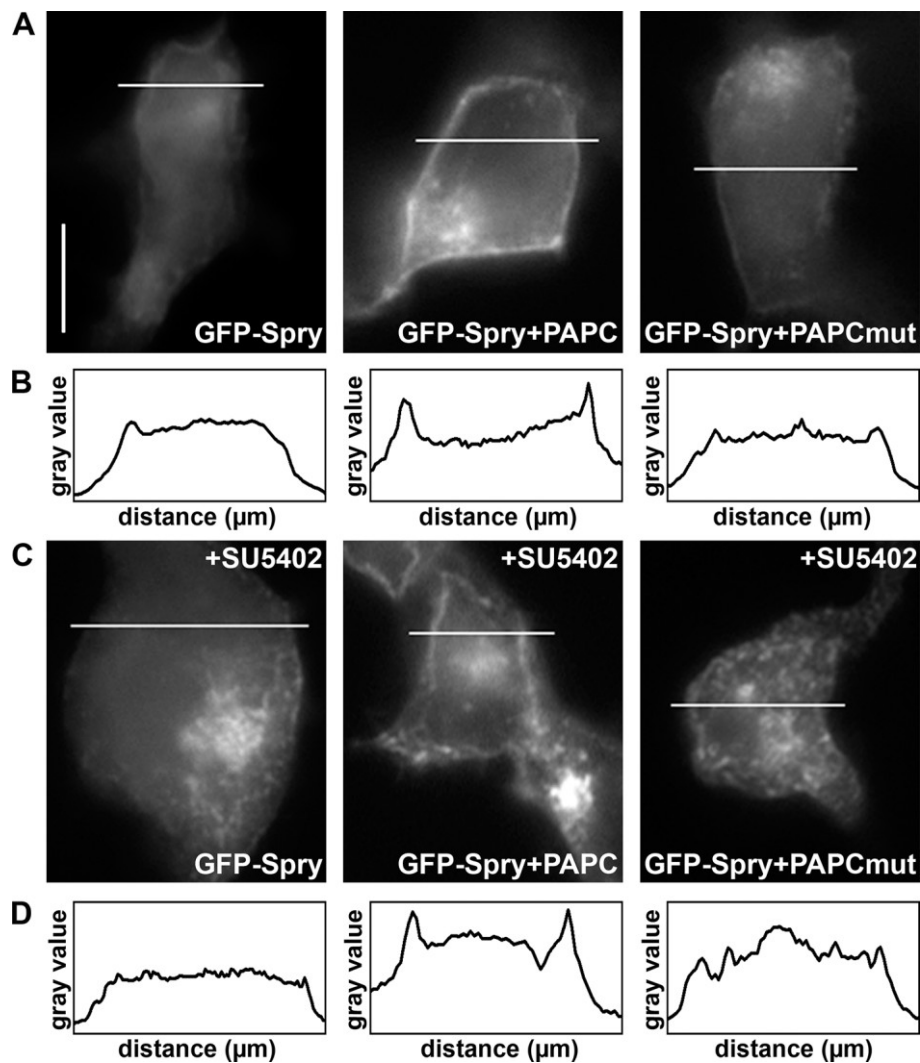


**Fig.10. PAPC recruits Spry to the membrane independently of FGF-signaling.** HEK293 cells were transfected with GFP-Spry alone or in combination with PAPC or PAPCmut. The cells were fixed and GFP-Spry localization was determined by fluorescent microscopy. (A) PAPC recruits GFP-Spry to the cell membrane, while PAPCmut is unable to do so. (B) Plot of fluorescent intensity measured along the lines in A. (C) In the presence of the FGF-receptor inhibitor SU5402 PAPC can still recruit GFP-Spry. (D) Plot of fluorescent intensity measured along the lines in C. Scale bar: 10μm.

Spry blocks morphogenetic movements in the embryo by inhibiting the recruitment of PCP signaling components downstream of Fz7. PAPC binds Spry, releases its block on PCP and thereby promotes morphogenetic movements (Wang et al., 2008). Since morphogenetic movements also require a modulation of cell adhesion (Brieher and Gumbiner, 1994; Jarrett et al., 2002) the question arose whether the ability of PAPC to bind Spry had any connection to the cell sorting properties of PAPC (Kim et al., 1998; Chen and Gumbiner, 2006). To address this point, an *in vivo* cell dispersion assay was used. The injection of a single blastomere with GFP at the 32-cell stage led to GFP-expressing cells extensively interspersed with unlabeled cells (Fig.11, A). In contrast, cells derived from GFP and PAPC, M-PAPC or PAPCmut injected blastomeres formed tight patches and maintained sharp borders with the unlabeled cells (Fig.11, B-D). These results show that there is no correlation between the ability to bind Spry and cell sorting induced by PAPC. Therefore the cell adhesion and signaling abilities of PAPC can be separated.

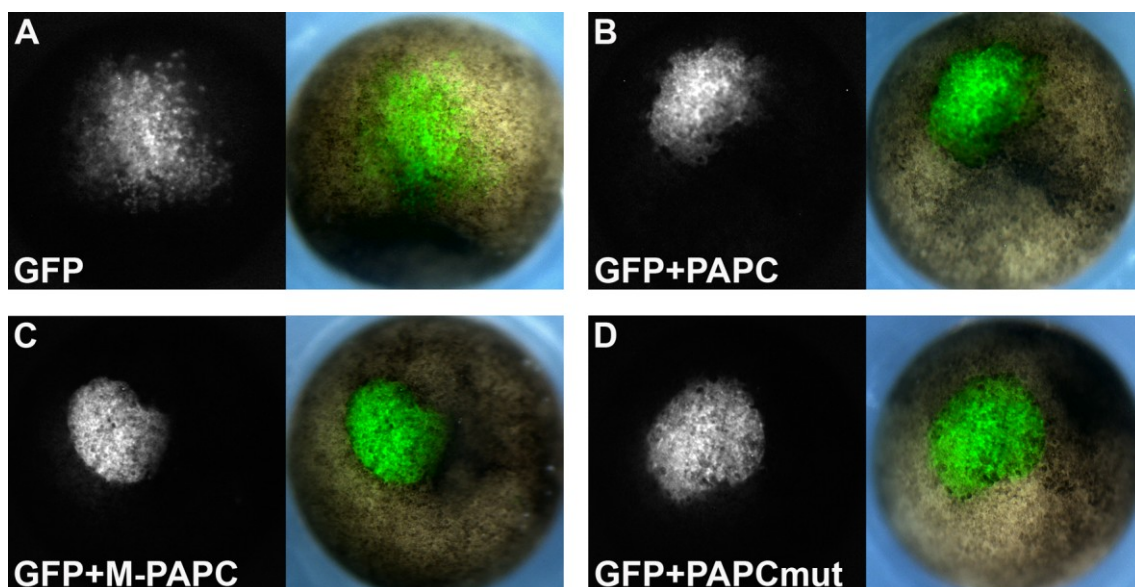


**Fig.11. The ability to bind Spry is independent of the cell sorting properties of PAPC.** GFP-mRNA (100pg) was injected alone or with PAPC, M-PAPC or PAPCmut (200pg each) into a single blastomere of the animal hemisphere at 32-cell stage. At st.12 the patch of GFP-expressing cells was analyzed for cohesion or dispersion. (A) GFP-injected cells resulted in a disperse patch of cells (12/12). (B) Coinjection of PAPC led to a patch with sharp boundaries in about 50% of cases (6/13). (C) M-PAPC caused the cells to cohere so strongly that the patch was even visible in the bright field image (10/11). (D) PAPCmut also led to a patch of cells with sharp boundaries (11/13).

### 3.1.3 PAPC does not signal by recruiting dsh-GFP to the cell membrane

Rho is activated downstream of Fz and dsh in the PCP-signal transduction pathway (Habas et al., 2001; Habas et al., 2003; Wallingford and Habas, 2005). Fz7 recruits dsh to the cell membrane, which is a necessary step in Rho activation (Park et al., 2005). What is the role of PAPC in this process? PAPC can inhibit Spry, a negative regulator of PCP signaling (Wang et al., 2008), but PAPC might activate the pathway more directly by recruiting dsh to the membrane as well.

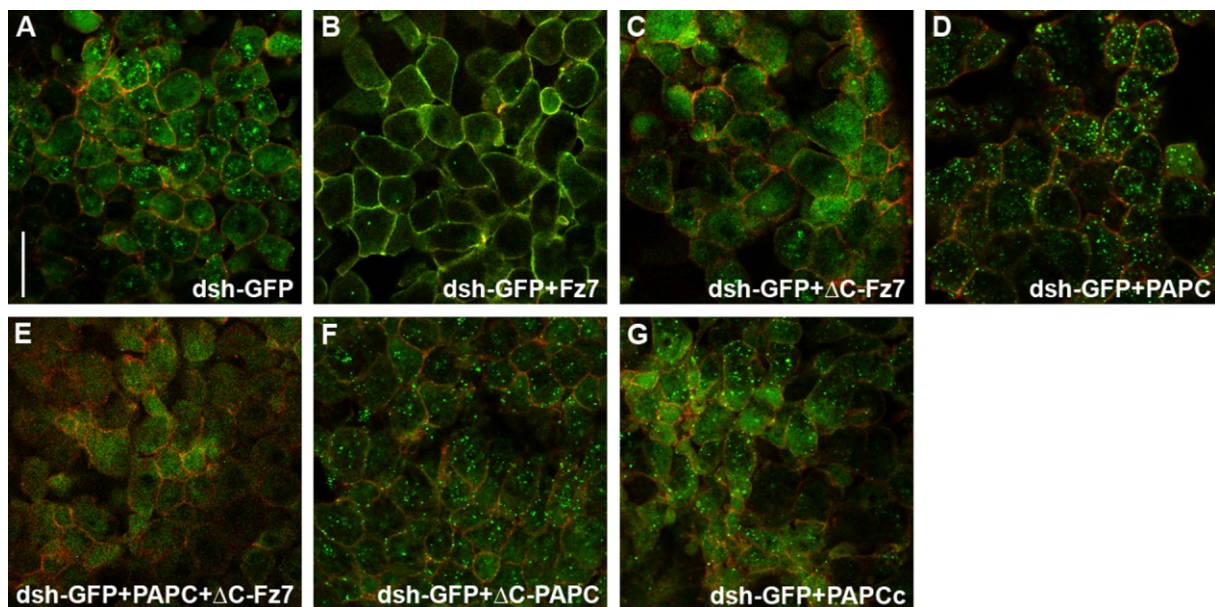


**Fig.12. PAPC does not recruit dsh-GFP to the cell membrane.** dsh-GFP (400pg) was injected alone or in combination with Fz7,  $\Delta$ C-Fz7, PAPC,  $\Delta$ C-PAPC or PAPCc (1ng each) into the 4-cell embryo. Membrane-bound (mb)-RFP marked the cell membrane. The animal cap was explanted and dsh-GFP localization was analyzed by confocal microscopy. (A) dsh-GFP was localized in the cytoplasm in a diffuse staining or a punctate pattern. (B) Fz7 recruited dsh-GFP to the membrane. (C)  $\Delta$ C-Fz7 could not recruit dsh-GFP because this is mediated by the intracellular domain of Fz7. (D) PAPC did not induce membrane localization of dsh-GFP. (E) The interaction between the extracellular domains of PAPC and Fz7 could not stimulate dsh-recruitment either. (F-G) Neither  $\Delta$ C-PAPC nor PAPCc could recruit dsh-GFP to the membrane. Scale bar: 50 $\mu$ m.

To test this hypothesis, dsh-GFP was expressed and its subcellular localization analyzed in animal cap cells. dsh-GFP, which shows a punctate localization pattern in the cytoplasm, was efficiently recruited to the membrane by the overexpression of Fz7 (Fig.12, A and B). This translocation depended on the cytoplasmic tail of Fz7 (Medina and Steinbeisser, 2000); consequently overexpressed  $\Delta$ C-Fz7, which lacks the cytoplasmic tail, was unable to recruit dsh-GFP (Fig.12, C). The presence of

PAPC was not sufficient to induce dsh-GFP membrane recruitment (Fig.12, D). PAPC and Fz7 interact via their extracellular domains (Medina et al., 2004). This interaction could be necessary to activate PAPC in order to stimulate membrane translocation of dsh. However, this was not the case, as PAPC together with  $\Delta$ C-Fz7 still did not recruit dsh-GFP (Fig.12, E). Accordingly, none of the PAPC fragments, neither  $\Delta$ C-PAPC nor PAPCc, could stimulate membrane translocation of dsh-GFP (Fig.12, F and G). In conclusion, PAPC does not activate Rho directly by recruiting dsh. The presence of Fz7 does not change the recruiting abilities of PAPC.

### 3.1.4 PAPCc is localized to the nucleus and to the cell membrane

The intracellular domain of PAPC (PAPCc) can rescue Rho activation and convergent extension movements in DMZ explants after knock-down of PAPC. PAPCc binds to and inhibits Spry, thereby releasing its block on PCP signaling (Wang et al., 2008). But other mechanisms of signaling downstream of PAPC are also possible. Unpublished data from our lab suggested that the overexpression of PAPC could regulate the transcription of target genes. In the original yeast-two-hybrid-screen for interaction partners of PAPCc, some transcription factors had been identified (Wang, 2007). Therefore it was an interesting observation that when embryos expressing PAPC-myc were subjected to Western blot analysis, two bands with a molecular weight of 150 and 60kDa were recognized by an  $\alpha$ -myc antibody (ab) (Fig.13, A). The band of 150kDa was the full length PAPC protein, but the band of 60kDa corresponded to a protein of unknown identity.

Since both cadherins and protocadherins had been shown to undergo ectodomain shedding and intracellular cleavage (Marambaud et al., 2002; Maretzky et al., 2005; Reiss et al., 2005; Reiss et al., 2006), it seemed possible that PAPC was also processed in that way. The 60kDa protein fragment could thus be the transmembrane and intracellular domain with some additional extracellular amino acids. If this was the case, could the intracellular domain of PAPC be cleaved off completely and enter the nucleus?

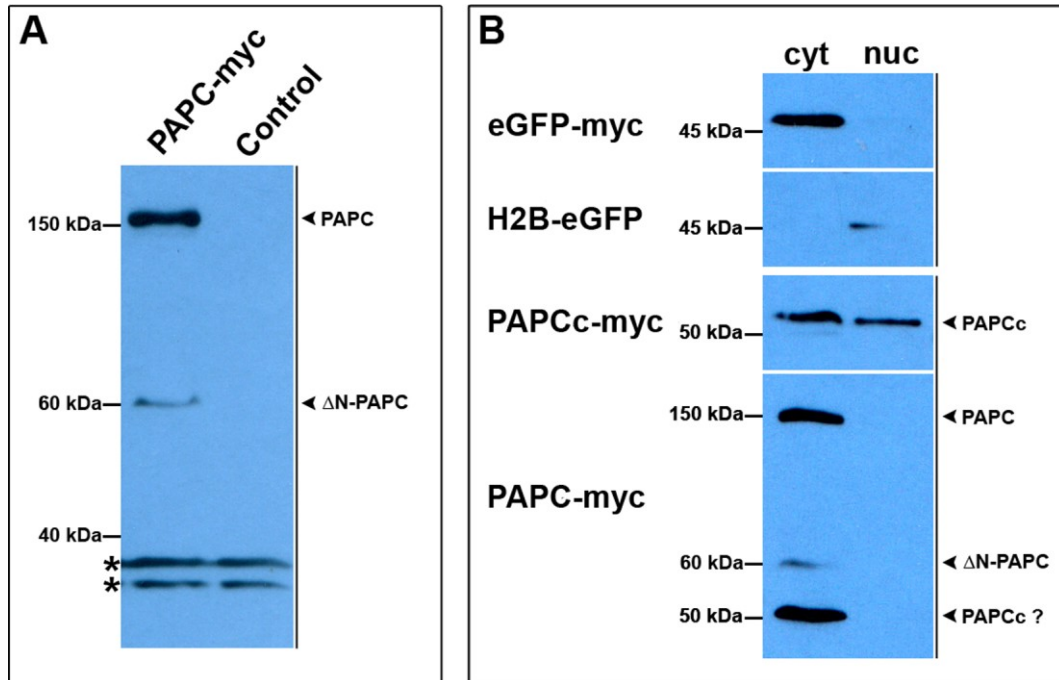


**Fig.13. The intracellular domain of PAPC is cleaved and can enter the nucleus.** (A) Western blot of embryos injected with PAPC-myc DNA (150pg). Asterisks mark nonspecific bands. (B) Western blot of the cytosolic and nuclear fraction of oocytes injected with eGFP-myc, H2B-eGFP, PAPCc-myc or PAPC-myc (500pg each). cyt, cytoplasmic fraction; nuc, nuclear fraction.

To test this hypothesis, *Xenopus* oocytes were used as assay system because the large nuclei can easily be separated from the cytoplasm by hand. The oocytes were injected with mRNA coding for eGFP-myc, histone 2B (H2B)-eGFP, PAPC-myc and PAPCc-myc and subjected to Western blot analysis (Fig.13, B). eGFP-myc and H2B-eGFP served as controls for the clean separation of nucleus and cytoplasm. As expected, eGFP-myc could only be detected in the cytoplasm and H2B-eGFP in the nucleus using an  $\alpha$ -GFP ab. PAPCc-myc was detected in the cytoplasm as well as in the nucleus of oocytes using the  $\alpha$ -myc ab. PAPC-myc showed three bands in the cytoplasmic but none in the nuclear fraction. The band with a molecular weight of 150kDa was the full length protein, while the bands of 60 and 50kDa could correspond to PAPC at different stages of extracellular cleavage. Several questions remained. If PAPC gives rise to a band of 50kDa in oocytes, why is there no corresponding fragment in embryos? It also was not apparent why the 50kDa-fragment of PAPC did not enter the nucleus just as PAPCc did. One explanation could be that the fragment of 50kDa was still membrane tethered and therefore could not be transported into the nucleus. Still, the observation that PAPCc was present in

the nuclear fraction was intriguing and raised the question, where PAPCc was located in the embryo.

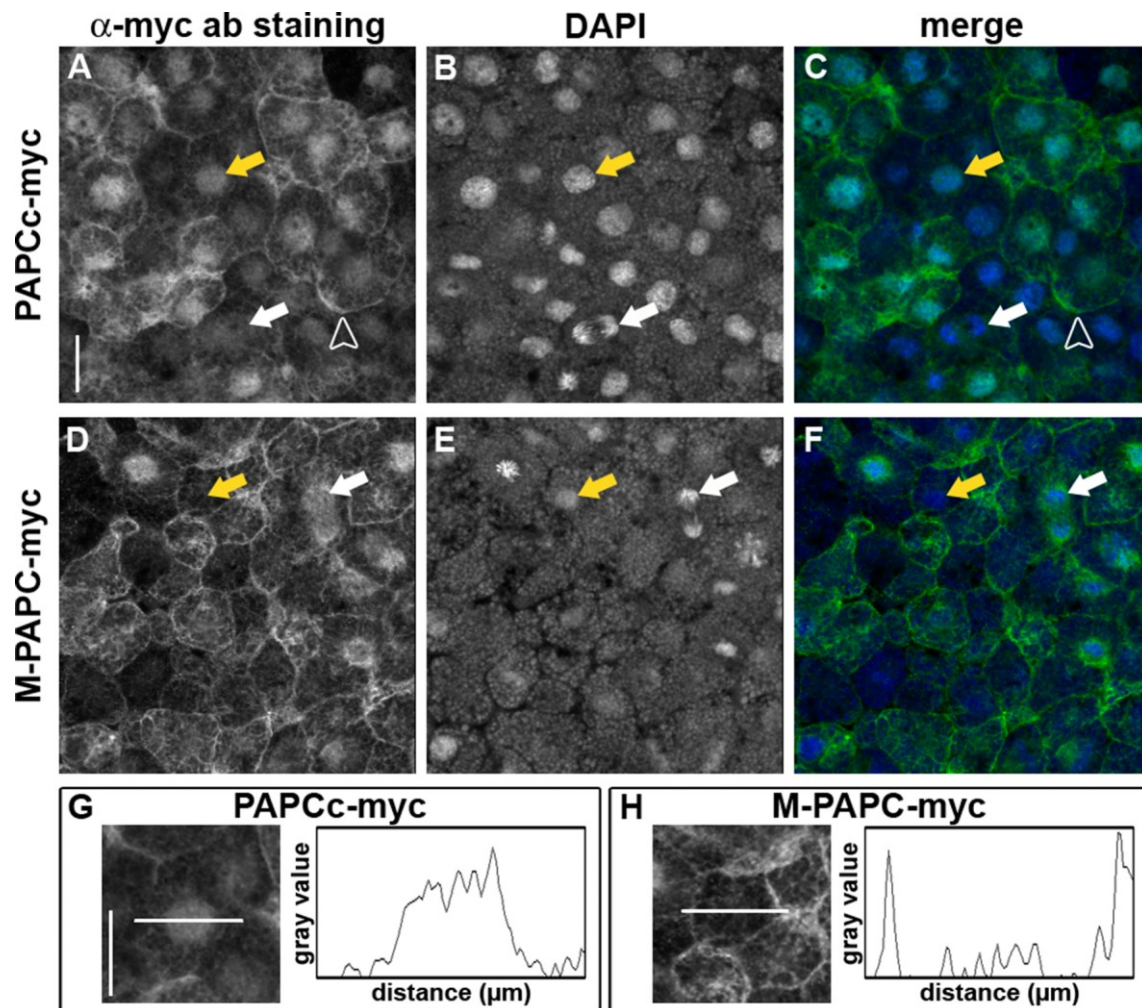


**Fig.14. PAPCc is localized to the nucleus and to the cell membrane.** mRNAs coding for PAPCc-myc or M-PAPC-myc (500pg each) were injected into the animal pole of 4-cell embryos. The animal caps were excised, fixed in formaldehyde and Dent's, and then stained with  $\alpha$ -myc ab and DAPI. The localization of PAPCc-myc and M-PAPC-myc was analyzed by confocal microscopy. (A-C) PAPCc-myc was localized to the nucleus (yellow arrow) and to the cell membrane (arrow head). In dividing cells PAPCc-myc could not be detected near the chromosomes (white arrow). (D-F) M-PAPC-myc is a transmembrane protein and absent from the nucleus (yellow arrow). Perinuclear stainings probably correspond to ER localization as they were still present in dividing cells (white arrow). (G, H) Magnifications of cells in A and D. Staining intensities were measured along the horizontal white line. Scale bars: 20 $\mu$ m.

To address this question, I excised animal caps of embryos expressing PAPCc-myc and, as a control for membrane localization, M-PAPC-myc. The caps were stained

with  $\alpha$ -myc ab and DAPI for analysis by confocal microscopy. PAPCc-myc was indeed localized to the nucleus (Fig.14, A-C, yellow arrow). A rather surprising fact was that it also localized to the cell membrane (Fig.14, A and C, open arrow head). Since PAPCc does not have any membrane-targeting signals, it must be bound to another protein at the cell membrane. M-PAPC-myc was present at the cell membrane and absent from the nucleus (Fig.14, D-F, yellow arrow). Representative cells were magnified and the intensity of  $\alpha$ -myc staining was measured to illustrate the different localization pattern of PAPCc-myc and M-PAPC-myc (Fig.14, G and H). To conclude, PAPC is subject to proteolytic cleavage in oocytes and in the embryo. Whether this cleaved C-terminal fragment can enter the nucleus cannot be answered, but PAPCc can localize to the nucleus in both cell types. There it might mediate transcription or repression of target genes.

### 3.1.5 Loss of PAPC leads to a change in cell shape and loss of cell polarity

Loss of PAPC inhibits the constriction but not the elongation of DMZ explants. As a consequence, MoPAPC-injected DMZ explants are broader and flatter in cross sections than those of control explants. This has been linked to random movement of mesoderm cells during convergent extension (Unterseher et al., 2004). While analyzing DMZ explants for Rho activation, it became obvious that the cells looked different after loss of PAPC. They appeared to be round instead of bipolarly shaped. To quantify this effect, I marked the cell membrane of dorsal marginal cells by expression of GAP43-GFP and measured their length and width. Only cells with a length to width ratio of 1.75 or more were counted as "elongated". 34% of control cells at stage 12 were elongated, while loss of PAPC reduced this population to 23% of cells (Fig.15, A and B). Coinjection of PAPC with MoPAPC worsened the effect; as a result only 18% of cells were elongated (Fig.15, C). This may be a problem of titrating the right amount of PAPC, since many components of PCP signaling have the same phenotype in loss or gain of function experiments (Tada and Smith, 2000; Wallingford et al., 2000; Tahinci and Symes, 2003). The regulation of cell shape seems to be a particularly sensitive system; other effects of PAPC loss of function, such as elongation of animal cap explants or tissue separation, can be rescued by expression of a PAPC rescue construct lacking the morpholino target sequence (Medina et al., 2004). The observed change in cell shape after knock-down of PAPC

is in agreement with experiments which show that inhibition of Rho leads to round cells at stage 12.5 in shaved DMZ explants (Tahinci and Symes, 2003). In this type of explant the deep mesodermal cells next to the epithelium are visible, as the other layers of deep cells have been peeled away (Shih and Keller, 1992). Nevertheless, these findings contradict other results which show no difference in cell shape after PAPC loss of function at later stages (Unterseher et al., 2004). This could be due to the small difference in cell shape, which may be recovered at later stages.

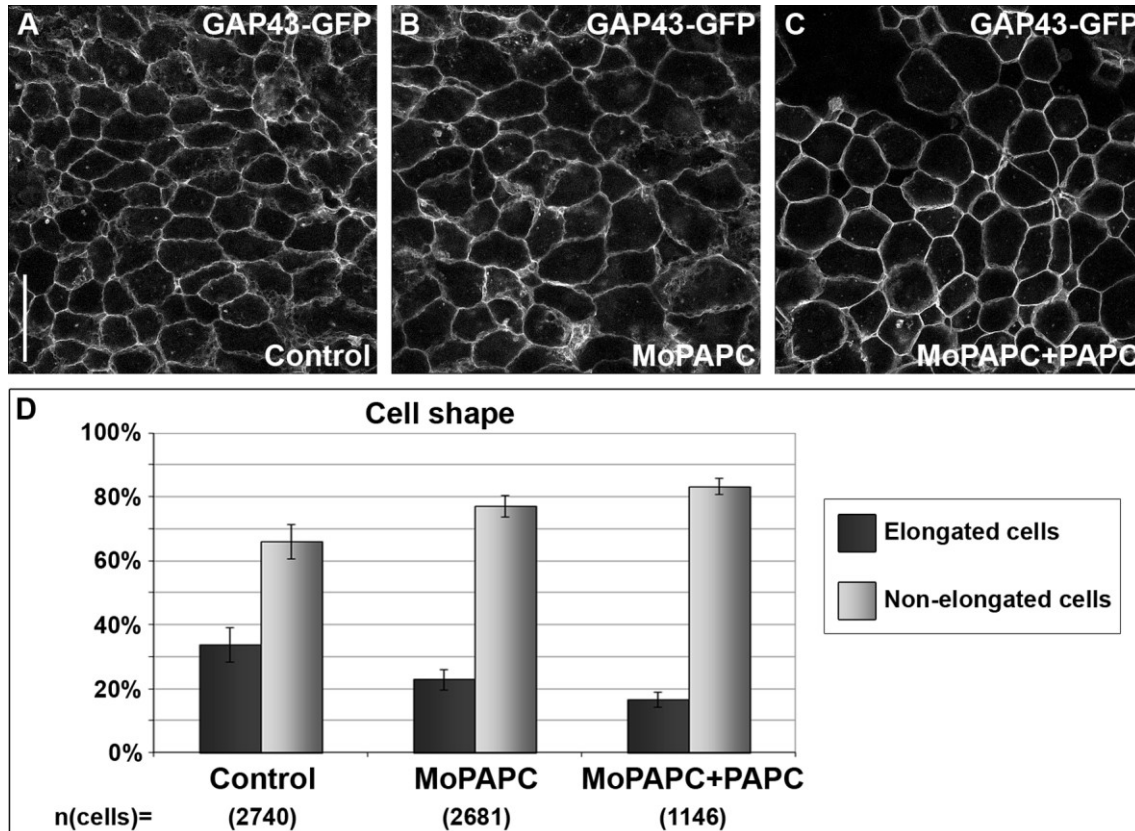


**Fig.15. Loss of PAPC leads to a change in cell shape.** (A-C) Embryos were injected with GAP43-GFP alone or in combination with MoPAPC (80ng) or MoPAPC and PAPC (200pg). The DMZs were explanted and analyzed by confocal microscopy. (D) The cell shape was determined as the ratio of cell length to cell width. Cells with a ratio  $\geq 1.75$  were counted as elongated. Error bars represent standard deviation. Scale bar: 50 $\mu$ m.

There could be different reasons why the cells without PAPC do not acquire a bipolar shape. Either the cells have lost their bipolar identity, that is, their orientation; or they cannot elongate because of physical restraints, like failures of the cytoskeletal architecture. To investigate whether the cells of the dorsal mesoderm retain their bipolarity after knock down of PAPC, the subcellular localization of Venus-protein kinase C $\lambda$  (Vn-PKC $\lambda$ ) was analyzed by confocal microscopy. PKC $\lambda$ , one of several

atypical protein kinases C, belongs to the partitioning defective (PAR) proteins and has been shown to localize to the tips of elongating mesodermal cells (Hyodo-Miura et al., 2006). Vn-PKC $\lambda$  was localized to the ends of cells in control DMZ explants at stage 12 (Fig.16, A, arrow heads). There it coincides with the lamellipodial protrusive activity that pulls cells between one another (Keller, 2002). In DMZ cells injected with MoPAPC Vn-PKC $\lambda$  failed to accumulate at specific sites of the cell (Fig.16, B). These findings corroborate data from time-lapse movies which show that MoPAPC-injected cells move randomly and change their orientation frequently (Unterseher et al., 2004).

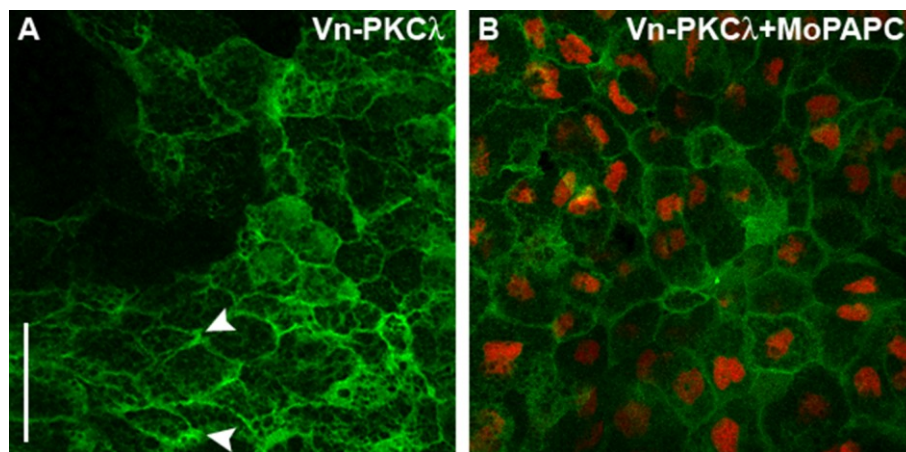


**Fig.16. Loss of PAPC leads to a loss of cell polarity.** Embryos were injected into the left side of the DMZ with Venus-PKC $\lambda$  (200pg) and into the right side with Venus-PKC $\lambda$  and MoPAPC (40ng) in addition to H2B-mRFP to mark the side of injection. The DMZs were explanted and the distribution of Venus-PKC $\lambda$  was analyzed by confocal microscopy. (A) Vn-PKC $\lambda$  is localized to the tips of elongating mesodermal cells in the control side. (B) Without PAPC Vn-PKC $\lambda$  is localized uniformly along the cell membrane. Scale bar: 50 $\mu$ m.

## 3.2 PAPC modulates cell adhesion

### 3.2.1 PAPC mediates cell sorting in reaggregation assays

PAPC can mediate cell sorting in dissociation and reaggregation assays (Kim et al., 1998; Chen and Gumbiner, 2006). As PAPC is a protocadherin and belongs to the cadherin superfamily, the cell sorting behavior of PAPC-expressing cells has been attributed to homophilic binding between PAPC proteins (Kim et al., 1998). A truncated form of PAPC which lacks most of the intracellular domain induces much stronger cell sorting than the full length protein. This observation led to the assumption that the intracellular domain inhibited the homophilic binding of the extracellular domain (Kim et al., 1998). However, it was shown later that PAPC induces cell sorting by reducing C-Cadherin mediated cell adhesion (Chen and Gumbiner, 2006). In this model the extracellular domain influences C-Cadherin via an unknown mechanism while the intracellular domain has no effect (Chen and Gumbiner, 2006).

I repeated the dissociation and reaggregation assay with different PAPC constructs in order to learn more about the role of the extra- and intracellular domain in cell sorting and adhesion. Embryos at the 4-cell stage were injected with Texas Red or Fluorescein dextrane alone or in combination with mRNAs encoding different PAPC constructs. At blastula stage the animal cap region was excised, dissociated in  $Mg^{2+}/Ca^{2+}$ -free medium, mixed and then reaggregated. In control aggregates the red and green cell populations mixed randomly in about 50% of cases (Fig.17, A). Surprisingly the other 50% of aggregates showed weak or even strong cell sorting. Injection of PAPC with Fluorescein dextrane raised the number of cell aggregates showing cell sorting to more than 70%, although the majority displayed only weak sorting (Fig.17, B). In agreement with previously published data, the deletion construct M-PAPC, which retains only 17 of the cytoplasmic amino acids, induced strong cell sorting in almost all aggregates (Fig.17, C).  $\Delta$ C-PAPC, which lacks even those 17 intracellular amino acids, also induced strong cell sorting (Fig.17, D). These results confirmed that the extracellular and transmembrane domains were sufficient to induce cell sorting. Furthermore, the cells which expressed the PAPC constructs seemed to sit on the outside of the aggregates (Fig.17, B-D). According to Steinberg's theory of differential cell adhesion (Steinberg, 1970; Foty and Steinberg, 2004), cells with weaker cell adhesion sort out to the periphery of aggregates.

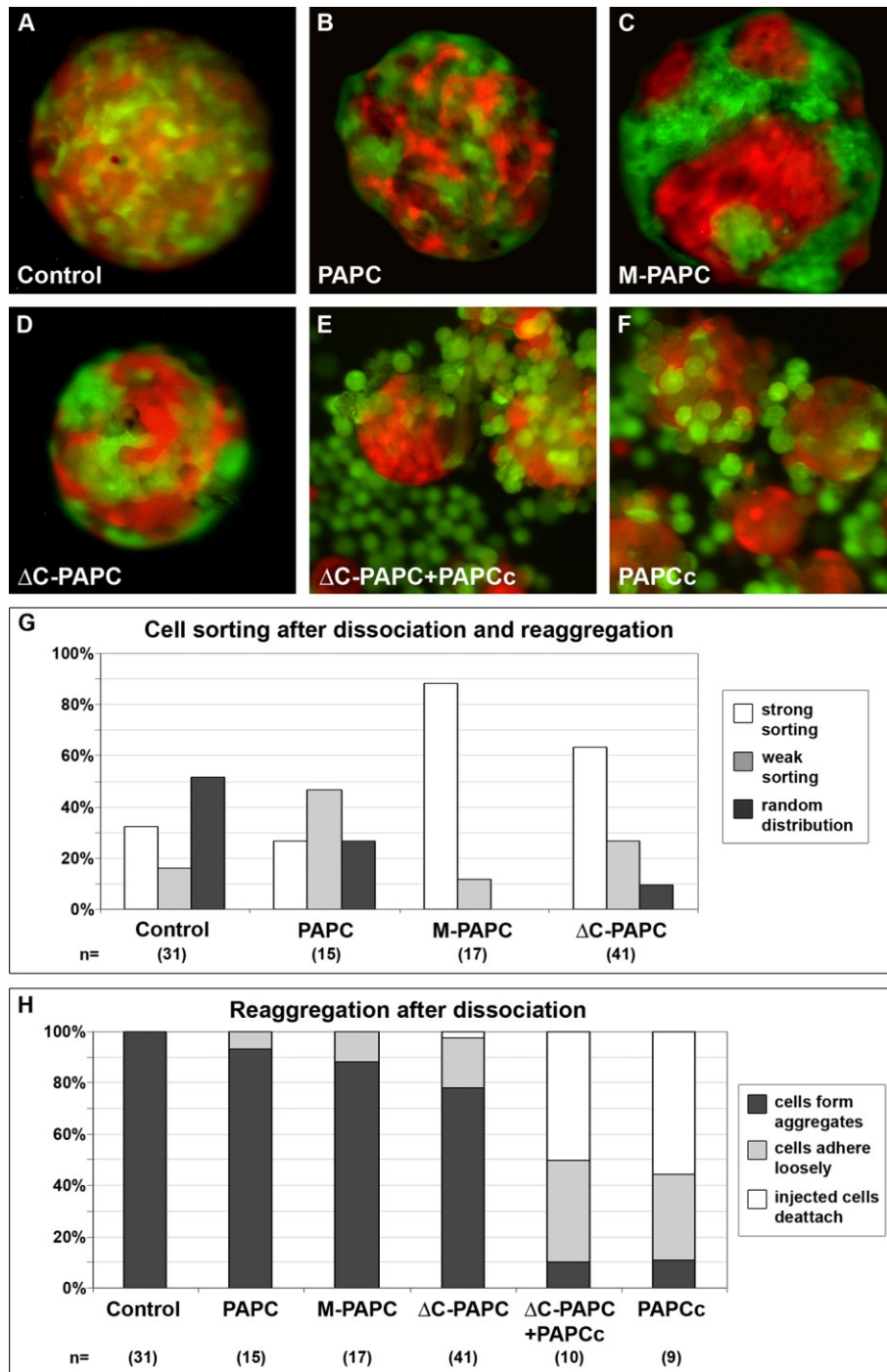


**Fig.17. PAPC mediates cell sorting.** Cells from embryos injected with Texas Red were dissociated and mixed with cells from embryos injected with Fluorescein and PAPC (1ng), M-PAPC,  $\Delta$ C-PAPC or PAPCc (600pg each). The cells were reaggregated and analyzed. (A) Cells in control aggregates were distributed randomly. (B) Cells expressing PAPC sorted out from control cells in small patches. (C) M-PAPC induced strong cell sorting. (D) Overexpression of  $\Delta$ C-PAPC also led to clearly separated patches of cells. (E)  $\Delta$ C-PAPC and PAPCc did not phenocopy PAPC but caused the cells to drastically reduce their adhesion. (F) PAPCc-expressing cells lost their adhesion to a great extent. (G) Summary of the sorting experiments. (H) Summary of the reaggregation behavior of cells.

This substantiated the idea that PAPC decreased cell adhesion instead of promoting it. Coexpression of  $\Delta C$ -PAPC together with the intracellular domain, PAPCc, did not cause the same weak sorting phenotype as PAPC. Instead the injected cells were excluded from the aggregates and sat loosely on top of them or were completely detached from the aggregates (Fig.17, E). The outcome was the same when only PAPCc was expressed; the injected cells neither adhered to each other nor to the control cells (Fig.17, F). This is in complete disagreement with previously published data that claimed that the intracellular domain of PAPC had no influence on cell adhesion (Chen and Gumbiner, 2006). The extracellular and transmembrane domains of PAPC are sufficient to induce cell sorting in aggregates. The intracellular domain, however, causes a state of complete non-adhesion. The results of the experiments are summarized in Fig.17, G and H.

Another indication that PAPCc does have an influence on cell adhesion came from experiments with DMZ explants. When PAPC was knocked down by injecting MoPAPC, the simultaneous expression of PAPCc sometimes caused the injected cells to drop out of the explants (Fig.18). This effect clearly depended on the amount of PAPCc injected, but even in lower concentrations the injected cells often became round and left gaps in the tissue (Fig.7, G, arrow heads). The cells which had fallen out of the explants were not dead and kept on dividing, as judged by the continued expression of H2B-mRFP and their small cell size (Fig.18).

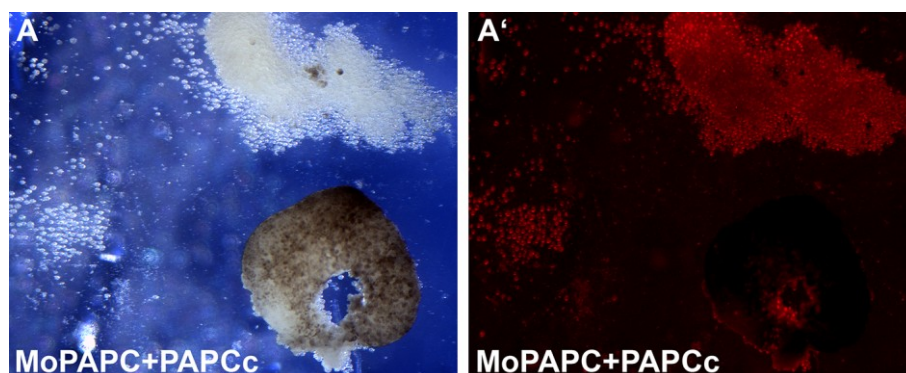


**Fig.18. PAPCc causes cells to detach in DMZ explants.** (A) The overexpression of PAPCc in the absence of endogenous PAPC led to the complete detachment of cells. (A') The injected cells are marked by H2B-mRFP expression.

### 3.2.2 P APC causes internalization of C-Cadherin in animal cap cells

P APC decreases C-Cadherin-mediated cell-cell adhesion; the total C-Cadherin protein levels, however, are not changed (Chen and Gumbiner, 2006). Nevertheless, P APC might affect the intracellular distribution of C-Cadherin, making less C-Cadherin available at the cell membrane. To test this hypothesis, C-Cadherin-eGFP was expressed in animal cap cells and its localization was analyzed by confocal microscopy. In 30% of samples C-Cadherin-eGFP was located exclusively at the plasma membrane with no cytoplasmic accumulation. In 50% of samples there was a weak cytoplasmic localization of C-Cadherin-eGFP visible, and in 20% a strong cytoplasmic localization (Fig.19, A-D). Coexpression of P APC with C-Cadherin-eGFP changed that subcellular distribution. Only very few animal caps had C-Cadherin-eGFP just at the cell membrane, most had intracellular protein particles (Fig.19, D). How does P APC influence the subcellular distribution of C-Cadherin-eGFP? Possible explanations could be that C-Cadherin-eGFP is held back inside the cell or that it is internalized from the membrane via endocytosis. In the latter case blocking endocytosis should reverse the effect of P APC. When endocytosis was blocked by injecting a dominant negative mutant of Dynamin1 (dnDyn) together with P APC and C-Cadherin-eGFP, the percentage of samples with no cytoplasmic C-Cadherin-eGFP dots increased slightly, while the percentage of samples with a strong cytoplasmic C-Cadherin-eGFP localization dropped dramatically. Most samples now showed a weak cytoplasmic C-Cadherin-eGFP localization (Fig.19, D). This suggested that P APC stimulated the endocytosis of C-Cadherin-eGFP in a Dynamin1-dependent manner.

Since Fz7 had been shown to decrease C-Cadherin-mediated adhesion in a cell adhesion assay (Medina et al., 2000), it was tested whether Fz7 also changed the distribution of C-Cadherin-eGFP. Indeed Fz7 led to the same increase in cytoplasmic C-Cadherin-eGFP dots as P APC did. The combination of P APC and Fz7 could not enhance the effect but caused the same degree of redistribution as each of the proteins alone (Fig.19, D). Both P APC and Fz7 stimulate the endocytosis of C-Cadherin, but they do not act synergistically.

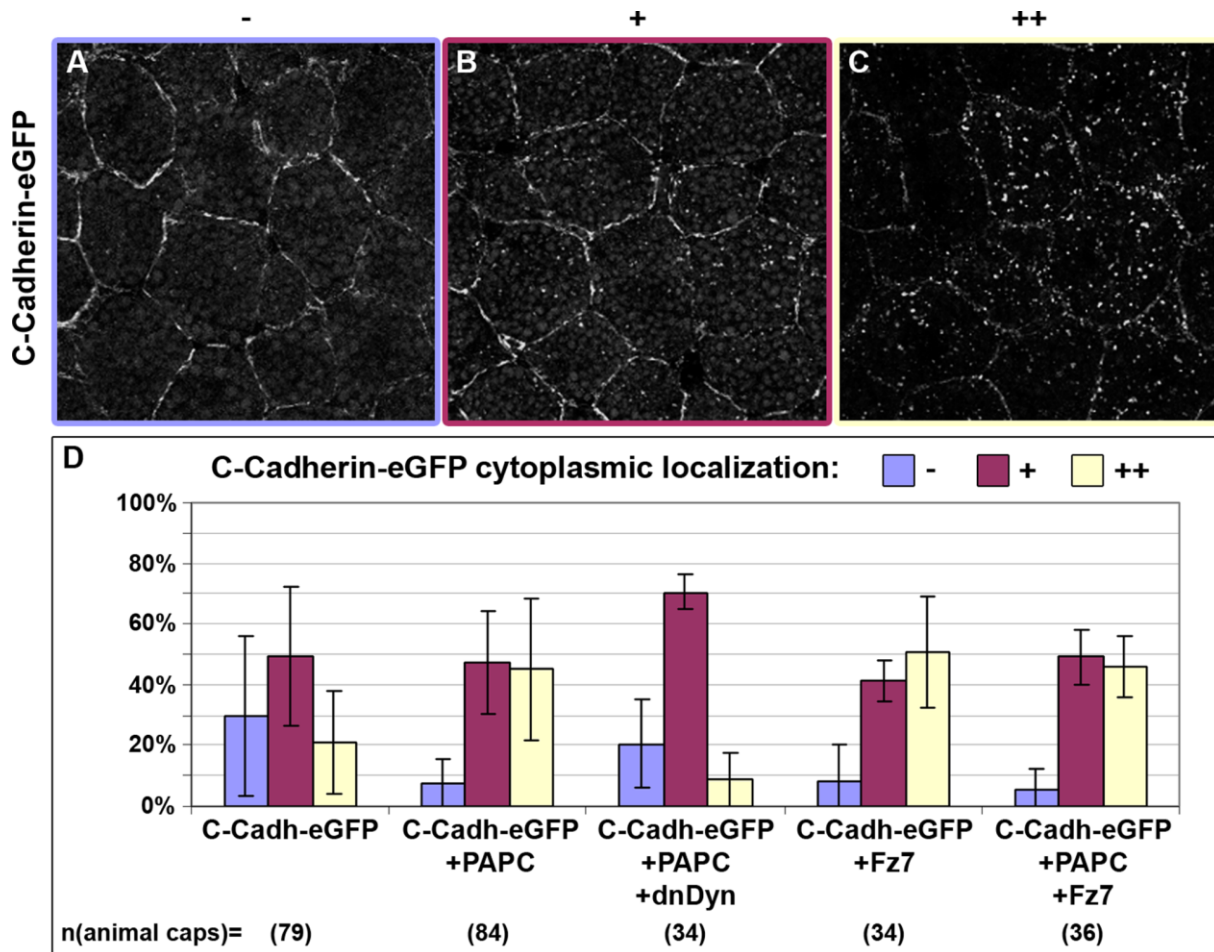


**Fig.19. PAPC increases the number of intracellular C-Cadherin-eGFP spots in animal caps.** Embryos were injected with C-Cadherin-eGFP (1ng) alone or in different combinations with PAPC (500pg), dnDynamin1 (50pg) or Fz7 (500pg). The animal caps were excised and the distribution of C-Cadherin-eGFP was analyzed by confocal microscopy. (A-C) Exemplary animal caps with (A) no cytoplasmic localization of C-Cadherin-eGFP (blue), (B) a weak (magenta) or (C) a strong cytoplasmic localization of C-Cadherin-eGFP (yellow). (D) Summary of experiments. Error bars represent standard deviation.

### 3.2.3 PAPC and C-Cadherin colocalize

When animal caps that expressed C-Cadherin-eGFP and PAPC were stained for PAPC, it was evident that PAPC and C-Cadherin-eGFP colocalized (Fig.20, A-C). Colocalization occurred mostly in punctate structures at the plasma membrane and in the cytoplasm (Fig.20, white arrow heads). C-Cadherin-eGFP was also found alone at the plasma membrane and in some cytoplasmic dots (Fig.20, green arrow heads). PAPC showed a weaker membrane staining and was found mainly in dot-like structures (Fig.20, red arrow heads). The colocalization of PAPC and C-Cadherin-eGFP could indicate that PAPC and C-Cadherin-eGFP are internalized together.

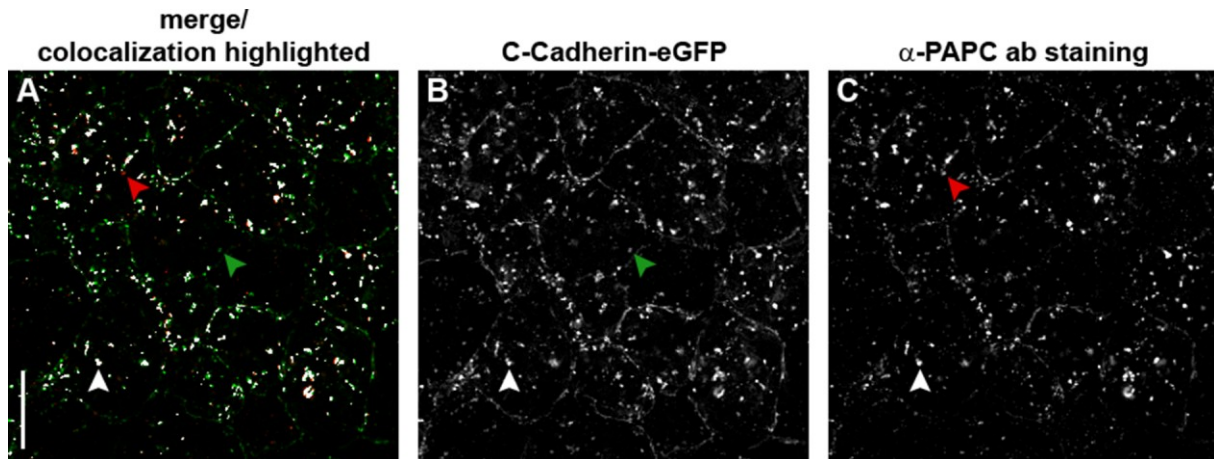


**Fig.20. C-Cadherin-eGFP and P APC colocalize in the dot-like structures.** C-Cadherin-eGFP (1ng) and P APC (500pg) were injected into 4-cell embryos. The animal cap was excised, stained with  $\alpha$ -P APC ab and analyzed by confocal microscopy. Scale bar: 25 $\mu$ m.

### 3.2.4 P APC is internalized with C-Cadherin-eGFP

While analyzing animal caps for C-Cadherin-eGFP and P APC localization, it became evident that C-Cadherin-eGFP and P APC were both internalized to such an extent, that P APC was hardly detectable anymore. P APC, when expressed alone, could be visualized by antibody staining at the cell membrane and in some dot-like structures (Fig.21, B'). C-Cadherin-eGFP alone was also localized clearly to the cell membrane (Fig.21, A). Coexpression of C-Cadherin-eGFP and P APC led to a noticeable reduction of P APC protein at the membrane and to an increase in cytoplasmic C-Cadherin-eGFP (Fig.21, C and C'). It was possible that P APC was still present in the cytoplasm and thus not detectable for the antibody, or that P APC had been degraded inside the cell. When endocytosis was blocked by expressing dnDyn in addition to C-Cadherin-eGFP and P APC, the cells showed again a strong P APC and C-Cadherin-eGFP staining at the cell membranes (Fig.21, D and D'). It was striking that blocking endocytosis promoted a change in cell shape and enhanced the exclusion of both P APC and C-Cadherin-eGFP from points of membrane contact between three or more cells (Fig.21, A and D, B' and D', white arrow heads). This was reminiscent of Dynamin-dependent recycling of adherens junctions during epithelial repacking in *Drosophila* wing tissue (Classen et al., 2005). In this process Dynamin is needed to recycle E-Cadherin from old to newly forming cell junctions. C-Cadherin-eGFP and P APC are thus internalized together in a Dynamin1-dependent manner in animal cap cells.

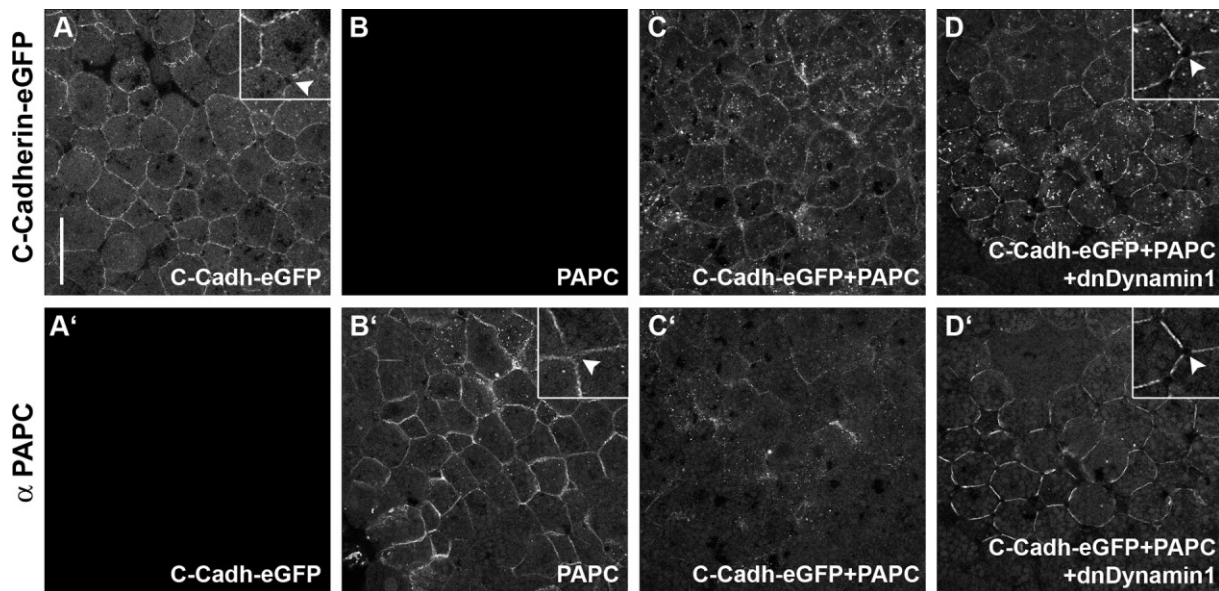


**Fig.21. Blocking endocytosis leads to accumulation of C-Cadherin-eGFP and PAPC at the cell membrane.** Embryos were injected with C-Cadherin-eGFP (1ng) alone or together with PAPC (500pg) or PAPC and dnDynamin1 (500ng). The animal caps were excised and stained with  $\alpha$ -PAPC ab. (A; B) C-Cadherin-eGFP and PAPC are both localized to the cell membranes when expressed alone. (C) Coexpression of PAPC and C-Cadherin-eGFP induces the removal of both C-Cadherin-eGFP and PAPC from the membrane. (D) Blocking endocytosis by overexpression of dnDynamin1 leads to the marked accumulation of C-Cadherin-eGFP and PAPC in the membrane. The contact points between several cells are free of C-Cadherin-eGFP or PAPC (arrow heads). Scale bar: 50 $\mu$ m.

### 3.2.5 PAPC and Fz7 mediate the relocalization of C-Cadherin from the membrane to the cytoplasm

Gain of PAPC function causes the internalization of C-Cadherin-eGFP in animal cap cells. Does this localization depend on the presence of PAPC? To answer this question the localization of C-Cadherin-eGFP was analyzed in cells of the DMZ. Dorsal cells of 4-cell embryos were injected with C-Cadherin-eGFP at the equator region; the DMZ was explanted at early gastrula stage and cultured until early neurula stages. The localization of C-Cadherin-eGFP was analyzed by confocal microscopy. About 45% of control DMZ explants showed a strong cytoplasmic localization of C-Cadherin-eGFP, 42% a weak cytoplasmic localization, and only 10% had none (Fig.22, A-D). When MoPAPC was coinjected together with C-Cadherin-eGFP, cytoplasmic C-Cadherin-eGFP was reduced and the levels of membrane-bound C-Cadherin-eGFP were elevated (Fig.22, D). This effect could be enhanced by knocking down PAPC and Fz7 at the same time. Only 4% of explants showed an

intense cytoplasmic C-Cadherin-eGFP signal, while 60% had a weak cytoplasmic localization, and 36% had none at all (Fig.22, D). These results show that both P APC and Fz7 contribute to internalization of C-Cadherin-eGFP in the DMZ.

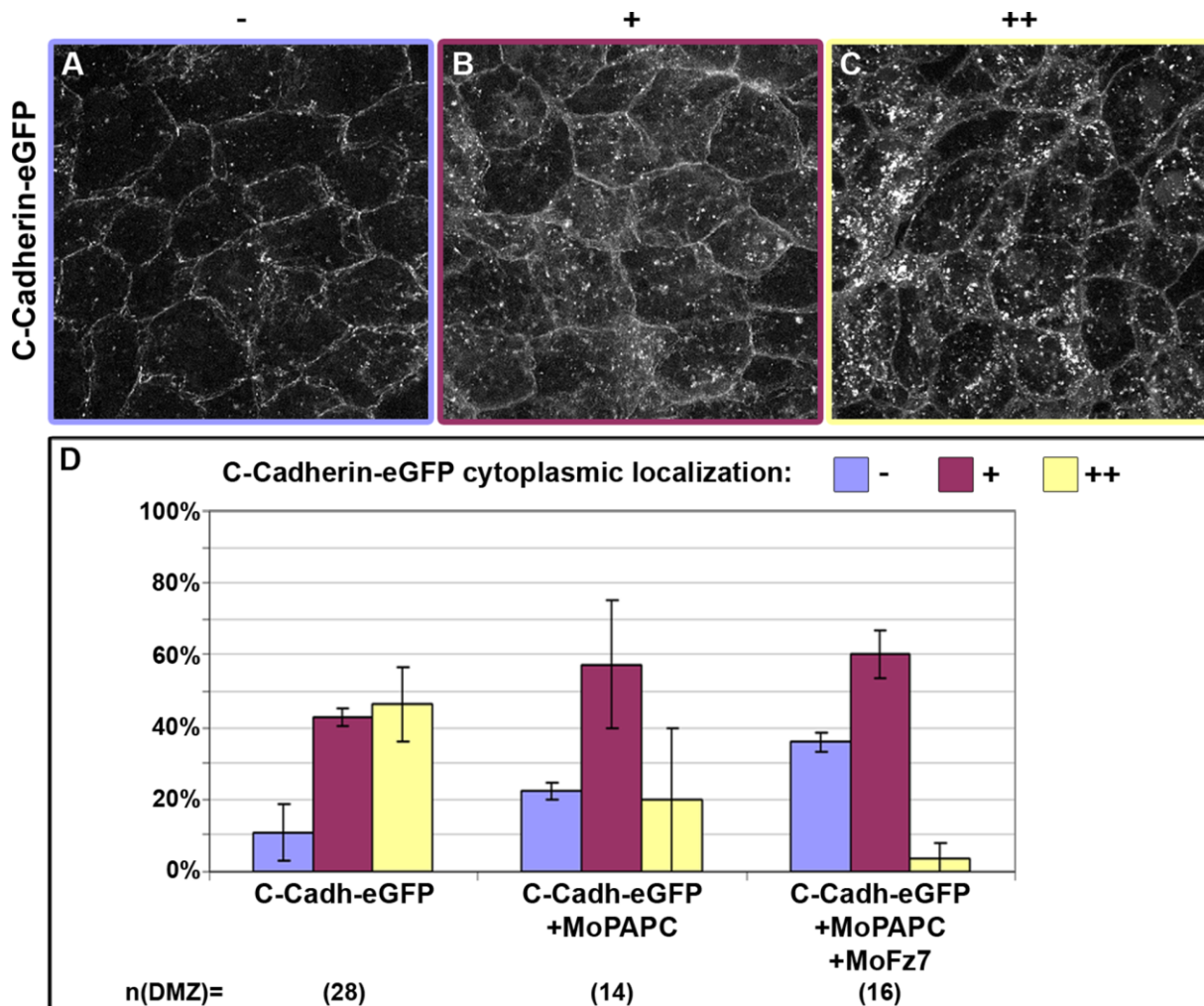


**Fig.22. Formation of intracellular C-Cadherin-eGFP spots depends on P APC and Fz7 function in dorsal mesoderm.** DMZs from embryos injected with C-Cadherin-eGFP (1ng) alone or in combination with MoPAPC (80ng) or MoPAPC and MoFz7 (160ng) were explanted and analyzed by confocal microscopy. The samples were divided into groups with (A) no cytoplasmic C-Cadherin-eGFP localization (blue), (B) a weak (magenta) or (C) a strong cytoplasmic C-Cadherin-eGFP localization (yellow). (D) Summary of experiments. Error bars represent standard deviation.

### 3.2.6 Rab5a, a marker of early endosomes, colocalizes with C-Cadherin

The cytoplasmic localization of C-Cadherin-eGFP depended on P APC and Fz7 in the DMZ. Gain of function experiments indicated that the intracellular distribution of C-Cadherin-eGFP was regulated by endocytosis. In the DMZ, however, the cytosolic C-Cadherin-eGFP pool had not yet been linked to this process. In order to investigate

the connection between internalization of C-Cadherin-eGFP and endocytosis, mCherry-Rab5a, a marker of early endosomes (Bucci et al., 1992; Ogata et al., 2007), was injected with C-Cadherin-eGFP into the DMZ.

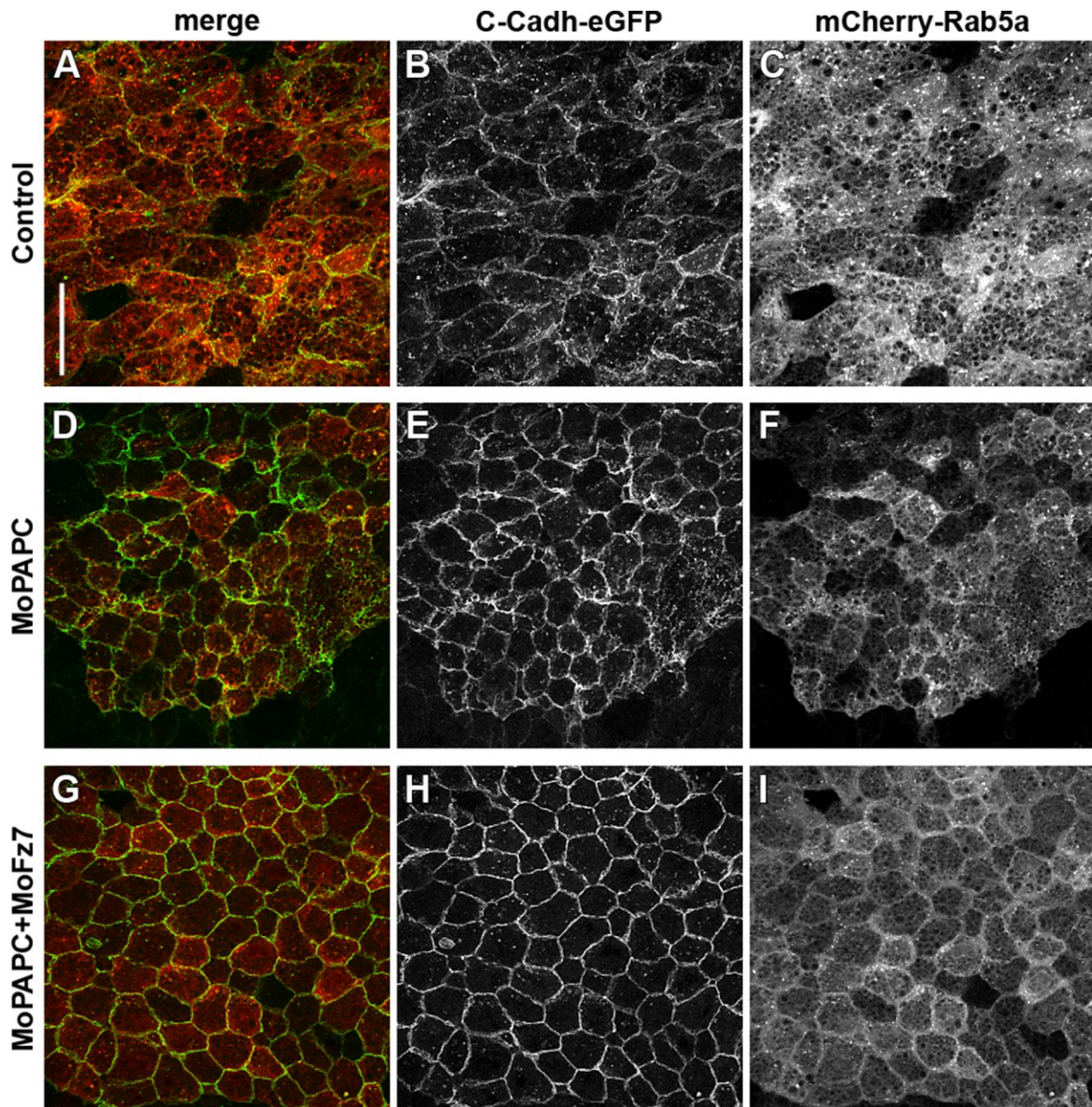


**Fig.23. The localization of C-Cadherin-eGFP and mCherry-Rab5a depend on PAPC and Fz7 in DMZs.** C-Cadherin-eGFP (1ng) and mCherry-Rab5a (1ng) were injected alone or in combination with MoPAPC (80ng) or MoPAPC and MoFz7 (160ng) into the dorsal marginal zone region of 4-cell stage embryos. Localization of the two fluorescent proteins was analyzed by confocal microscopy at early neurula stages.

mCherry-Rab5a showed a disperse cytoplasmic staining with varying intensity. C-Cadherin-eGFP and mCherry-Rab5a colocalized to a great extent at the plasma membrane and in the cytoplasm (Fig.23, A-C). Injection of MoPAPC caused a relocalization of mCherry-Rab5a and C-Cadherin-eGFP to the cell membrane (Fig.23, D-F). The loss of function of both PAPC and Fz7 triggered a pronounced membrane localization of both mCherry-Rab5a and C-Cadherin-eGFP (Fig.23, G-I). This indicates that the intracellular localization of C-Cadherin-eGFP in the DMZ is controlled by endocytosis. These results complement the data from overexpression experiments in animal caps. PAPC and Fz7 are sufficient and necessary to internalize C-Cadherin from the cell membrane to early endosomes in a Dynamin1-dependent manner.

### 3.3 Interaction partners of PAPC

Both gain and loss of function approaches had demonstrated that PAPC and Fz7 prompted the internalization of C-Cadherin-eGFP via endocytosis. But so far, the mechanism behind this internalization had not been addressed. Interestingly, the mouse ortholog of PAPC has been shown to physically interact with N-Cadherin and to trigger the controlled endocytosis of N-Cadherin/PAPC-complexes at the synapse (Yasuda et al., 2007). A similar mechanism could also exist for PAPC and C-Cadherin. The fact that PAPC and C-Cadherin-eGFP colocalized and were internalized together points in that direction. Also, PAPCmut, which is deficient in antagonizing Spry, still mediates cell sorting (Fig.11). It is therefore probable that PAPC modulates C-Cadherin-mediated cell adhesion not via the PCP pathway but via triggering endocytosis by binding directly to C-Cadherin. The role of Fz7 in this process remains unclear. Fz7 could modulate adhesion via the PCP signaling pathway. Tissue separation, for instance, clearly requires the presence of the cytoplasmic tail of Fz7 and can be rescued by activation of PKC $\alpha$  (Winklbauer et al., 2001). But there could also be another way how Fz7 influences cell adhesion. Fz7 might bind directly to C-Cadherin to mediate its endocytosis, either via its extracellular or transmembrane domain. To test these hypotheses, I decided to investigate whether PAPC or Fz7 interact directly with C-Cadherin.

#### 3.3.1 Bimolecular fluorescence complementation

Recently new assays have been developed which allow the detection of protein interaction *in vivo* (Hu et al., 2002; Kerppola, 2008). The two proteins of interest are cloned in frame with the N- or C-terminal half of YFP (named YN or YC). If the proteins interact, the YFP-halves can reconstitute a functional protein, and YFP-fluorescence is detected (Fig.24). This Bimolecular Fluorescence Complementation (BIFC) has been used to visualize the interaction between the transcription factors Jun and Fos in Cos-1 cells (Hu et al., 2002). I wanted to use this method to investigate whether PAPC and Cadherin or Fz7 and Cadherin interact *in vivo*. First I tried to recapitulate the interaction of PAPC and Fz7 with BIFC to test the assay system.

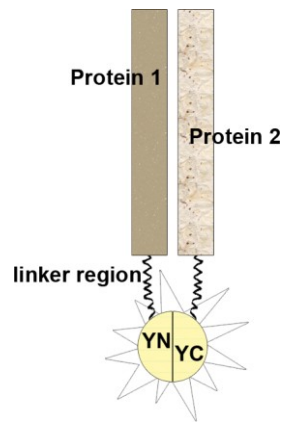


**Fig.24. Schematic drawing of the Bimolecular Fluorescent Complementation (BIFC) principle.**

The proteins of interest are linked to the N- or C-terminal half of YFP via a flexible linker region. If the proteins interact, the YFP-halves reconstitute a functional YFP protein and a fluorescent signal can be detected.

I cloned PAPC-myc and Fz7-myc upstream of YN or YC and expressed the fusion constructs in HEK293 cells. The interaction between Jun and Fos was easily detected, but no complementation between PAPC and Fz7 was visible (data not shown). Several explanations were possible as to why there was no complementation signal: (i) PAPC and Fz7 from different cells interact in trans; (ii) PAPC and Fz7 interact within the same cell but the seven transmembrane-domains of Fz7 sterically hinder the reconstitution of YFP; (iii) PAPC and Fz7 do not interact in cell culture but only in the *Xenopus* embryo. To test the second hypothesis Fz7 was truncated after the first intracellular loop creating Fz7-TM1. Additionally the incubation temperature of the HEK293 cells after transfection was lowered to 30°C because YFP maturation has been described to be sensitive to higher temperatures (Kerppola, 2006; Shyu et al., 2006). Since there was only a faint interaction signal between PAPC and Fz7-TM1, the incubation temperature was lowered again for the following experiments. At 26°C the interaction between Jun and Fos was still normally localized to the nucleus, enriched in the nucleoli (Fig.25, A). As expected, a Fos construct without the interaction interface (Fos $\Delta$ ZIP) did not complement with Jun (data not shown). Transfection of PAPC and Fz7 did not result in the reconstitution of YFP although the proteins were expressed as determined by  $\alpha$ -myc antibody staining (Fig.25, B, and data not shown). This was probably due to the large distance between the cytoplasmic domains of PAPC and Fz7, as the expression of PAPC and the truncated Fz7-TM1 resulted in a fluorescent signal (Fig.25, C). The interaction seemed to take place in the ER and sometimes in round structures of unknown identity.

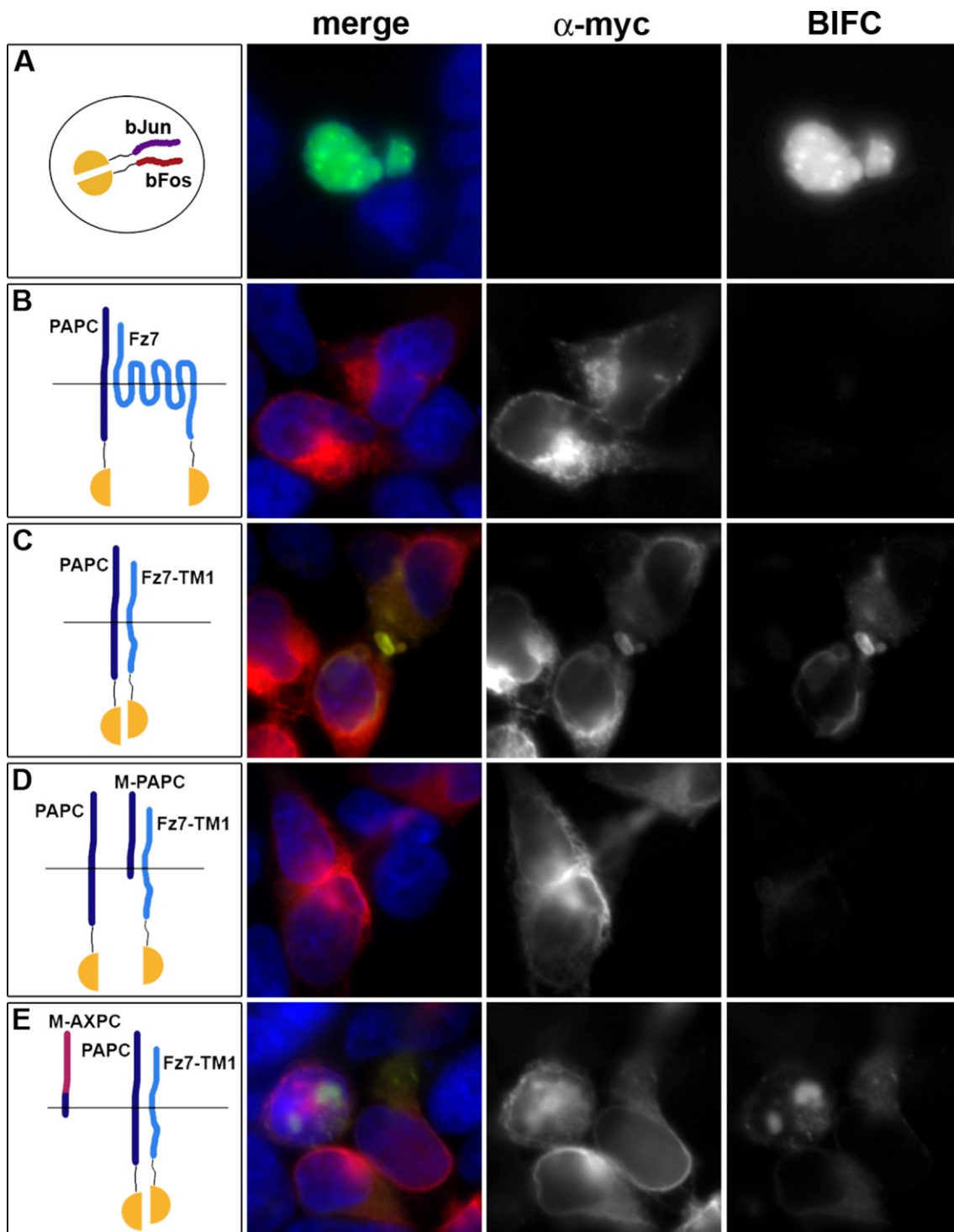


**Fig.25. The interaction of PAPC and Fz7-TM1 can be detected using the BIFC assay.** HEK293 cells were transfected with the constructs indicated in the boxes in (A-E). The cells were fixed and stained with DAPI (blue) and  $\alpha$ -myc ab (red) to localize the constructs. YFP-fluorescence (green, named BIFC in figure) marks the site of protein interaction.

Coexpression of M-PAPC abolished the interaction between PAPC and Fz7-TM1 probably because it competed for binding (Fig.25, D). M-AXPC, the truncated form of the related Axial Protocadherin, which does not interact with Fz7 (Medina et al., 2004), did not interfere with the complementation (Fig.25, E). This shows that BIFC

can be used to show the specific interaction of *Xenopus* transmembrane proteins in HEK293 cells and that PAPC and Fz7 interact *in vivo* in the same cell. Next I wanted to address the question whether PAPC and C-Cadherin interact. Therefore C-Cadherin-myc was used to generate the corresponding BIFC constructs. Overexpression of PAPC and C-Cadherin led to a strong interaction signal in the ER of HEK293 cells (Fig.26, A). When C-Cadherin without YFP-tag was additionally transfected, the fluorescent signal decreased to a great extent (Fig.26, B). By contrast, when Fz7-TM1 and C-Cadherin were expressed together, only a faint signal was detectable (Fig.26, C). In preliminary experiments, C-Cadherin showed stronger complementation with the full length Fz7-BIFC construct than with Fz7-TM1 (data not shown). These data demonstrate for the first time that PAPC and C-Cadherin and Fz7 and C-Cadherin can interact *in vivo*.

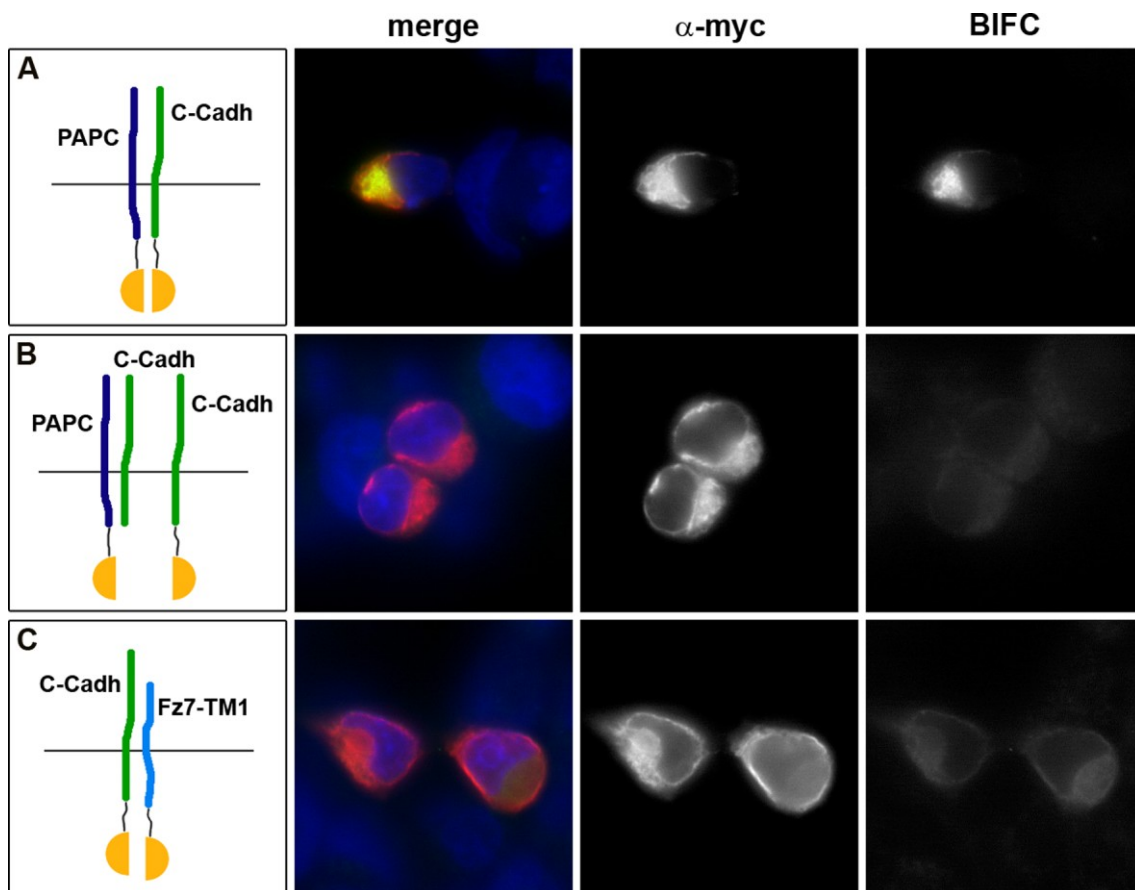


**Fig.26. PAPC and C-Cadherin interact *in vivo*.** HEK293 cells were transfected with the constructs indicated in the boxes in (A-C). The cells were fixed and stained with DAPI (blue) and  $\alpha$ -myc ab (red) to localize the constructs. YFP-fluorescence (green, named BIFC in figure) marks the site of protein interaction.

PAPC and Fz7 interact via their extracellular domains (Medina et al., 2004), yet the domains involved in binding C-Cadherin are not identified. If PAPC interacts with Fz7 and C-Cadherin via the same protein domain, the two proteins could compete for binding to PAPC or, on the contrary, enhance each other's interaction. To address this point, the BIFC constructs of PAPC and Fz7-TM1 were expressed in the absence or presence of untagged C-Cadherin (Fig.27, A and B). Coexpression of C-Cadherin led to a strong complementation signal in round structures (Fig.27, B, arrow head). The increase in signal strength could mean that the interaction between PAPC and Fz7 is intensified in the presence of C-Cadherin, or that the interacting proteins are more restricted to certain domains of the cell. In any case, the presence of C-Cadherin does not impede the interaction of Fz7 with PAPC.

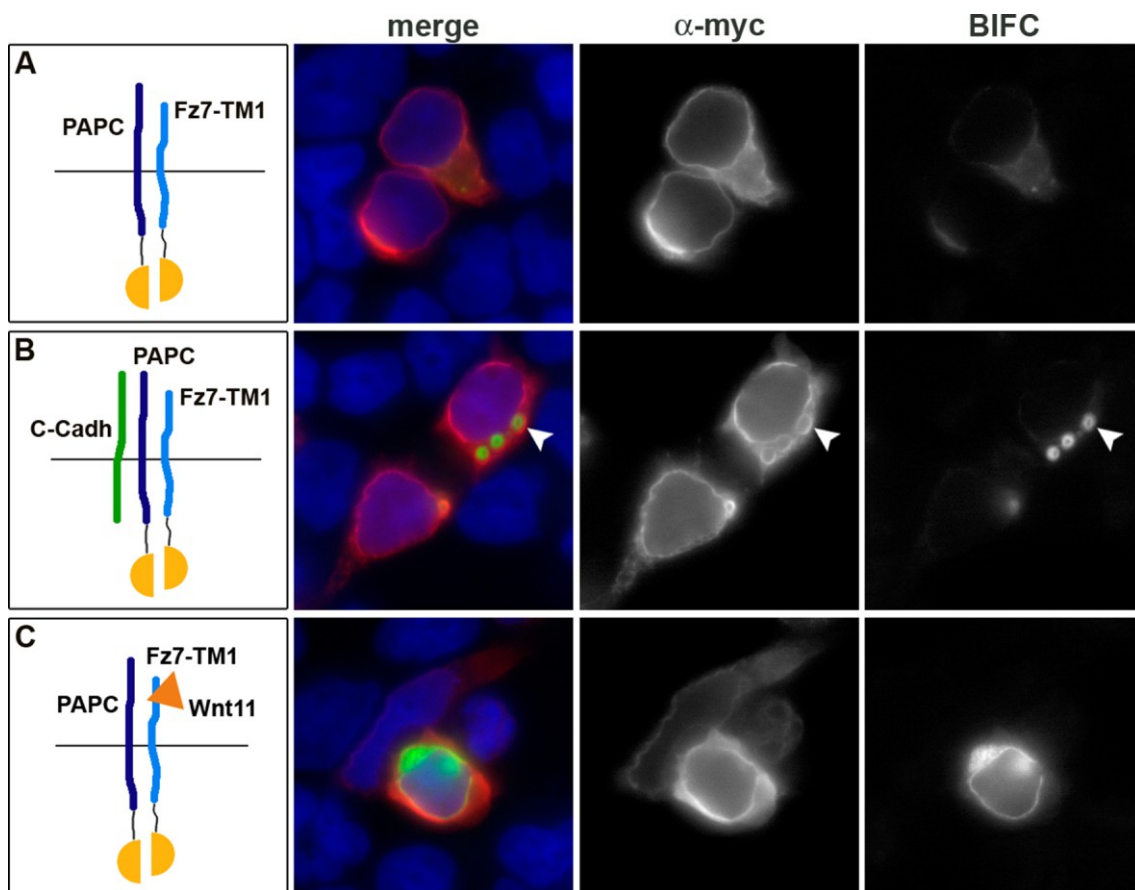


**Fig.27. The interaction between PAPC and Fz7-TM1 can be modulated.** HEK293 cells were transfected with the constructs indicated in the boxes in (A-C). The cells were fixed and stained with DAPI (blue) and  $\alpha$ -myc ab (red) to localize the constructs. YFP-fluorescence (green, named BIFC in figure) marks the site of protein interaction.

Wnt11 has been shown to recruit Fz7 to discrete spots at cell-cell contacts (Witzel et al., 2006; Yamanaka and Nishida, 2007). Does the presence of the ligand change the interaction between PAPC and Fz7? When Wnt11 was transfected with PAPC and

Fz7-TM1 into HEK293 cells, the fluorescence was stronger than in cells without Wnt11 (Fig.27, A and C). In contrast to the cells cotransfected with C-Cadherin, the interaction between PAPC and Fz7-TM1 still seemed to take place in the ER. Therefore, Wnt11 enhances the interaction of PAPC and Fz7 without stimulating a relocalization of the proteins.

The interaction between proteins as detected by BIFC can be quantified. Since the detection of interaction relies on a fluorescent signal, flow cytometry can be used to rapidly analyze large numbers of cells. BIFC coupled to flow cytometry has already been used as a fast screening method for interaction partners in bacteria (Morell et al., 2008). To quantify the interaction between PAPC and Fz7-TM1 I transfected HEK293 cells with the plasmids indicated in Fig.29. The cells were harvested, washed and resuspended in PBS buffer. The cell suspensions had a density of about  $8.2 \times 10^5$  cells/ml. During flow cytometry the side and forward scatter plots of samples were used to gate the cells, so that cell debris and clumps were excluded from further analysis (Fig.28). For each sample 10 000 gated cells were analyzed for frequency of fluorescent signal and signal intensity (Fig.29).

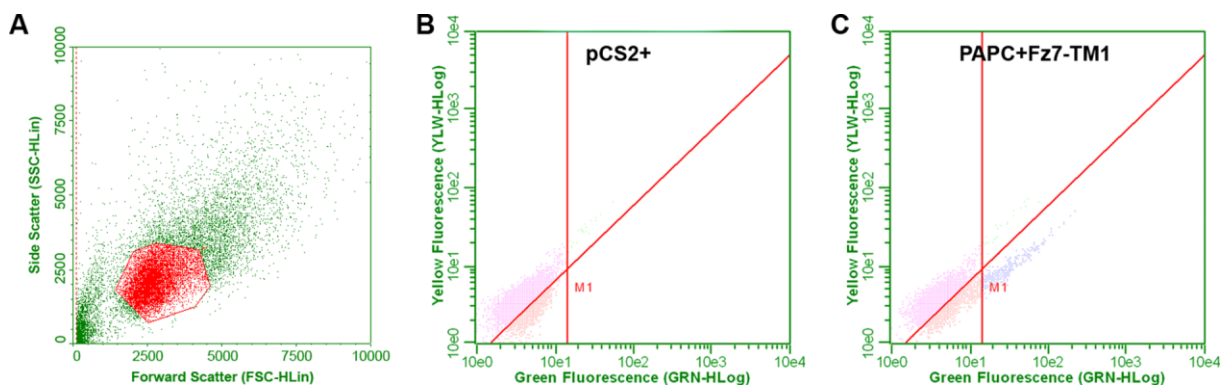


**Fig.28. Example of flow cytometry analysis.** (A) The cells were gated according to their side and forward scatter plot to exclude cell debris and clumps from further analysis. The cells represented in red were analyzed for fluorescence while the ones in green were discarded. (B) Cells transfected with empty vector were used to determine the background level of green fluorescence. (C) The cells in the lower right area (depicted in blue) showed green fluorescence above background level.

Transfection of the empty vector or of constructs with non-complementing YFP-halves did not result in any fluorescent signal (Fig.29, and data not shown). After transfection of the PAPC- and Fz7-TM1-BIFC constructs, about 4% of gated cells

exhibited fluorescence. This number dropped to almost 0% when M-PAPC was cotransfected, while M-AXPC decreased it to 1.7% of cells (Fig.29, blue bars). These data essentially confirm the results I obtained by fluorescence microscopy (Fig.25). But it was surprising to see that M-AXPC led to a partial decrease in interaction frequency. M-AXPC is a hybrid construct which consists of 5 extracellular cadherin-repeats (EC1-5) of AXPC fused to EC6, the transmembrane domain and the 17 intracellular amino acids of M-PAPC (Kim et al., 1998). Coimmunoprecipitation experiments have shown that the secreted form of AXPC (EC1-5) does not interact with Fz7, and therefore it should not compete with PAPC for interaction. EC6 from PAPC, however, might be involved with binding to Fz7, at least to some degree. In contrast to M-PAPC, the presence of C-Cadherin did not change the frequency of interaction between PAPC and Fz7-TM1 (Fig.29), which is in accordance with earlier results (Fig.27). The overall transfection rate was around 9% as judged by the transfection of GFP (data not shown).

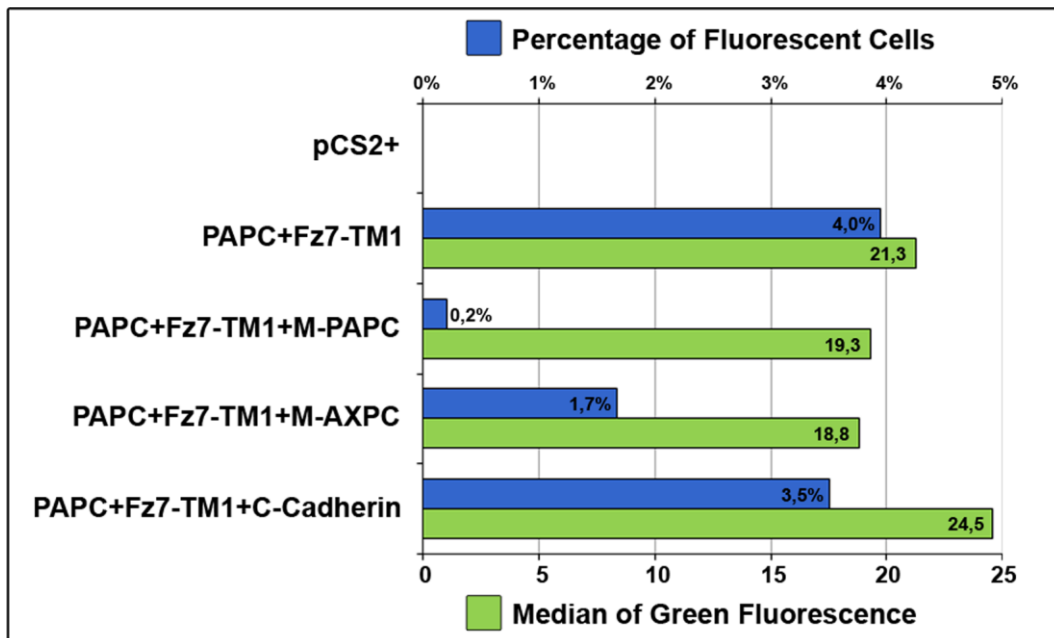


**Fig.29. Frequency and intensity of BIFC signal can be measured by flow cytometry.** HEK293 cells were transfected with empty pCS2+ vector or with the plasmids as indicated. The cells were harvested, washed and analyzed by flow cytometry. The cells were gated according to their side and forward scatter plot. Percentages of fluorescent cells (blue) refer to the number of gated cells. The median of the green fluorescence (green) is measured in relative fluorescent units.

The median of the green fluorescence signal strength did not vary considerably between samples (Fig.29, green bars). It seemed that YFP was either reconstituted or not, but there were no intermediate stages of low fluorescence.

My next goal was to look at the interaction between PAPC and Fz7-TM1 in the *Xenopus* embryo. Therefore I injected the BIFC constructs of these proteins into 4-cell stage embryos, explanted the animal caps, fixed and stained them with  $\alpha$ -myc ab. The samples were analyzed by confocal microscopy. In animal cap cells the proteins were located to the cell membrane and to round vesicular structures close to the membrane (Fig.30). The interaction, as judged by BIFC-signal, took place mainly in these round structures (Fig.30, arrow head). They looked reminiscent of the round particles that formed in HEK293 cells in the presence of C-Cadherin (Fig.27, B, arrow head). C-Cadherin is expressed in the animal cap region at blastula stages (Kühl and Wedlich, 1996) and could be the cause for these structures in the embryo just as in HEK293 cells.

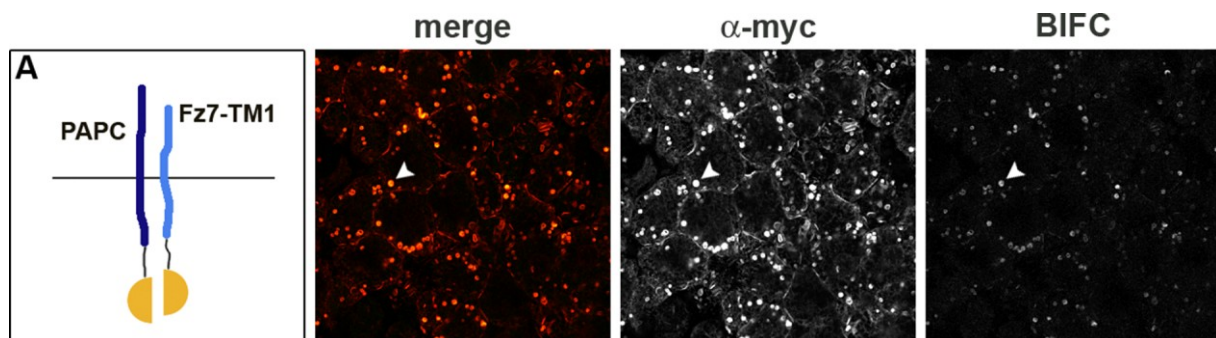


**Fig.30. The interaction between PAPC and Fz7-TM1 can be detected in *Xenopus* using BIFC.** (A) mRNA coding for the BIFC constructs of PAPC and Fz7-TM1 (1ng each) was injected into the animal pole of 4-cell stage embryos. The animal caps were stained with  $\alpha$ -myc ab (red) to localize the constructs. YFP-fluorescence (green, named BIFC in figure) marks the sight of protein interaction.

In summary, I could show that bimolecular fluorescence complementation can be used to investigate protein interactions not only in cell culture but also in *Xenopus* (Table 1). PAPC and Fz7 interact specifically within the same cell. Coexpression of C-Cadherin strengthens the interaction and leads to a relocalization of the interacting complex, while Wnt11 also increases the interaction without affecting its localization. Both PAPC and Fz7 interact with C-Cadherin, but possibly not with the same domains as when interacting with each other.

BIFC constructs	Cotransfection with	Interaction (HEK293)	Interaction ( <i>Xenopus</i> )
<b>bJun+bFos</b>		+	+
<b>bJun+bFos<math>\Delta</math>Zip</b>		-	-
<b>PAPC+Fz7</b>		-	-
<b>PAPC+Fz7-TM1</b>		+	+
	M-PAPC	-	n.d.
	M-AXPC	+	n.d.
	C-Cadherin	+	n.d.
	Wnt11	+	n.d.
<b>PAPC+C-Cadherin</b>		+	n.d.
	C-Cadherin	-	n.d.
<b>Fz7-TM1+C-Cadherin</b>		+	n.d.

**Table 1. Summary of BIFC experiments.**

### 3.3.2 Tissue separation

The interaction between the extracellular domains of PAPC and Fz7 is essential for tissue separation (Medina et al., 2004). And as shown by BIFC assay, PAPC and Fz7 interact within the same cell. A question which remained unresolved was whether the interaction must occur within the same cell to trigger tissue separation. To investigate this issue an *in vitro* separation assay was performed. Cells from embryos injected with PAPC and Fluorescein or Fz7 and Texas Red were dissociated and mixed. The cells were reaggregated and placed on the inner layer of uninjected animal caps. After 45min almost 80% of mixed aggregates had sunk in (Fig.31, A-B', E). In some cases the aggregates did not contain any PAPC-expressing cells and were not counted. This was probably due to the decreased cell adhesion brought about by PAPC. Cells that expressed both PAPC and Fz7 stayed separated from the animal caps (Fig.31, C-E), confirming the published data (Medina et al., 2004). This shows for the first time that the interaction between PAPC and Fz7 from neighboring cells is not enough to induce tissue separation. PAPC and Fz7 must be in the same cell to make the cells separate.

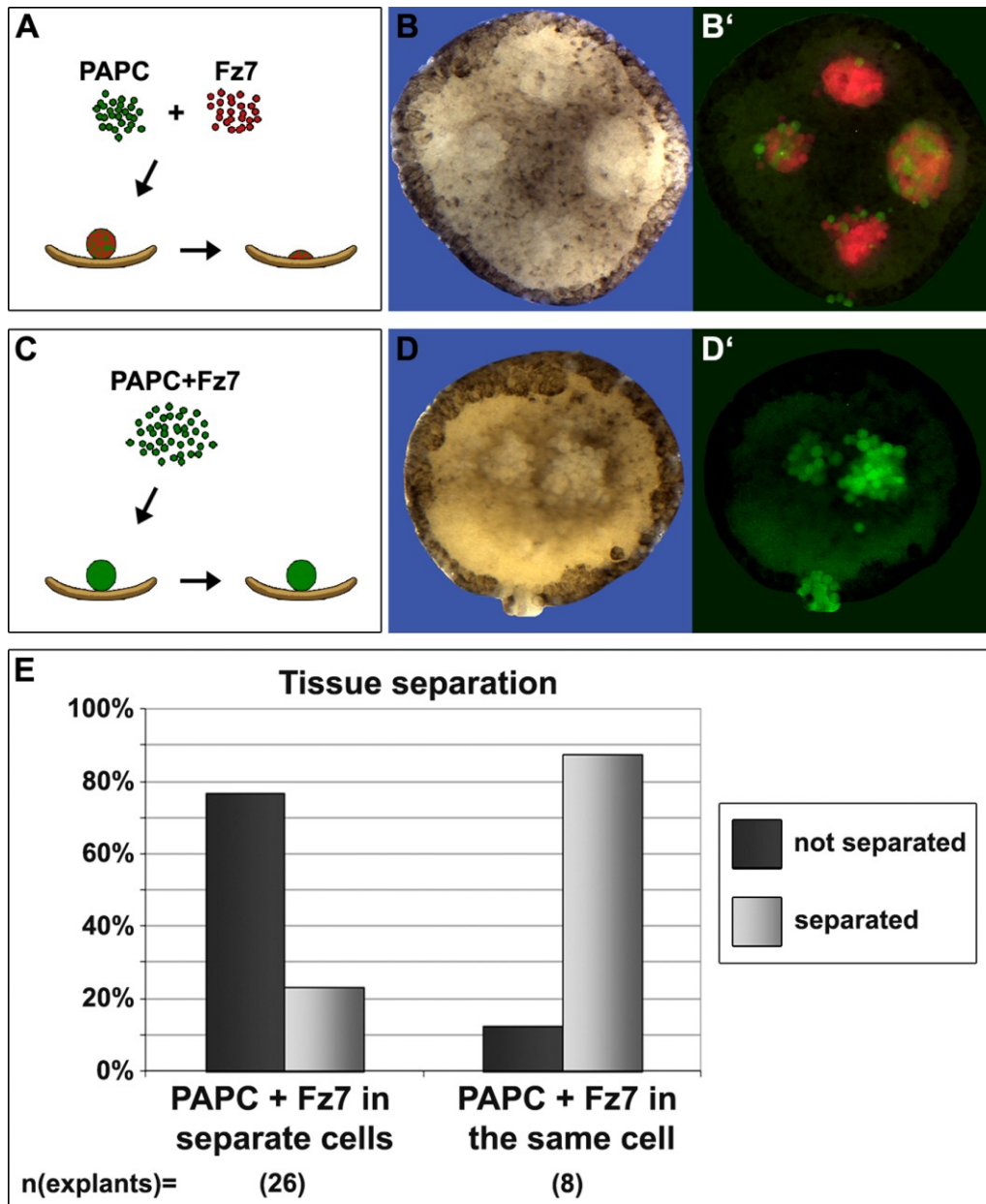


**Fig.31. PAPC and Fz7 must be in the same cell to trigger tissue separation.** (A) Cells from embryos expressing PAPC or Fz7 were mixed and aggregated. The aggregates sunk into the uninjected animal caps. (B, B') Bright field and fluorescent picture of mixed cell-aggregates. (C) Aggregates of cells expressing both PAPC and Fz7 stayed separated from the animal caps. (D, D') Bright field and fluorescent picture of uniform cell-aggregates. (E) Summary of experiments.

### 3.3.3 Functional consequence of the interaction between PAPC, Fz7 and C-Cadherin

Although both PAPC and Fz7 can interact with C-Cadherin as shown by BIFC, the interaction between PAPC and Fz7 is not disrupted by the presence of C-Cadherin. PAPC and Fz7 have each been shown to reduce C-Cadherin-mediated cell adhesion

(Medina et al., 2000; Chen and Gumbiner, 2006), but it is not known whether the two proteins influence cell adhesion jointly. To address this question a reaggregation assay was performed. C-Cadherin is a maternal cadherin and mainly responsible for cell adhesion at early stages (Ginsberg et al., 1991; Heasman et al., 1994b). The zygotic cadherin, E-Cadherin, can be detected in the ectoderm from stage 9,5 onwards but its expression is predominantly in the outer ectodermal layer (Choi and Gumbiner, 1989). Cells of the inner layer of the animal cap were dissociated and reaggregated. After 3h the aggregates were photographed.

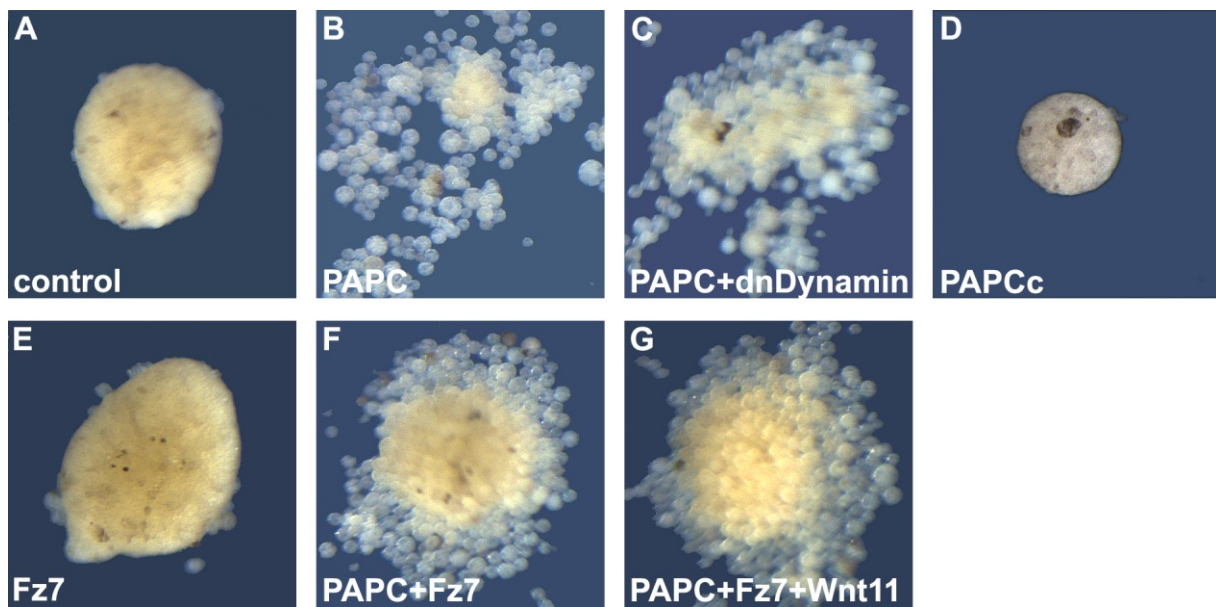


**Fig.32. Fz7 can reverse the loss of adhesion induced by PAPC in dissociated cells.** mRNAs coding for PAPC, dnDynamin1, PAPCc, Fz7 (500pg each) or Wnt11 (10pg) were injected into embryos. The animal cap was excised, dissociated and reaggregated. After 3h the aggregates were analyzed. (A) Control cells form aggregates with sharp borders. (B) Expression of PAPC impedes the aggregation of cells. (C) This effect is not dependent on endocytosis as dnDynamin cannot rescue it. (D) PAPCc-expressing cells reaggregate like control cells. (E) Fz7 does not change the aggregation behavior of cells. (F) Coexpression of Fz7 can partially reverse the PAPC-induced non-aggregation. (G) Wnt11 does not further enhance this effect of Fz7.

Uninjected control cells aggregated to form round spheres in all cases (Fig.32, A). PAPC-expressing cells failed to reaggregate (Fig.32, B), which confirms the results from previous experiments (Chen and Gumbiner, 2006). Surprisingly this defect in reaggregation did not depend on Dynamin-mediated endocytosis (Fig.32, C). PAPCc did not influence the reaggregation behavior unlike in previous dissociation and reassociation experiments (Fig.32, D; Fig.17, F). Cells that expressed Fz7 formed

aggregates just as the control cells (Fig.32, E). Although Fz7 has been shown to reduce cell binding to C-Cadherin matrices (Medina et al., 2000), the reaggregation of blastomeres is never affected (unpublished data). When PAPC and Fz7 were expressed together in animal cap cells, the cells formed aggregates that were loosely structured and left some cells out (Fig.32, F). This means that Fz7 can partially reverse the lack of reaggregation induced by PAPC. Wnt11, which intensified the interaction between PAPC and Fz7 in BIFC assays, did not enhance any further the reaggregation of cells expressing PAPC and Fz7 (Fig.32, G). These results show that PAPC reduces cell reaggregation, and that Fz7 can reverse this effect of PAPC. Endocytosis is not involved in regulating cell reaggregation in this context.

## 4 Discussion

Successful completion of gastrulation movements requires the finely orchestrated interplay of signaling pathways which regulate gene expression and changes in cytoskeleton and cell adhesion. These aspects are delicately intertwined. A new cell fate often results in the activation of signaling pathways which change cellular behavior. On the other hand, structural components of the cell can activate signaling cascades or modulate gene expression directly. The seemingly discrete systems of signaling, gene expression and physical cell properties act in concert to allow for morphogenetic movements to take place.

The protocadherin PAPC is right at the interface of these cell functions. It is involved in signaling, cell adhesion and transcription. PAPC integrates signal input from various sources: its expression is regulated by the transcription factor Xlim1 (Hukriede et al., 2003),  $\beta$ -catenin-dependent Wnt and nodal-related signaling (Wessely et al., 2004), as well as by  $\beta$ -catenin-independent Wnt signaling (Schambony and Wedlich, 2007). PAPC interacts functionally with proteins induced by FGF signaling, such as Spry and ANR5 (Chung et al., 2007; Wang et al., 2008), and the cell adhesion protein C-Cadherin (Chen and Gumbiner, 2006). Furthermore, PAPC modulates the activities of downstream effectors of  $\beta$ -catenin-independent Wnt signaling, such as Rho, Rac and JNK (Medina et al., 2004; Unterseher et al., 2004; Wang et al., 2008), and may even play a role in  $\beta$ -catenin-dependent Wnt signaling and direct regulation of gene transcription (Wang, 2007). How PAPC exerts these functions is largely unknown. An important feature of PAPC function, however, is the physical interaction with other proteins. So far, several interaction partners of PAPC have been identified: the receptor Fz7 interacts with the extracellular domain of PAPC (Medina et al., 2004), while Spry and ANR5 bind to its cytoplasmic domain (Chung et al., 2007; Wang et al., 2008). These interactions are essential for the regulation of tissue separation and convergent extension (Medina et al., 2004; Wang et al., 2008).

In this work several aspects of PAPC protein interaction have been studied. I could show using Bimolecular Fluorescence Complementation (BIFC) that PAPC interacts physically with C-Cadherin (Fig.26). BIFC experiments in combination with functional studies demonstrated that the interaction between PAPC and Fz7 in *cis* is essential for tissue separation (Fig.25, Fig.31). Finally I could provide evidence that PAPC and

Spry bind to each other independently of FGF signaling, and that the putative phosphorylation sites at serines 741/955 of PAPC are essential for this interaction (Fig.10).

#### 4.1 PAPC physically interacts with C-Cadherin

Classical cadherins usually bind to other classical cadherins. Cadherin-mediated adhesion is initiated by lateral, parallel *cis*-dimerization followed by an antiparallel adhesive *trans* contact of *cis*-dimers on opposing cells (Halbleib and Nelson, 2006). There are still controversies concerning the domains involved, the contact sites, and the specificity of interactions among members of the same cadherin subfamily (Ahrens et al., 2002). Protocadherins, on the other hand, form *cis*-homodimers and *cis*-heterodimers (Murata et al., 2004; Hamsch et al., 2005; Triana-Baltzer and Blank, 2006). No direct link between oligomerization and protocadherin function has been established so far (Chen et al., 2007).

Despite their similar extracellular (EC) domain structure, a  $\beta$ -sandwich composed of 7  $\beta$ -strands, it seems unlikely that classical cadherins and protocadherins could interact (Morishita and Yagi, 2007). Protocadherins lack the conserved tryptophan residue and the corresponding hydrophobic pocket to accommodate it, both of which seem to be indispensable for cadherin dimerization (Patel et al., 2003; Morishita and Yagi, 2007). Furthermore, protocadherins contain numerous conserved cysteines in their EC domains, which are crucial for their oligomerization, but which are absent in classical cadherins (Murata et al., 2004; Chen et al., 2007).

Yet when PAPC and C-Cadherin were expressed together as BIFC-fusion proteins in HEK293 cells, they interacted as judged by the strong YFP-signal (Fig.26). Expression of untagged C-Cadherin together with these constructs suppressed the interaction probably by competing for binding to PAPC (Fig.26). If PAPC interacts with C-Cadherin in the embryo, the proteins should have overlapping localization patterns. This was the case. In animal cap cells PAPC and C-Cadherin colocalized to a large extent when both proteins were overexpressed (Fig.20). Therefore I propose that PAPC and C-Cadherin interact and that the mechanism of interaction is different from the dimerization observed in both protein families.

#### 4.1.1 Localization of interaction

The interaction between PAPC and C-Cadherin took place mainly in a perinuclear compartment which might correspond to the ER or Golgi (Fig.26). This intracellular compartment could be identified by costaining ER and Golgi marker proteins. Why PAPC and C-Cadherin interact mainly in intracellular compartments instead of at the cell membrane could have several reasons. The fusion proteins could be trapped in the ER/Golgi as a consequence of the overexpression. In this case the strong intracellular interaction signal would not allow the detection of faint fluorescence from the cell membrane. Another reason could be that protocadherin transport from intracellular compartments to the cell membrane is regulated (Murata et al., 2004). Pcdh $\alpha$  expressed in cultured cells and Pcdh $\gamma$  *in vivo* are largely retained in intracellular compartments such as the ER, Golgi, and tubulovesicular structures (Phillips et al., 2003; Murata et al., 2004). Only at points of cell contact protocadherins seem to be stabilized (Triana-Baltzer and Blank, 2006). The same has been observed for PAPC (unpublished data). The main localization of the interaction between PAPC and other proteins in intracellular compartments might therefore reflect the absence of membrane transport cues in HEK293 or other cell lines.

## 4.2 Binding between PAPC and C-Cadherin reduces cell adhesion

It was evident from both gain and loss of function experiments that PAPC caused the relocalization of C-Cadherin from the plasma membrane to intracellular structures (Fig.19, Fig.22). As a matter of fact, PAPC was internalized together with C-Cadherin in a Dynamin1-dependent process (Fig.21). Therefore I propose that PAPC binds to C-Cadherin, and the two proteins are endocytosed together. Support of this idea comes from the rat/mouse ortholog of PAPC, which has recently been shown to bind to N-Cadherin and to trigger the controlled endocytosis of the N-Cadherin/PAPC-complex in hippocampal neurons (Yasuda et al., 2007).

#### 4.2.1 Endocytosis and cell adhesion

On a functional level, PAPC decreases C-Cadherin-mediated adhesion. This has been demonstrated by plating single cells onto a C-Cadherin matrix or by reaggregating dissociated cells (Chen and Gumbiner, 2006). I could confirm these

results; dissociated animal cap cells expressing PAPC failed to reaggregate (Fig.32). Endocytosis of C-Cadherin would be a simple way to decrease cell adhesion, but endocytosis is not necessarily involved. Binding between PAPC and C-Cadherin at the cell surface could be sufficient to block the adhesive function of C-Cadherin, possibly by interfering with *cis*- or *trans*-clustering of C-Cadherin. Supporting evidence comes from reaggregation experiments in which blocking endocytosis did not reverse the loss of adhesion induced by PAPC (Fig.32). The fact that a specific activating antibody targeting C-Cadherin can undo the effect of PAPC on adhesion points in the same direction (Zhong et al., 1999; Chen and Gumbiner, 2006). Endocytosis of PAPC/C-Cadherin might be a regulatory mechanism to release the block on cell adhesion. In this model the regulated availability of PAPC at the cell surface would control C-Cadherin mediated cell adhesion. Endocytosis would be a consequence but not the cause of decreased cell adhesion.

What happens to PAPC and C-Cadherin after being endocytosed is not clear. The proteins could be retained intracellularly, recycled back to the cell surface or degraded, either together or individually (Bryant and Stow, 2004). Data from the PAPC rat/mouse ortholog show that while the amount of PAPC and N-Cadherin at the cell surface decreases, the total amount remains the same (Yasuda et al., 2007). This argues against protein degradation playing a substantial role in the regulation of PAPC or the bound cadherin.

#### 4.2.2 Tissue versus single cells

In *Xenopus*, both cell surface and total level of C-Cadherin are unchanged upon expression of PAPC, although cell adhesion is inhibited (Chen and Gumbiner, 2006). This led to the initial assumption that PAPC modulated C-Cadherin-mediated adhesion not through endocytosis but via another, yet unknown mechanism (Chen and Gumbiner, 2006). But although endocytosis might not be necessary to decrease C-Cadherin-mediated adhesion, as discussed above, it most certainly took place when PAPC and C-Cadherin were expressed together (Fig.19, Fig.21). The use of different experimental approaches could explain these apparently contradictory data; for some experiments cells forming a tissue were used, and for others single cells. In the case of mouse PAPC and N-Cadherin, endocytosis is strongly enhanced when PAPC interacts *in trans* with other PAPC molecules (Yasuda et al., 2007). Endocytosis can therefore be triggered by adding secreted PAPC extracellular

domains or  $\alpha$ -PAPC antibodies to the medium (Yasuda et al., 2007). If the same held true for PAPC and C-Cadherin, PAPC would decrease cell adhesion in both intact tissues and single cells by binding to C-Cadherin, but endocytosis would only take place in tissues where a *trans* PAPC-PAPC interaction was possible. To investigate this point one could try to show reduction of surface C-Cadherin in the presence of PAPC in animal cap tissue, or trigger endocytosis of C-Cadherin/PAPC with recombinant PAPC EC domains in single cells.

### 4.3 Regulators of cell adhesion

C-Cadherin is not the only protein known to interact with PAPC (Medina et al., 2004; Chung et al., 2007; Wang, 2007; Wang et al., 2008). Some of PAPC's other interaction partners also modulate cell adhesion (Fig.6), but it has not been investigated how.

**Spry**, a cytoplasmic interaction partner of PAPC, negatively regulates tissue separation and convergent extension movements (Wang et al., 2008). For this function Spry blocks  $\beta$ -catenin-independent Wnt signaling downstream of Fz7 (Wang et al., 2008). It does not have an effect on cell adhesion via PAPC; a PAPC mutant which cannot bind Spry has the same cell sorting abilities as wild type PAPC (Fig.10, Fig.11). Another cytoplasmic protein, **ANR5**, also interacts with PAPC, and both are necessary for tissue separation (Chung et al., 2007). In reaggregation experiments using dissociated DMZ cells, ANR5 loss of function suppresses cell reaggregation (Chung et al., 2007), but the connection between ANR5 and adhesion has not been investigated so far.

The receptor **Fz7**, which interacts with PAPC via the extracellular domain, is also involved in regulating tissue separation and convergent extension (Djiane et al., 2000; Medina et al., 2000; Winklbauer et al., 2001; Medina et al., 2004). Regarding the influence of Fz7 on cell adhesion, contradictory results have been published. One report has shown that overexpression of Fz7 decreases cell adhesion to C-Cadherin by 50%, while another one failed to detect any effect using both gain and loss of function experiments (Medina et al., 2000; Chen and Gumbiner, 2006). Thus the effects observed upon Fz7 manipulation have been largely attributed to its function in Wnt signaling. In this work, I could show using the BIFC assay that Fz7 interacted

with C-Cadherin in HEK293 cells (Fig.26). In the embryo, Fz7 induced the internalization of overexpressed C-Cadherin from the cell membrane, just as PAPC did (Fig.19, Fig.22). Yet in functional experiments, Fz7 did not influence the reaggregation of dissociated animal cap cells (Fig.32). Therefore I conclude that Fz7 binds to C-Cadherin and induces its endocytosis without affecting C-Cadherin-mediated cell adhesion. Nevertheless, Fz7 was able to antagonize the effect which PAPC had on adhesion and partially rescued cell reaggregation (Fig.32). There are several possibilities to explain the role of Fz7 in this process. (i) Binding of Fz7 could be necessary for endocytosis of non-adhesive PAPC/C-Cadherin-complexes. Expression of Fz7 would therefore facilitate cell adhesion mediated by unbound C-Cadherin. (ii) Interaction with Fz7 could separate PAPC from C-Cadherin, thus promoting C-Cadherin dimerization and cell adhesion. (iii) The interaction between Fz7 and PAPC could allow intracellular regulators to bind or modify PAPC, thereby modulating its effect on cell adhesion. (iv) Fz7 could modify cell adhesion by modulating the cytoskeleton via PCP signaling independently of PAPC.

It is clearly difficult to separate the functions of Fz7.  $\Delta$ C-Fz7, which lacks the cytoplasmic tail, could not decrease the cell sorting activity of PAPC when both proteins were overexpressed (Chen and Gumbiner, 2006). The cytoplasmic tail of Fz7 is necessary for its signaling activities (Medina et al., 2000; Medina and Steinbeisser, 2000; Sumanas et al., 2000) (Fig.12), emphasizing the dual character of Fz7 function. To investigate the role of the different Fz7 domains further, it could be tested whether  $\Delta$ NFz7, which lacks the extracellular domain and is not expected to interact with PAPC, could still antagonize PAPC function in downregulating cell adhesion. In any case, both the extracellular and cytoplasmic domains are necessary for Fz7-dependent tissue separation. In contrast to full length Fz7 the deletion constructs are both unable to induce tissue separation in animal cap tissue in the presence of FGF (Medina et al., 2000).

In zebrafish **Wnt11**, a ligand of Fz7, increases cell adhesion by inducing the Rab5c-mediated endocytosis of E-Cadherin (Ulrich et al., 2005). Additionally Wnt11 accumulates Fz7 at certain membrane micro domains, which display increased cell contact persistence (Witzel et al., 2006). In *Xenopus* the effect of Wnt11 on C-Cadherin localization has not yet been tested. But the reaggregation of dissociated animal cap cells expressing PAPC and Fz7 was not enhanced by coexpression of

Wnt11 (Fig.32). The role of Wnt11 in regulating C-Cadherin-mediated cell adhesion remains therefore to be investigated.

#### 4.4 Tissue separation

The regulation of tissue separation combines several of the aspects of cell adhesion and signaling discussed above (Steinbeisser, 2007). Downregulation of maternal cadherin activity is a necessary step for cells in order to stay separated from the ectoderm (Wacker et al., 2000). On the other hand, tissue separation can be rescued after Fz7 or PAPC loss of function approaches by expressing certain downstream signaling components (Winklbauer et al., 2001; Medina et al., 2004).

It was published that both Fz7 and PAPC, and especially the interaction of their extracellular domains, are necessary for the establishment of tissue separation (Winklbauer et al., 2001; Medina et al., 2004). In this work I could show that Fz7 and PAPC interacted in *cis*, and that this interaction within the same cell was essential for tissue separation (Fig.25, Fig.31). Therefore Fz7 and PAPC do not act as ligand and receptor across cell boundaries, but modulate simultaneously cell adhesion and parallel signaling pathways inside the same cell.

If the interaction between PAPC and Fz7 is so vital for tissue separation, can it be modulated by other proteins? C-Cadherin, which interacts with both PAPC and Fz7, could theoretically disrupt the interaction between the two proteins, or it could become part of a ternary PAPC/Fz7/C-Cadherin-complex. The latter seems to be the case. In HEK293 cells the coexpression of C-Cadherin did not impede the interaction between Fz7 and PAPC, but changed its localization (Fig.27). PAPC and C-Cadherin probably interact each with different domains of Fz7. PAPC binds to Fz7 via their extracellular domains (Medina et al., 2004). Fluorescent complementation between PAPC and Fz7 could only be detected using a truncated form of Fz7, which retains the first of seven transmembrane domains (Fig.25). The full length Fz7-BIFC construct might sterically impede the interaction of PAPC with the C-terminally-fused YFP while binding to the Fz7 extracellular domain. C-Cadherin, on the other hand, interacted more strongly with the wild type than the truncated receptor in preliminary experiments, pointing to an interaction site closer to the C-terminal end of Fz7 (data not shown). Wnt11, which can accumulate Fz7 at certain membrane micro domains

(Witzel et al., 2006; Yamanaka and Nishida, 2007; Kim et al., 2008), enhanced the interaction between Fz7 and PAPC without affecting its localization (Fig.27). The stronger fluorescent signal could be due to increased or stabilized interaction. Which influence C-Cadherin and Wnt11 exert on tissue separation induced by PAPC and Fz7 is still to be addressed in future experiments.

#### 4.5 Model of dynamic cell adhesion

During gastrulation the dorsal mesoderm undergoes massive cell rearrangements due to intercalation. Medial and lateral protrusions appear to exert traction on adjacent cells, and generate tension in the mediolateral axis (Keller et al., 2003). The cells are held together by many small contact points along their elongated sides, which are constantly being made and broken (Fig.33, green dots). On the whole, a large number of these adhesions lock the cells into a rigid array, but locally, periodic breakdown of these adhesions allows local shearing of cells past one another (Keller et al., 2003).

PAPC is the ideal candidate to execute this dynamic adhesion. It is expressed in the mesoderm during gastrulation (Kim et al., 1998). The intracellular localization of PAPC in vesicular structures is very dynamic (unpublished observations); only at the tips of elongated mesoderm cells PAPC is stable (Unterseher et al., 2004; Chung et al., 2007). PAPC binds C-Cadherin (Fig.26) and reduces its adhesive properties (Fig.32). Furthermore, PAPC is necessary and sufficient to cause the endocytosis of C-Cadherin (Fig.19, Fig.22, and Fig.23).

I therefore propose that PAPC is transported to the cell membrane, where it binds to C-Cadherin. The interaction between PAPC and C-Cadherin decreases C-Cadherin-mediated adhesion. Upon interaction with another PAPC in *trans*, the PAPC/C-Cadherin-complex is internalized via endocytosis. C-Cadherin is recycled back to the membrane restoring adhesion locally. At the tips of elongated cells, PAPC is stabilized, while C-Cadherin-mediated adhesion is restored.

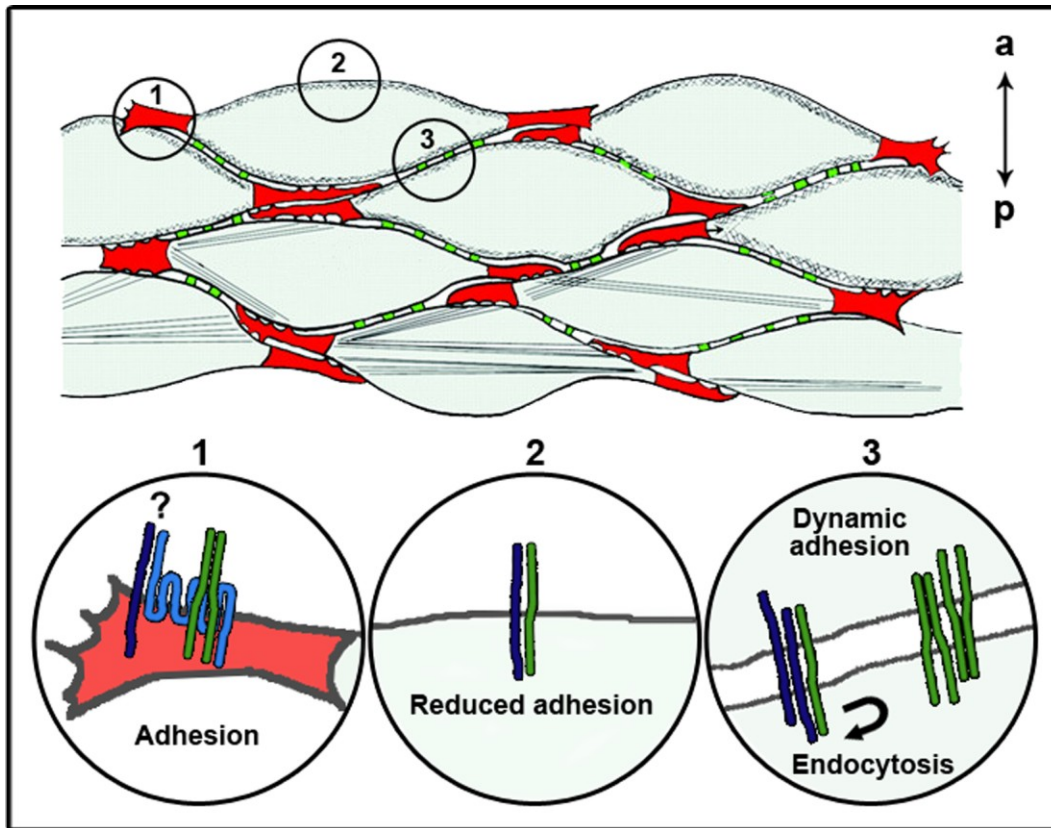


**Fig.33. Model of dynamic cell adhesion in dorsal mesoderm cells.** (1) At the tips of elongated cells, PAPP (navy blue) is stabilized by Fz7 (cyan) or other unidentified factors, while adhesive activity via C-Cadherin (green) takes place. (2) Along the anterior and posterior sides of the cell, C-Cadherin-mediated binding is reduced by the interaction between PAPP and C-Cadherin. (3) The non-adhesive complexes of PAPP and C-Cadherin are internalized upon binding to other PAPP molecules in *trans*. Adhesion is restored by C-Cadherin oligomers. a, anterior; p, posterior. Picture adapted from Keller et al. (2003).

This model would allow for dynamic regulation of cell adhesion along the anterior and posterior sides of the cell (Fig.33, 2 and 3), while maintaining adhesive protrusions at the medial and lateral tips (Fig.33, 1). The function of PAPP could be fine-tuned by intracellular proteins, like kinases and other interaction partners. Additionally, extracellular binding partners could confer binding specificity or stabilize PAPP at certain membrane domains in analogy to the asymmetrically localized PCP components in the fly (Strutt, 2008).

The roles of Fz7 and Wnt11 in the process of dynamic adhesion are not clear yet. Wnt11 could accumulate Fz7 at the tips of mesodermal cells (Witzel et al., 2006), where Fz7 would cluster with and stabilize other Fz7 molecules in *trans* (Yamanaka and Nishida, 2007). Via its interaction with Fz7 PAPP could be stabilized at the tips

as well. Questions to be addressed are what distinguishes the tip region of the cell, and how is the adhesive activity regulated there.

## 4.6 Additional roles of P APC

### 4.6.1 Signal transduction

Not all of the functions of P APC involve the regulation of cell adhesion. P APC is also part of  $\beta$ -catenin-independent Wnt-signaling and can modulate the activities of downstream signaling components such as Rac, Rho and JNK (Medina et al., 2004; Unterseher et al., 2004). Recruitment of the adaptor protein dsh to the cell membrane is a necessary step in the activation of PCP signaling (Axelrod et al., 1998; Park et al., 2005). Expression of Fz7, but not of  $\Delta$ C-Fz7, resulted in membrane recruitment of dsh-GFP (Fig.12), which is in agreement with previously published data (Medina and Steinbeisser, 2000). P APC did not recruit dsh-GFP to the cell membrane (Fig.12). When P APC and  $\Delta$ C-Fz7 were coexpressed, P APC did not cause membrane translocation of dsh-GFP either, even though it could interact extracellularly with  $\Delta$ C-Fz7 (Fig.12). Thus, P APC is not a direct activator of PCP signaling via dsh. The interaction between P APC and Fz7 does not function as a switch to activate the signaling activities of P APC. Instead, P APC antagonized the inhibitor of  $\beta$ -catenin-independent Wnt-signaling, Spry, by binding to it (Fig.10). This interaction released the block Spry exerts on the activation of dsh, PKC $\delta$  and Rho, allowing gastrulation movements to take place (Wang et al., 2008). Spry serves as an interface through which FGF signaling can feed into the PCP signal pathway (Nutt et al., 2001; Sivak et al., 2005; Wang et al., 2008). Nevertheless, the interaction and thus the antagonism between P APC and Spry were independent of FGF signaling (Fig.9, Fig.10).

The small GTPase Rho is an important regulator of a variety of cellular functions, including the dynamics of the actin cytoskeleton, cell adhesion, transcription, cell growth and membrane trafficking (Wunnenberg-Stapleton et al., 1999). Both dominant negative and constitutively active forms of Rho disrupt gastrulation of *Xenopus* embryos (Tahinci and Symes, 2003). The activation of Rho in the dorsal mesoderm depended on P APC function (Fig.7). Many of the effects observed upon P APC loss of function can be attributed to a loss of Rho activation. Knock-down of P APC in DMZ explants impaired cell elongation with cells retaining a round cell

shape (Fig.15). This is in line with results showing that the expression of dominant negative Rho induces a round cell shape in the mesoderm (Tahinci and Symes, 2003). The establishment of a bipolar morphology is a result of the extension of cytoplasmic protrusions, such as lamellipodia in a mediolateral direction (Shih and Keller, 1992; Wallingford et al., 2000). Both activation or inhibition of Rho disturb the normal bipolar pattern of cytoplasmic protrusions, creating a more even distribution of protrusions between the cells' elongated and short sides (Tahinci and Symes, 2003). This may explain why coinjection of PAPC did not rescue the loss of function phenotype (Fig.15), as the regulation of cell shape requires such a delicate balance of Rho signaling.

PAPC has been shown by independent groups to be localized mainly to the tips of elongated cells (Unterseher et al., 2004; Chung et al., 2007). There PAPC could activate Rho locally to promote protrusive activity in mediolateral directions. Staining endogenous activated Rho *in situ* I could detect it enriched at the tips of mesodermal cells (Fig.8). Unfortunately the cell elongation was not robust at early gastrulation stages, when PAPC is expressed according to *in situ* hybridization (Kim et al., 1998). Therefore I could not analyze whether the localization of activated Rho depended on PAPC. Nevertheless, the overall activation status of Rho was PAPC-dependent.

Loss of Rho leads to a reduction of cell protrusions at the tips of elongated cells (Tahinci and Symes, 2003). Thus the mesodermal cells could remain round after PAPC loss of function because lacking the protrusions, they could not be able to exert traction on their neighbors anymore. Another possibility would be that the cells have lost their sense of direction, or polar identity. This seems to be the case. After knock-down of PAPC, the polarity marker PKC $\lambda$  fails to localize to specific membrane sub domains (Fig.16). Besides regulating cell adhesion in the mesoderm, PAPC activates Rho in an indirect manner by antagonizing Spry. PAPC confers polar identity on the mesoderm cells which enables them to elongate.

#### 4.6.2 Gene transcription

In addition to the immediate morphological remodeling described above, PAPC might also induce long-term changes by regulating gene transcription. Protocadherins are subject to regulated Presenilin-dependent intramembrane proteolysis, during which

the extracellular and the intracellular domains are successively released (Haas et al., 2005; Hamsch et al., 2005; Bonn et al., 2007). The intracellular domain localizes to the nucleus and can activate transcription (Hamsch et al., 2005; Bonn et al., 2007). In a yeast-two-hybrid-screen several transcription factors were identified as interaction partners of PAPCc (Wang, 2007). Although they were considered to be false positives (Wang, 2007), other unpublished results from our lab suggest that PAPC indeed regulates transcription. Consistent with a Presenilin-dependent intramembrane proteolysis of PAPC, I could detect C-terminal PAPC fragments of 60kDa and 50kDa in oocyte and embryo lysates (Fig.13). These fragments may correspond to PAPC after sequential matrix metallo-protease and  $\gamma$ -secretase proteolysis, generating  $\Delta$ N-PAPC and then releasing the cytoplasmic fragment. But the identity of these fragments remains uncertain. In the case of Protocadherin $\alpha$ 4 the difference in size between the fragments after extracellular and intramembrane cleavage is just 4kDa, and the smaller fragment is not stable (Bonn et al., 2007). It is possible that both PAPC fragments were still membrane bound and that the free cytoplasmic domain was not detectable. Therefore it would be useful to investigate whether these fragments would accumulate using inhibitors of matrix metallo-proteinases and the  $\gamma$ -secretase complex like TAPI-1 and DAPT or the proteasome inhibitor lactacystin (Bonn et al., 2007). It is also unclear whether the cleavage of PAPC is regulated.

After overexpression in *Xenopus* oocytes PAPCc was detected in the nucleus, but none of the fragments derived from the overexpressed full length PAPC was (Fig.13). This could only be explained if the fragments were still membrane-tethered, which underlines the need to identify them. In any case, from these data I conclude that whenever unbound PAPCc is available in the cytoplasm it enters actively the nucleus. Passive diffusion of molecules  $\geq 30$ kDa through the nuclear pores is not observed (Görllich and Kutay, 1999). Since no nuclear localization signal has been identified in PAPCc, it is possible that PAPCc enters the nucleus bound to an interacting protein in the way of a shuttle. In animal cap cells PAPCc can be detected in the nucleus, confirming the results from oocyte lysates, and at the cell membrane (Fig.14). Its localization at the membrane must be due to its interaction with a membrane-bound protein. In fact Spry and ANR5, both cytoplasmic interaction partners of PAPC, are also found at the cell membrane even in the absence of PAPC (Chung et al., 2007; Wang et al., 2008). The identity of this membrane-associated

protein remains unknown. As a conclusion, PAPC is processed by proteolysis, and its overexpressed cytoplasmic domain, PAPCc, can enter the nucleus where it possibly regulates transcription.

#### **4.7 PAPC functions can be mapped to its protein domains**

Cell adhesion and signaling functions of PAPC can be separated according to its protein domains. PAPC decreases C-Cadherin-mediated adhesion, which causes PAPC-expressing cells to sort out from control cells (Chen and Gumbiner, 2006). M-PAPC, a construct lacking all but 17 cytoplasmic amino acids, still induces cell sorting (Fig.17) (Kim et al., 1998; Chen and Gumbiner, 2006). This raised the question whether the 17 juxtamembrane amino acids of the cytoplasmic domain contributed to the effect of PAPC. In dissociation and reaggregation experiments, I could show that even in the total absence of the cytoplasmic domain,  $\Delta$ C-PAPC still induced cell sorting (Fig.17). This is in agreement with results of other groups (Chen et al., 2007). The extracellular and/or transmembrane domains are therefore sufficient for PAPC function with regard to cell adhesion.

In mouse, the interaction between PAPC and N-Cadherin has been mapped to the transmembrane domain of N-Cadherin (Yasuda et al., 2007). Yet in functional assays in *Xenopus*, neither the extracellular nor the transmembrane domain of PAPC by themselves were sufficient to induce cell sorting in animal cap cells (Chen et al., 2007). The activating antibody AA5, which blocks the effects of PAPC on C-Cadherin, has been shown to recognize specifically EC5 of C-Cadherin, the most juxtamembrane of the extracellular domains (Zhong et al., 1999; Chen and Gumbiner, 2006). Consequently I propose that PAPC and C-Cadherin interact via their extracellular and transmembrane domains. This interaction decreases C-Cadherin-mediated adhesion.

What the cytoplasmic domain, PAPCc, does with regard to cell adhesion, is less clear. Even though PAPCc was not necessary to induce cell sorting, its expression in animal cap cells inhibited cell reaggregation cell-autonomously (Fig.17). This effect has not been observed with a membrane-tethered construct of PAPCc (Chen and Gumbiner, 2006). Additionally, the expression of PAPCc in DMZ explants induced cell detachment in the absence of endogenous PAPC (Fig.18). Since PAPCc has not

been implied in regulating C-Cadherin adhesiveness, it must exert its effects via other mechanisms. PAPCc might influence cell adhesion indirectly via its signaling properties which will be discussed in more detail later in this chapter.

The PAPC domains involved in signaling are different from those involved in cell adhesion. In contrast to Fz7 and C-Cadherin, Spry binds to the intracellular domain of PAPC (PAPCc). The putative phosphorylation sites S741 and S955 of PAPCc are especially important for the interaction with Spry (Wang et al., 2008). When these amino acids were mutated, the interaction between PAPC and Spry was abolished (Fig.10). These results confirmed data obtained from functional experiments with DMZ explants. The expression of PAPCc, but not of the mutated PAPCc, was sufficient to antagonize Spry and to allow gastrulation movements to take place (Wang et al., 2008). The importance of PAPCc for signaling was also reflected in the activation status of Rho. Loss of PAPC in the dorsal mesoderm, which resulted in loss of Rho activation, could be rescued by the intracellular (PAPCc), but not by the extracellular and transmembrane domains (M-PAPC) (Fig.7). The PAPC-S741A/S955A point mutant (PAPCmut), which cannot bind Spry, failed to rescue Rho activation after PAPC loss of function (Fig.11, Fig.7). These results confirm that PAPC activates Rho signaling by inhibiting Spry function. Since PAPCmut still mediates cell sorting (Fig.11), the cell sorting properties of PAPC are distinct from its signaling functions.

As Rho activity can also influence cell adhesion and endocytosis (Braga et al., 1997; Ellis and Mellor, 2000), it is difficult to differentiate between direct and indirect effects of PAPCc. The observation that in dissociation and reaggregation experiments and in DMZ explants PAPCc-expressing cells simply did not adhere (Fig.17, Fig.18) may be a titration problem of PAPCc resulting in overactivation of Rho. The total detachment of the cells need not be a consequence of altered cadherin adhesiveness, but could be due to increased cell-cortex tension generated by the cortical actomyosin network (Harris, 1976; Krieg et al., 2008). In order to investigate whether this non-adhesive state of PAPCc-expressing cells is due to modulation of cadherin function or the cytoskeleton, beads coated with C-Cadherin ectodomains could be used. Adhesion to these beads depends solely on direct adhesion between the molecules studied, without interference from other factors (Hammerschmidt and Wedlich, 2008).

PAPC is essential for convergent extension and tissue separation during gastrulation (Medina et al., 2004; Unterseher et al., 2004; Chen and Gumbiner, 2006; Wang et al., 2008). How PAPC controls these complex processes is still not well understood; but the regulation of cell adhesion and Wnt-signaling seem to be at the core of its function. Considering the diverse functions of PAPC it is not surprising that PAPC is also involved in somitogenesis and may be a tumor suppressor of breast cancer (Kim et al., 2000; Rhee et al., 2003; Yu et al., 2008). The study of its protein domains will contribute greatly to elucidate the role of PAPC during development, as will the further characterization of its interaction partners.

## 5 Material

### 5.1 Chemicals

All chemicals, if not stated otherwise, were obtained from J.T.Baker, Merck, Roth, and Sigma-Aldrich.

Ampicillin	biomol
Bacto tryptone	BD
Bacto yeast extract	BD
Bromophenol Blue	Serva
DAPI	Roth
Fluorescein	Molecular Probes/Invitrogen
Freon	Fluka
Gelatin from cold water fish skin	Sigma
HEPES	biomol
Hi-Di formamide	Roche
L-cystein	biomol
LE Agarose	Biozym
Mowiol	Calbiochem
PEI, linear, MW 25000	Polysciences, Inc.
Penicillin	PAA Laboratories
Phenol-chloroform-isoamylalcohol	Fluka
Poly (2-hydroxyethyl methacrylate)	Sigma
TEMED	biomol
Texas Red	Molecular Probes/Invitrogen
TurboFect	Fermentas

### 5.2 Buffers

3x SDS-sample buffer	150mM Tris-HCl (pH 6.8), 6% SDS, 0.3% Bromophenol Blue, 30% glycerol, 300mM DTT
6x loading buffer	40% glycerol, 0.25% Bromophenol Blue
Blocking solution	3% bovine serum albumin (BSA), 20% normal goat serum (NGS), 0.1M glycine
Ca <sup>2+</sup> /Mg <sup>2+</sup> -free MBSH	88mM NaCl, 1mM KCl, 2.4mM NaHCO <sub>3</sub> , 7.5mM Tris-HCl (pH 7.6)
Dent's	4V methanol, 1V DMSO
DMEM high-glucose medium	PAA Laboratories
DMEM Ready Mix	PAA Laboratories
Gurdon buffer	88mM NaCl, 10mM Tris-HCl (pH 7.4), sterilely filtered
HEMA	12 mg/ml Poly (2-hydroxyethyl methacrylate) in 95% EtOH
HGNT buffer	50mM NaCl, 25mM HEPES, 10% glycerol, 1% TritonX-100
LB (2l)	20g bacto tryptone, 10g yeast extract, 20g NaCl

LB-Amp plate	1.5% agar in LB-Amp
LB-Amp	50µg/ml ampicillin in LB
MBSH buffer	88mM NaCl, 1mM KCl, 2.4mM NaHCO <sub>3</sub> , 0.82mM MgSO <sub>4</sub> , 0.33mM Na(NO <sub>3</sub> ) <sub>3</sub> , 0.41mM CaCl <sub>2</sub> , 10mM HEPES (pH 7.4), 10µg/ml streptomycin-sulfate, 10µg/ml penicillin
MEMFA	0.1M MOPS (pH 7.4), 2mM EGTA, 1mM MgSO <sub>4</sub> , 3.7% formaldehyde
Milk buffer	5% milk powder in PBS/0.1% Tween-20
MMR	0.1M NaCl, 2mM KCl, 1mM MgSO <sub>4</sub> , 2mM CaCl <sub>2</sub> , 5mM HEPES
Mowiol	20mg Mowiol, 80ml PBS, 50ml glycerol
Opti-MEM® I medium	Invitrogen
PBS for cell culture	PAA Laboratories
PBS	126mM NaCl, 2.7mM KCl, 1.5mM KH <sub>2</sub> PO <sub>4</sub> , 6.5mM Na <sub>2</sub> HPO <sub>4</sub>
RIPA buffer	0.1% SDS, 0.5% Na-deoxycholate, 1% NP-40, 150mM NaCl, 50mM Tris-HCl (pH 7.4), proteinase inhibitor
SDS-PAGE running buffer	24.8mM Tris, 192mM glycine, 0.1% SDS
Transfer buffer	24.8mM Tris, 192mM glycine, 20% methanol
Tris/NaCl	100mM Tris-HCl (pH 7.4), 100mM NaCl

### 5.3 Oligonucleotides

The following oligonucleotides were ordered from Operon.

BIFC_YC_f	ATC CCA TCG ATT CGA ATT CCC GTC CGG CGT GCA AAA TCC CG
BIFC_YC_r	CGG GAT TTT GCA CGC CGG ACG GGA ATT CGA ATC GAT GGG AT
BIFC_YN_f	GGA TCC CAT CGA TTC GAA TTC CAG ATC CAT CGC CAC CAT GG
BIFC_YN_r	CCA TGG TGG CGA TGG ATC TGG AAT TCG AAT CGA TGG GAT CC
C-Cadh_BIFC_r	GAC TCA CTA TAG TTC TTT CGA AGT CCT CCT CGG AGA TC
Fz7_1171_f	AAC AGC GTG GAC TCT CTG CG
Fz7_781_f	GAG CGG CCC ATC ATC TTC CT
Fz7_myc_BIFC_f2	TTC GAA ATG TCC TCT ACA GTC TCG CTG
Fz7_TM1_f	ATC GAT ATG TCC TCT ACA GTC TCG CT
Fz7_TM1_r	ATC GAT GCC GCT CGG GGT AAC TGA AG
IF-myc_f	TTC GAA TGT GTA CCT GTA AAA AGA AAG CTG G
M13f	GTA AAA CGA CGG CCA G
M13r	CAG GAA ACA GCT ATG AC
M-PAPC-myc_r	TTC GAA CGT GTT GTT CAG GTA C
PAPC_1441_f	AGT GAT GAG AAT GAC AAT GCA CCT G
PAPC_1746_f	TCG CGT TCA ACT AAA TCT CAG AAT A
PAPC_2651_f	AAF AAF AFC ATT GAG CAG CCA A
PAPC_4_f	CGT AGT AGT GGC AGT GTA TGA C
PAPC_4_r	CGG AAG GTT GTA GCG ATC TCT G
PAPC_5_r	GTG TTC GAA AGG TTG TAG CAA GTA CTG

PAPC_6_f	GAG TCC GTG AGA GTG ATG GGC AG
PAPC_6_r	GCT GTT TCT GGA ATA TAG GCA ACT CC
PAPC_myc_BIFC_f	TAC TTC GAA ATG CTG CTT CTC TTC AGA
PAPC_myc_BIFC_r2	CTC TTC GAA TGA ATT CAA GTC CTC TTC AGA
PAPC_myc_f	AGC TAC TTG TTC TTT TTG C
PAPC-GFP_f	GGT CTT CGA AAT GGT GAG CAA GGG
PAPC-GFP_r	GGT ATG GCT GAT TAT GAT CTA GAG TCG C
SP6	ATT TAG GTG ACA CTA TAG
T7 all	TAA TAC GAC TCA CTA TAG GG
YC155_f	TCA GAA TTC CGT CCG GCG TGC AAA ATC
YC155_r	TTA CTC GAG GCT TAC TTG TAC AGC TCG TC
YN155_f	TAG AGA ATT CAG ATC CAT CGC CAC CAT G
YN155_r	GGA CTC GAG GGC CAT GAT ATA GAC GTT G

The following morpholino oligonucleotides were purchased from Gene Tools. MoPAPC is a mixture of MoPAPC\_1 and MoPAPC\_2 targeting both PAPC alleles.

MoFz7_1	CCA ACA AGT GAT CTC TGG ACA GCA G
MoControl	CCT CTT ACC TCA GTT ACA ATT TAT A
MoPAPC_1	CCT AGA AAC AGT GTG GCA ATG TGA A
MoPAPC_2	CTT GCC TAG AAA GAG TGC TGC TGT G

## 5.4 Plasmids

Plasmid	Source
p13-pCS-H2B-mRFP	JB. Wallingford
pBIFC-bFosYN155	(Hu et al., 2002)
pBIFC-bFos $\Delta$ ZIPYN155	(Hu et al., 2002)
pBIFC-bJunYC155	(Hu et al., 2002)
pcDNA3.1(+) xC-Cadherin-eGFP	(Ogata et al., 2007)
pCMT-Fz7-myc-eGFP	KM. Kürner
pCS2+	R. Rupp and D. Turner
pCS2+ 3xHA	R. Swain
pCS2+ C-Cadherin-myc	B. Gumbiner
pCS2+ C-Cadherin-myc-YC, pCS2+ C-Cadherin-myc-YN	C-Cadherin-myc was amplified from pCS2+ C-Cadherin-myc using primers SP6 and C-Cadh_BIFC_r and ligated into the <i>Asu</i> II-restriction site of pCS2+ YC or YN.
pCS2+ DN-Dynamin1	(Jarrett et al., 2002)
pCS2+ FL-PAPC (-UTR)	(Medina et al., 2004)
pCS2+ Fz7	(Medina et al., 2000)
pCS2+ Fz7-myc	KM. Kürner
pCS2+ Fz7-myc-YN, pCS2+ Fz7-myc-YC	Fz7-myc was amplified from pCS2+ Fz7-myc using primers Fz7_myc_BIFC_f2 and PAPC_myc_BIFC_r2 and ligated into the <i>Asu</i> II-restriction site of pCS2+ YC or YN.

pCS2+ Fz7-TM1-myc-YN, pCS2+ Fz7-TM1-myc-YC	A fragment corresponding to amino acids 1-262 of Fz7 was amplified from pCS2+ Fz7 using primers Fz7_TM1_f and Fz7_TM1_r and ligated into the <i>Cla</i> I-restriction site of pCS2+ mt. Subsequently Fz7-TM1-myc was ligated into the <i>Eco</i> RI/ <i>Xho</i> I-restriction sites of pCS2+ YN* or YC*.
pCS2+ GAP43-GFP	(Moriyoshi et al., 1996; Kim et al., 1998)
pCS2+ M-AXPC	(Kim et al., 1998)
pCS2+ mb-RFP	(lioka et al., 2004)
pCS2+ mCherry-xRab5 $\alpha$	(Ogata et al., 2007)
pCS2+ M-PAPC	(Kim et al., 1998)
pCS2+ M-PAPC-myc	M-PAPC was amplified from pCS2+ M-PAPC using primers PAPC-myc_f and M-PAPC-myc_r and ligated into the <i>Cla</i> I-restriction sites of pCS2+ mt.
pCS2+ mt	R. Rupp and D. Turner
pCS2+ PAPC-3xHA	PAPC was amplified from pCS2+ FL-PAPC (-UTR) using primers PAPC-myc_f und PAPC_5_r and ligated into the <i>Cla</i> I-restriction site of pCS2+ 3xHA.
pCS2+ PAPCc-flag	(Wang et al., 2008)
pCS2+ PAPCc-myc	PAPCc was amplified from pCS2+ FL-PAPC(-UTR) using primers lf-myc_f and PAPC_5_r and ligated into the <i>Cla</i> I-restriction site of pCS2+ mt.
pCS2+ PAPC-eGFP	eGFP was amplified from pEGFP-N1 using primers PAPC-GFP_f and PAPC-GFP_r and ligated into the <i>Asu</i> II/ <i>Xba</i> I-restriction sites of pCS2+ PAPC-3xHA.
pCS2+ PAPCmut	(Wang et al., 2008)
pCS2+ PAPC-myc	PAPC was amplified from pCS2+ FL-PAPC(-UTR) using primers PAPC-myc_f and PAPC_5_r and ligated into the <i>Cla</i> I-restriction site of pCS2+ mt.
pCS2+ PAPC-myc-YN, pCS2+ PAPC-myc-YC	PAPC-myc was amplified from pCS2+ PAPC-myc using primers PAPC_myc_BIFC_f and PAPC_myc_BIFC_r2 and ligated into the <i>Asu</i> II-restriction site of pCS2+ YN or YC.
pCS2+ Venus-xPKC $\lambda$	(Hyodo-Miura et al., 2006)
pCS2+ Wnt11	E. deRobertis
pCS2+ xSpry1-GFP	(Wang, 2007)
pCS2+ YN*, pCS2+ YC*	Using primers BIFC_YC_f, BIFC_YC_r, BIFC_YN_f and BIFC_YN_r a nucleotide was added to the multiple cloning site of pCS2+ YN and pCS2+ YC via PCR-based mutagenesis.
pCS2+ YN, pCS2+ YC	Using primers YC155_f, YC155_r, YN155_f and YN155_r the N- and C-terminal fragment of YFP (corresponding to amino acids 1-155 and 156-239) was amplified with the linker region from pBIFC-bFosYC155 and pBIFC-bJunYN155 and ligated into the <i>Eco</i> RI/ <i>Xho</i> I-restriction sites of pCS2+.
pCS2+ $\Delta$ C-Fz7	(Medina et al., 2000)
pCS2+ $\Delta$ C-PAPC	CD. Berger
pEGFP-N1	Clontech

**Table 2. Table of plasmids used in this work.**

## 5.5 Proteins, enzymes, inhibitors, and markers

All enzymes were obtained from Fermentas, Roche, and New England Biolabs if not stated otherwise. RBD-GFP protein was purified according to Berger et al. (2009).

10x protease inhibitor complete Mini	Roche
bFGF	Invitrogen
BSA	Sigma
EuroTaq	Biocat
GeneRuler 1kb DNA ladder Plus	Fermentas
Human chorionic gonadotropin	Sigma
Normal goat serum	Dako
PageRuler Prestained protein ladder	Fermentas
PageRuler Unstained protein ladder	Fermentas
Phusion® High Fidelity	Finnzymes
Poly-L-Lysine	Sigma
SU5402	Calbiochem
Trypsin	PAA Laboratories

## 5.6 Antibodies

$\alpha$ -GFP	mouse	Roche
$\alpha$ -mouse Alexa 594	goat	Molecular Probes/Invitrogen
$\alpha$ -mouse peroxidase	goat	Dianova
$\alpha$ -myc 9E10 supernatant	mouse	
$\alpha$ -myc Ab-1	mouse	Oncogene
$\alpha$ -PAPC 11A6	mouse	(Chen and Gumbiner, 2006)

## 5.7 Bacteria and cells

*E.coli* Q 358 XL1

HEK293 cells

## 5.8 Kits

Big Dye Terminator Cycle	Applied Biosystems
JETSTAR 2.0 Midi columns	Genomed
JETSTAR 2.0 Mini columns	Genomed
Lumi-light <sup>plus</sup> Western Substrate	Roche
mMessage mMachine	Ambion
QIAquick Gel Extraction	Qiagen
QIAquick PCR Purification	Qiagen

Super Signal West Femto	Pierce
-------------------------	--------

## 5.9 Other material

Cassettes 1.0mm	Invitrogen
Cronex 5 Film	Agfa
Protran BA 85 membrane	Whatman
Self-adhesive hole reinforcements	Zweckform
Superfrost Plus	Thermo Scientific

## 5.10 Microscopes and equipment

ABI PRISM 3100 Genetic Analyzer	Applied Biosystems
C1Si confocal laser scanning system	Nikon
Cryostat CM 30505	Leica
DS-1QM CCD camera	Nikon
Easyject Prima Electroporator	Equibio
Eclipse 80i upright microscope	Nikon
Eclipse 90i upright microscope	Nikon
Guava EasyCyte	Guava Technologies
IM300 Microinjector	Narishige
Micromanipulator	Micro Instruments
NanoDrop ND-1000	Thermo Scientific
Novex XCell SureLock mini	Invitrogen
SZX12 stereo microscope	Olympus
Ti inverted microscope	Nikon

## 5.11 Computer programs

Adobe Photoshop CS3	Adobe
EZ-C1 3.30 FreeViewer	Nikon
Guava CytoSoft 5.1	Guava Technologies
ImageJ 1.41n	NIH, USA
NIS-Elements 2.30	Nikon
Vector NTI Advance 10.3	Invitrogen

## 6 Methods

### 6.1 DNA/RNA-methods

#### 6.1.1 Isolation of nucleic acids

If not mentioned otherwise, the nucleic acids were isolated with the appropriate kits (see 5.8 Kits) according to the manufacturers' instructions. For the isolation of plasmid DNA from bacteria, 2ml (Miniprep) or 50ml (Midiprep) of LB-Amp were inoculated with a single colony and cultured overnight at 37°C with shaking. The buffer volume used for Midipreps was increased by 50% compared to the instructions.

##### 6.1.1.1 Phenol-chloroform extraction

Phenol-chloroform extraction was used to separate nucleic acids from proteins and lipids. The aqueous solution was mixed with 1V phenol-chloroform-isoamylalcohol and centrifuged for 2min at 13200rpm. The upper phase was transferred to a new tube, mixed with 1V chloroform, and centrifuged again. The upper phase was transferred to a new tube and the nucleic acid was precipitated with ethanol or isopropanol.

##### 6.1.1.2 Alcohol precipitation

Alcohol precipitation was used to purify and/or concentrate RNA or DNA from aqueous solutions. The nucleic acid solution was mixed with 1/10V 3M Sodium Acetate (pH 5.2), 2.5V ethanol (95%) or 1V isopropanol were added, and the mixture was incubated 20min at RT or overnight at -20°C.

#### 6.1.2 PCR

The proofreading polymerase Phusion was used to introduce restriction sites into DNA sequences for cloning purposes. For a 50µl reaction 40ng plasmid template, 0.5µM of forward and reverse primers, 0.2mM of each dNTP, 10µl 5x HF-buffer, H<sub>2</sub>O, and 1U Phusion were mixed. The fragment was amplified according to Table 3 with 25 cycles (steps 2-4). The PCR fragment was isolated using the QIAquick PCR Purification kit according to the manufacturer's instructions. Restriction of fragments was carried out overnight with 10U of the corresponding restriction enzyme.

Step	Temperature (°C)	Duration
1	95	40sec
2	95	10sec
3	variable	20sec
4	72	variable
5	4	∞

**Table 3. PCR program used for cloning.**

##### 6.1.2.1 Mutagenesis

Point mutations or new nucleotides were introduced into plasmids by site-directed mutagenesis using PCR. Primers for mutagenesis were designed to have 15-18 nucleotides flanking the mutated

nucleotides on each side. A 50 $\mu$ l PCR reaction was set up including 50ng template DNA, 5 $\mu$ l 10x buffer with MgSO<sub>4</sub>, 0.5mM dNTPs each, 0.5 $\mu$ M of forward and reverse primers, H<sub>2</sub>O, and 5U Pfu polymerase. The vector was amplified according to Table 4 with 20 cycles (steps 2-4).

Step	Temperature (°C)	Duration
1	94	2min
2	94	30sec
3	60	45sec
4	72	10min
5	4	$\infty$

**Table 4. PCR program used for mutagenesis.**

The DNA was isolated using the QIAquick PCR Purification kit. The template was digested with 10U *DpnI* at 37°C for 1-4h. The PCR product was purified with phenol-chloroform extraction and ethanol precipitation. The plasmid solution was dialyzed and transformed into *E.coli* by electroporation. After identification of the clone carrying the mutation by colony PCR and sequencing, the mutated sequence was subcloned into the original vector.

#### 6.1.2.2 Colony PCR

Colony PCR was used to detect bacterial clones which had incorporated the vector with the desired insert after cloning and transformation. A standard 10 $\mu$ l reaction contained H<sub>2</sub>O, 0.1mM of each dNTP, 1 $\mu$ l 10x buffer, 1mM MgCl<sub>2</sub>, 0.5 $\mu$ M of forward and reverse primer, and 0.75U Taq polymerase. A single colony was picked, dipped onto a LB-Amp plate and then into the PCR reaction. The colony PCR was carried out according to Table 5 with 30 cycles (steps 2-4).

Step	Temperature (°C)	Duration
1	95	5min
2	95	30sec
3	variable	45sec
4	72	variable
5	4	$\infty$

**Table 5. PCR program used for colony PCR.**

#### 6.1.3 Cloning

Cloning was performed using the standard protocols of PCR-based fragment amplification, restriction, ligation, and plasmid transformation. The bacterial clones were analyzed by colony PCR, the plasmid DNA was isolated using the appropriate kit, and the sequence was confirmed by sequencing.

#### 6.1.4 Sequencing

Sequencing was performed using the Big Dye Terminator Cycle kit. For a 10 $\mu$ l reaction 400ng Plasmid-DNA, 0.5 $\mu$ M primer, 2 $\mu$ l 5x buffer, H<sub>2</sub>O, and 1 $\mu$ l Big Dye were mixed on ice. The target sequence was amplified according to Table 6 with 28 cycles (steps 2-3), purified by ethanol precipitation and dissolved in 20 $\mu$ l Hi-Di formamide. The sequencing was performed on an ABI PRISM 3100 Genetic Analyzer. The sequences were examined using Vector NTI Advance 10.3.

Step	Temperature (°C)	Duration
1	95	2min30sec
2	95	30sec
3	55	4min15sec
4	4	∞

**Table 6. PCR program used for sequencing.**

### 6.1.5 Cap-mRNA

Cap-mRNA was synthesized with the mMessage mMachine kit according to the manufacturer's instructions. A 10 $\mu$ l reaction was set up using 0.5 $\mu$ g linearized plasmid and 1 $\mu$ l enzyme mix. The cap-mRNA was purified with phenol-chloroform extraction followed by isopropanol precipitation.

## 6.2 Biochemical and immunological methods

### 6.2.1 Protein extraction from cell culture cells

The cells were washed with ice-cold PBS and then transferred to tubes in 70-200 $\mu$ l HGNT buffer with protease inhibitor. The cells were incubated for 30min on ice and vortexed 2x during incubation. The proteins were pelleted by centrifugation for 30min at 4°C at 13200rpm and the supernatant was removed. The extracted proteins were mixed with 3x SDS sample buffer and heated for 20min to 70°C or 5min to 95°C.

### 6.2.2 Protein extraction from embryos

The embryos were collected in tubes and the buffer was removed. The embryos were homogenized by pipetting in 7.5 $\mu$ l RIPA buffer per embryo, and were then incubated on ice for 15min. After centrifuging for 5min at 4°C at 5000rpm the protein solution was transferred without fat, cell debris or yolk to a new tube and was mixed with 1V Freon. After vortexing and centrifuging for 5min at 4°C at 5000rpm the different phases separated. The upper aqueous phase containing the proteins was transferred to a new tube and stored as aliquots at -80°C.

### 6.2.3 SDS-PAGE and Western blot

The proteins were separated with discontinuous SDS-PAGE (Laemmli, 1970). The acrylamide concentration of the gels varied between 8-12% according to the expected protein sizes. The molecular weight of the proteins was estimated by loading 4  $\mu$ l of standard size markers. Proteins were transferred to nylon membrane by wet transfer in Novex XCell SureLock mini chambers. Blocking of the membrane was carried out in milk buffer for 1h at RT. Antibody incubation times were overnight at 4°C for primary, and 1h at RT for secondary antibodies. Antibody dilutions used were  $\alpha$ -GFP (1:1000),  $\alpha$ -myc (1:1000), and  $\alpha$ -mouse peroxidase (1:10000).

### 6.2.4 Immunostainings of cell culture cells

The cells were washed with ice-cold PBS and then fixed for 20min at RT in 3.7% formaldehyde/PBS. After washing the cells 2x for 10min with PBS, they were incubated for 10min in Tris/NaCl, followed by

another 10min in PBS. The cells were permeabilized for 5min with 0.3% Triton X-100/PBS, washed 2x for 10min with PBS and then incubated for 1h at RT in blocking solution. The cells were transferred to a wet chamber and incubated overnight at 4°C with  $\alpha$ -myc supernatant (1:30) in blocking solution. After 3x 10min washing with PBS the cells were incubated for 1h at RT with  $\alpha$ -mouse Alexa 594 ab (1:300) in blocking solution. The cells were washed 3x with PBS, stained with 20 $\mu$ g/ml DAPI/PBS for 3min, washed again 2x for 10min and fixed on slides with Mowiol.

### 6.2.5 Immunostainings of animal caps

The animal caps were fixed for 30min at RT in 3.7% formaldehyde/PBS. After washing the animal caps 2x for 15min with PBS, they were incubated for 30min in Tris/NaCl, followed by another 15min in PBS. The animal caps were permeabilized for 10min with 0.3% Triton X-100/PBS, washed 2x for 15min with PBS and then incubated for 1h at RT in blocking solution. The animal caps were incubated overnight at 4°C with  $\alpha$ -PAPC ab (1:20) in blocking solution. After several washes with PBS the animal caps were incubated again overnight at 4°C with  $\alpha$ -mouse Alexa 594 ab (1:200) in blocking solution. The animal caps were washed with PBS and fixed inside of self-adhesive reinforcement labels between slides and cover slips using Mowiol.

### 6.2.6 RBD-GFP staining

Sections (or DMZs) were permeabilized with 0.3% TritonX-100/PBS for 10 min, washed with PBS for 15min and with H<sub>2</sub>O for 20sec. Specimens were blocked in blocking solution for 1h at room temperature. Incubation with 10 $\mu$ g RBD-GFP protein in blocking solution was carried out overnight at 4°C in the dark. The sections (DMZs) were washed 3(6)x with PBS for 10 min and mounted using Mowiol. For simultaneous RBD-GFP and antibody staining, RBD-GFP protein can be added to the fluorescent secondary antibody.

## 6.3 Bacteria and cell culture methods

### 6.3.1 Chemical transformation of bacteria

Chemical transformation was used to introduce foreign DNA into bacteria. Plasmid-DNA (100-150ng) and 50 $\mu$ l chemocompetent *E.coli* cells were mixed and incubated for 40min on ice. The bacteria were heat-shocked for 2min at 42°C and then put on ice for 5min. After the addition of 1ml LB the bacteria were incubated for 1h at 37°C with shaking and then plated on LB-Amp plates.

### 6.3.2 Electroporation of bacteria

Electroporation was used to achieve higher transformation efficiency than with chemical transformation. The cuvette used for electroporation was sterilized for 10min with UV light and then precooled on ice. The salt-free DNA solution was mixed with 50 $\mu$ l of electrocompetent *E.coli* cells and filled into the cuvette. The cells were electroporated. Afterwards 250 $\mu$ l of LB were added and the bacteria were incubated for 1h at 37°C before plating them on LB-Amp plates.

### 6.3.3 Maintaining cell lines

HEK293 cells were grown in DMEM Ready Mix supplemented with 100µg/ml penicillin and streptomycin at 37°C in a humidified 5% CO<sub>2</sub> incubator. At 80-90% confluency cells were subcultured. For microscopic analyses cells were seeded onto coverslips coated with poly-L-lysine in 6-well plates. For FACS analysis cells were seeded into 12-well plates.

### 6.3.4 Transfection of cultured cells

The HEK293 cells were transfected using PEI and DMEM high-glucose medium or TurboFect and Opti-MEM I according to the manufacturer's instructions. The total amount of transfected DNA was kept constant by adding empty pCS2+ vector. For fluorescence microscopy experiments DNA was transfected using a ratio of 1µg DNA to 4µl PEI. For FACS experiments 1.5µg DNA was transfected using 1.5µl TurboFect.

### 6.3.5 bFGF treatment of cultured cells

All plastic material was coated with 5% BSA prior to contact with bFGF. After transfection the cells were grown in DMEM Ready Mix or serum-free DMEM high-glucose medium for 18h. The medium was then exchanged for fresh DMEM Ready Mix, serum-free medium, or serum-free medium containing 5 ng/ml bFGF and 0.1 mg/ml BSA or 5 µM SU5402 or both. Cells were washed with ice-cold PBS and fixed in 4% formaldehyde. The localization of GFP-Spry was analyzed by fluorescent microscopy.

### 6.3.6 FACS

After transfection cells were cultured for 48h at 26° in a humidified 5% CO<sub>2</sub> incubator. The cells were trypsinized, washed with PBS, resuspended in 200µl PBS and stored on ice. The cells were diluted 1:1 with PBS (about 8.2×10<sup>5</sup> cells/ml) in a 96-well flat bottom cell culture dish and analyzed for BIFC signal using the Guava EasyCyte flow cytometer.

## 6.4 Embryological methods

### 6.4.1 Embryo culture and manipulations

*In vitro* fertilization, embryo culture and microinjections were performed as described (Medina et al., 2004). Embryos were staged according to Nieuwkoop and Faber (1967). The dorsal blastomeres of 4-cell embryos were identified according to Klein (1987).

### 6.4.2 Cell dispersion assay

Sample mRNA, together with GFP as a tracer, was injected into one blastomere at the animal hemisphere of 32-cell stage embryos. At st.12, the injected embryos were observed under fluorescence microscope for distribution of GFP-labeled blastomeres.

### 6.4.3 Dissociation and reaggregation assay

The embryos were injected animally with mRNA and Fluorescein or just Texas Red at the 4-cell stage. The vitelline membrane was removed at st.9 and the animal caps were explanted. 3 caps of each sample were dissociated together with 3 control caps in 1x  $\text{Ca}^{2+}/\text{Mg}^{2+}$ -free MBSH in plastic dishes coated with 1% agarose in the same buffer. The outer pigmented layer of the ectoderm was removed. The inner cells were transferred to tubes, which contained a 1% agarose/1xMMR floor, and were pelleted for 30sec at 0.8rpm. The buffer was exchanged for 0.7x MMR buffer; the cells were centrifuged again and reaggregated over night at 15°C.

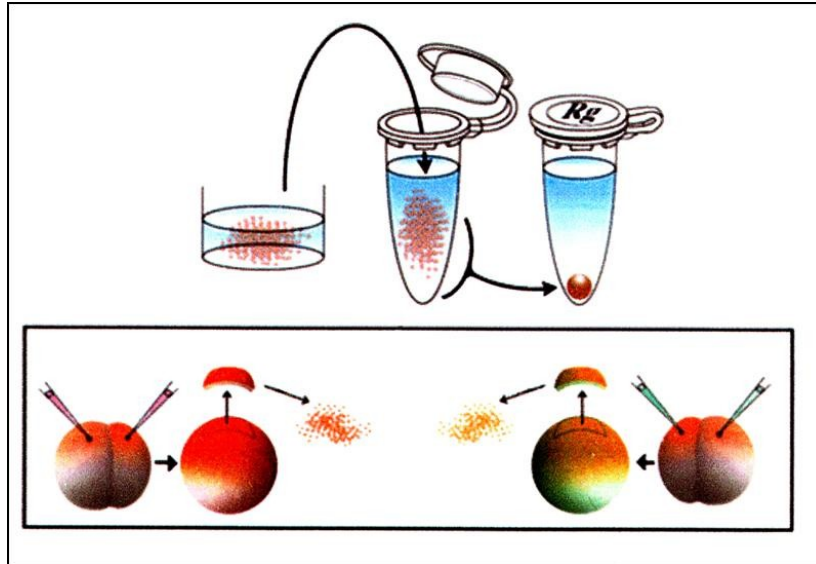


**Fig.34. Schematic outline of the dissociation and reaggregation experiment.** Picture adapted from Kuroda et al. (2002).

### 6.4.4 Reaggregation assay

The embryos were injected animally at the 4-cell stage. The vitelline membrane was removed at st.9 and 10 animal caps of each sample were explanted. The animal caps were dissociated in 1x  $\text{Ca}^{2+}/\text{Mg}^{2+}$ -free MBSH in cell culture plates coated with HEMA. The outer pigmented layer of the ectoderm was removed. The dissociated inner cells of each sample were distributed into 8 wells of a 96-well plate coated with 1% agarose/1x MBSH. The cells were reaggregated in 1x MBSH for 3h, the first hour with horizontal shaking.

### 6.4.5 Dorsal marginal zone (DMZ) explants

The vitelline membrane of embryos at st.10 was removed. Using knives made from eye lashes the dorsal third part of the embryo was explanted. The cells of the anterior mesendoderm still attached to the explant were carefully removed. The bottle cells were cut off, and the explant was placed in a plastic dish coated with 5% BSA. The DMZ explants were restrained by a cover slip on silicone feet and cultured in 1x MBSH until sibling embryos reached st.12. The DMZ explants were fixed with MEMFA for 30min at RT, washed in PBS and stored at 4°C.

#### 6.4.6 Tissue separation

The embryos were injected at the 4-cell stage. At st.9 the vitelline membrane was removed and the animal caps were excised. The animal caps were dissociated in 1x  $Mg^{2+}/Ca^{2+}$ -free MBSH in plastic dishes coated with 1% agarose in the same buffer. The outer, pigmented layer of the animal cap was removed. The cells of the inner layer were mixed and reaggregated in tubes coated with 1% agarose in 1x MBSH by centrifuging 30sec at 0.8rpm. The aggregates were divided in smaller pieces with eye lash-knives. The animal caps of uninjected st.10.5 embryos were explanted and placed upside-down on a plastic dish without agarose. The small aggregates were placed on the inner side of the animal cap and fixed by placing a cover slip with silicone feet on top of them. After 45min tissue separation was scored.

#### 6.4.7 Cryosections

Cryosections were generated largely as has been described (Fagotto and Gumbiner, 1994). Briefly, embryos (or DMZ explants) were fixed in MEMFA for 1h (30min) at room temperature, washed in PBS, rinsed in Tris/NaCl for 1h and washed again in PBS. The embryos (DMZ explants) were then embedded in 15% fish gelatin, 15% sucrose overnight followed by 25% fish gelatin, 15% sucrose overnight. Specimens were frozen in 15% gelatin at  $-80^{\circ}C$ .  $12\mu m$  sections were cut at  $-19^{\circ}C$ , collected on Superfrost Plus precoated glass slides and dried at  $37^{\circ}C$  overnight. The dried cryosections were fixed with acetone for 5min and stained with RBD-GFP.

### 6.5 Microscopy

Microscopy was mainly carried out at the Nikon Imaging Center at the University of Heidelberg. Fluorescent images were acquired using an Eclipse 80i or 90i upright microscope equipped with a DS-1QM CCD camera. Confocal images were acquired at  $0.5\mu m$  intervals using a C1Si confocal laser scanning system on a Ti fully automated inverted microscope. Maximum z-stack projection was performed using EZ-C1 Free Viewer Gold Version 3.30 build 647. Further image processing was carried out with ImageJ 1.41n and Adobe Photoshop CS3 Extended Version 10.0.1.

## 7 References

- Ahrens T, Pertz O, Haussinger D, Fauser C, Schulthess T, Engel J. 2002. Analysis of Heterophilic and Homophilic Interactions of Cadherins Using the c-Jun/c-Fos Dimerization Domains. *J. Biol. Chem.* 277:19455-19460.
- Angres B, Muller AH, Kellermann J, Hausen P. 1991. Differential expression of two cadherins in *Xenopus laevis*. *Development* 111:829-844.
- Axelrod JD, Miller JR, Shulman JM, Moon RT, Perrimon N. 1998. Dishevelled provides signaling specificity in the planar cell polarity and Wingless signaling pathways. *Genes & Development* 12:2610-2622.
- Berger CD, März M, Kitzing TM, Grosse R, Steinbeisser H. 2009. Detection of activated Rho in fixed *Xenopus* tissue. *Developmental Dynamics* 9999:NA.
- Bonn S, Seeburg PH, Schwarz MK. 2007. Combinatorial expression of alpha- and gamma-protocadherins alters their presenilin-dependent processing. *Mol Cell Biol* 27:4121-4132.
- Boutros M, Paricio N, Strutt DI, Mlodzik M. 1998. Dishevelled activates JNK and discriminates between JNK pathways in planar polarity and wingless signaling. *Cell* 94:109-118.
- Bradley RS, Espeseth A, Kintner C. 1998. NF-protocadherin, a novel member of the cadherin superfamily, is required for *Xenopus* ectodermal differentiation. *Curr Biol* 8:325-334.
- Braga VM, Machesky LM, Hall A, Hotchin NA. 1997. The small GTPases Rho and Rac are required for the establishment of cadherin-dependent cell-cell contacts. *J Cell Biol* 137:1421-1431.
- Brieher WM, Gumbiner BM. 1994. Regulation of C-cadherin function during activin induced morphogenesis of *Xenopus* animal caps. *J Cell Biol* 126:519-527.
- Brieher WM, Yap AS, Gumbiner BM. 1996. Lateral dimerization is required for the homophilic binding activity of C-cadherin. *J Cell Biol* 135:487-496.
- Bryant DM, Stow JL. 2004. The ins and outs of E-cadherin trafficking. *Trends Cell Biol* 14:427-434.
- Bucci C, Parton RG, Mather IH, Stunnenberg H, Simons K, Hoflack B, Zerial M. 1992. The small GTPase rab5 functions as a regulatory factor in the early endocytic pathway. *Cell* 70:715-728.
- Cabrita M, Christofori G. 2008. Sprouty proteins, masterminds of receptor tyrosine kinase signaling. *Angiogenesis* 11:53-62.
- Chen CP, Posy S, Ben-Shaul A, Shapiro L, Honig BH. 2005. Specificity of cell-cell adhesion by classical cadherins: Critical role for low-affinity dimerization through beta-strand swapping. *Proc Natl Acad Sci U S A* 102:8531-8536.
- Chen X, Gumbiner BM. 2006. Paraxial protocadherin mediates cell sorting and tissue morphogenesis by regulating C-cadherin adhesion activity. *J Cell Biol* 174:301-313.
- Chen X, Molino C, Liu L, Gumbiner BM. 2007. Structural elements necessary for oligomerization, trafficking, and cell sorting function of paraxial protocadherin. *J Biol Chem* 282:32128-32137.
- Choi YS, Gumbiner B. 1989. Expression of cell adhesion molecule E-cadherin in *Xenopus* embryos begins at gastrulation and predominates in the ectoderm. *J. Cell Biol.* 108:2449-2458.
- Choi YS, Sehgal R, McCrea P, Gumbiner B. 1990. A cadherin-like protein in eggs and cleaving embryos of *Xenopus laevis* is expressed in oocytes in response to progesterone. *J Cell Biol* 110:1575-1582.
- Chung HA, Yamamoto TS, Ueno N. 2007. ANR5, an FGF target gene product, regulates gastrulation in *Xenopus*. *Curr Biol* 17:932-939.
- Clark HF, Brentrup D, Schneitz K, Bieber A, Goodman C, Noll M. 1995. Dachshous encodes a member of the cadherin superfamily that controls imaginal disc morphogenesis in *Drosophila*. *Genes Dev* 9:1530-1542.
- Classen AK, Anderson KI, Marois E, Eaton S. 2005. Hexagonal packing of *Drosophila* wing epithelial cells by the planar cell polarity pathway. *Dev Cell* 9:805-817.
- Curtin JA, Quint E, Tshipouri V, Arkell RM, Cattanach B, Copp AJ, Henderson DJ, Spurr N, Stanier P, Fisher EM, Nolan PM, Steel KP, Brown SD, Gray IC, Murdoch JN. 2003. Mutation of *Celsr1* disrupts planar polarity of inner ear hair cells and causes severe neural tube defects in the mouse. *Curr Biol* 13:1129-1133.

- Davies A, Formstone C, Mason I, Lewis J. 2005. Planar polarity of hair cells in the chick inner ear is correlated with polarized distribution of c-flamingo-1 protein. *Dev Dyn* 233:998-1005.
- Djiane A, Riou J, Umbhauer M, Boucaut J, Shi D. 2000. Role of frizzled 7 in the regulation of convergent extension movements during gastrulation in *Xenopus laevis*. *Development* 127:3091-3100.
- Drechsel DN, Hyman AA, Hall A, Glotzer M. 1997. A requirement for Rho and Cdc42 during cytokinesis in *Xenopus* embryos. *Curr Biol* 7:12-23.
- Duguay D, Foty RA, Steinberg MS. 2003. Cadherin-mediated cell adhesion and tissue segregation: qualitative and quantitative determinants. *Dev Biol* 253:309-323.
- Eaton S, Wepf R, Simons K. 1996. Roles for Rac1 and Cdc42 in planar polarization and hair outgrowth in the wing of *Drosophila*. *J Cell Biol* 135:1277-1289.
- Ellis S, Mellor H. 2000. Regulation of endocytic traffic by rho family GTPases. *Trends Cell Biol* 10:85-88.
- Fagotto F, Gumbiner BM. 1994. Beta-catenin localization during *Xenopus* embryogenesis: accumulation at tissue and somite boundaries. *Development* 120:3667-3679.
- Fanto M, Clayton L, Meredith J, Hardiman K, Charroux B, Kerridge S, McNeill H. 2003. The tumor-suppressor and cell adhesion molecule Fat controls planar polarity via physical interactions with Atrophin, a transcriptional co-repressor. *Development* 130:763-774.
- Fanto M, Weber U, Strutt DJ, Mlodzik M. 2000. Nuclear signaling by Rac and Rho GTPases is required in the establishment of epithelial planar polarity in the *Drosophila* eye. *Curr Biol* 10:979-988.
- Formstone CJ, Mason I. 2005a. Combinatorial activity of Flamingo proteins directs convergence and extension within the early zebrafish embryo via the planar cell polarity pathway. *Dev Biol* 282:320-335.
- Formstone CJ, Mason I. 2005b. Expression of the Celsr/flamingo homologue, c-fmi1, in the early avian embryo indicates a conserved role in neural tube closure and additional roles in asymmetry and somitogenesis. *Dev Dyn* 232:408-413.
- Foty RA, Steinberg MS. 2004. Cadherin-mediated cell-cell adhesion and tissue segregation in relation to malignancy. *Int J Dev Biol* 48:397-409.
- Foty RA, Steinberg MS. 2005. The differential adhesion hypothesis: a direct evaluation. *Dev Biol* 278:255-263.
- Frank M, Kemler R. 2002. Protocadherins. *Curr Opin Cell Biol* 14:557-562.
- Ginsberg D, DeSimone D, Geiger B. 1991. Expression of a novel cadherin (EP-cadherin) in unfertilized eggs and early *Xenopus* embryos. *Development* 111:315-325.
- Glickman NS, Kimmel CB, Jones MA, Adams RJ. 2003. Shaping the zebrafish notochord. *Development* 130:873-887.
- Görlich D, Kutay U. 1999. Transport between the cell nucleus and the cytoplasm. *Annual Review of Cell and Developmental Biology* 15:607-660.
- Goulimari P, Kitzing TM, Knieling H, Brandt DT, Offermanns S, Grosse R. 2005. Galpha12/13 is essential for directed cell migration and localized Rho-Dia1 function. *J Biol Chem* 280:42242-42251.
- Goulimari P, Knieling H, Engel U, Grosse R. 2008. LARG and mDia1 link Galpha12/13 to cell polarity and microtubule dynamics. *Mol Biol Cell* 19:30-40.
- Haas IG, Frank M, Veron N, Kemler R. 2005. Presenilin-dependent processing and nuclear function of gamma-protocadherins. *J Biol Chem* 280:9313-9319.
- Habas R, Dawid IB. 2005. Dishevelled and Wnt signaling: is the nucleus the final frontier? *J Biol* 4:2.
- Habas R, Dawid IB, He X. 2003. Coactivation of Rac and Rho by Wnt/Frizzled signaling is required for vertebrate gastrulation. *Genes Dev* 17:295-309.
- Habas R, Kato Y, He X. 2001. Wnt/Frizzled activation of Rho regulates vertebrate gastrulation and requires a novel Formin homology protein Daam1. *Cell* 107:843-854.
- Hacohen N, Kramer S, Sutherland D, Hiromi Y, Krasnow MA. 1998. sprouty encodes a novel antagonist of FGF signaling that patterns apical branching of the *Drosophila* airways. *Cell* 92:253-263.

- Halbleib JM, Nelson WJ. 2006. Cadherins in development: cell adhesion, sorting, and tissue morphogenesis. *Genes & Development* 20:3199-3214.
- Hambusch B, Grinevich V, Seeburg PH, Schwarz MK. 2005.  $\gamma$ -Protocadherins, presenilin-mediated release of C-terminal fragment promotes locus expression. *J Biol Chem* 280:15888-15897.
- Hammerschmidt M, Wedlich D. 2008. Regulated adhesion as a driving force of gastrulation movements. *Development* 135:3625-3641.
- Hanafusa H, Torii S, Yasunaga T, Nishida E. 2002. Sprouty1 and Sprouty2 provide a control mechanism for the Ras/MAPK signalling pathway. *Nat Cell Biol* 4:850-858.
- Hardin J. 1989. Local shifts in position and polarized motility drive cell rearrangement during sea urchin gastrulation. *Dev Biol* 136:430-445.
- Harris AK. 1976. Is Cell sorting caused by differences in the work of intercellular adhesion? A critique of the Steinberg hypothesis. *J Theor Biol* 61:267-285.
- Heasman J, Crawford A, Goldstone K, Garner-Hamrick P, Gumbiner B, McCrea P, Kintner C, Noro CY, Wylie C. 1994a. Overexpression of cadherins and underexpression of beta-catenin inhibit dorsal mesoderm induction in early *Xenopus* embryos. *Cell* 79:791-803.
- Heasman J, Ginsberg D, Geiger B, Goldstone K, Pratt T, Yoshida-Noro C, Wylie C. 1994b. A functional test for maternally inherited cadherin in *Xenopus* shows its importance in cell adhesion at the blastula stage. *Development* 120:49-57.
- Heisenberg CP, Solnica-Krezel L. 2008. Back and forth between cell fate specification and movement during vertebrate gastrulation. *Curr Opin Genet Dev* 18:311-316.
- Hikasa H, Shibata M, Hiratani I, Taira M. 2002. The *Xenopus* receptor tyrosine kinase Xror2 modulates morphogenetic movements of the axial mesoderm and neuroectoderm via Wnt signaling. *Development* 129:5227-5239.
- Hill E, Broadbent ID, Chothia C, Pettitt J. 2001. Cadherin superfamily proteins in *Caenorhabditis elegans* and *Drosophila melanogaster*. *J Mol Biol* 305:1011-1024.
- Hu CD, Chinenov Y, Kerppola TK. 2002. Visualization of interactions among bZIP and Rel family proteins in living cells using bimolecular fluorescence complementation. *Mol Cell* 9:789-798.
- Hukriede NA, Tsang TE, Habas R, Khoo PL, Steiner K, Weeks DL, Tam PP, Dawid IB. 2003. Conserved requirement of Lim1 function for cell movements during gastrulation. *Dev Cell* 4:83-94.
- Hyodo-Miura J, Yamamoto TS, Hyodo AC, Iemura S, Kusakabe M, Nishida E, Natsume T, Ueno N. 2006. XGAP, an ArfGAP, is required for polarized localization of PAR proteins and cell polarity in *Xenopus* gastrulation. *Dev Cell* 11:69-79.
- Iioka H, Ueno N, Kinoshita N. 2004. Essential role of MARCKS in cortical actin dynamics during gastrulation movements. *J Cell Biol* 164:169-174.
- Irvine KD, Wieschaus E. 1994. Cell intercalation during *Drosophila* germband extension and its regulation by pair-rule segmentation genes. *Development* 120:827-841.
- Ishitani T, Ninomiya-Tsuji J, Nagai S-i, Nishita M, Meneghini M, Barker N, Waterman M, Bowerman B, Clevers H, Shibuya H, Matsumoto K. 1999. The TAK1-NLK-MAPK-related pathway antagonizes signalling between  $\beta$ -catenin and transcription factor TCF. *Nature* 399:798-802.
- Jarrett O, Stow JL, Yap AS, Key B. 2002. Dynamin-dependent endocytosis is necessary for convergent-extension movements in *Xenopus* animal cap explants. *Int J Dev Biol* 46:467-473.
- Keller R. 2002. Shaping the vertebrate body plan by polarized embryonic cell movements. *Science* 298:1950-1954.
- Keller R, Danilchik M. 1988. Regional expression, pattern and timing of convergence and extension during gastrulation of *Xenopus laevis*. *Development* 103:193-209.
- Keller R, Davidson LA, Shook DR. 2003. How we are shaped: the biomechanics of gastrulation. *Differentiation* 71:171-205.
- Keller RE. 1986. The cellular basis of amphibian gastrulation. In: Browder CW, editor. *Developmental biology: A comprehensive synthesis*. New York/London: Plenum Press. pp 241-327.
- Kerppola TK. 2006. Design and implementation of bimolecular fluorescence complementation (BiFC) assays for the visualization of protein interactions in living cells. *Nat Protoc* 1:1278-1286.

- Kerppola TK. 2008. Bimolecular fluorescence complementation (BiFC) analysis as a probe of protein interactions in living cells. *Annu Rev Biophys* 37:465-487.
- Kim G-H, Han J-K. 2005. JNK and ROK $\alpha$  function in the noncanonical Wnt/RhoA signaling pathway to regulate *Xenopus* convergent extension movements. *Developmental Dynamics* 232:958-968.
- Kim G-H, Her J-H, Han J-K. 2008. Ryk cooperates with Frizzled 7 to promote Wnt11-mediated endocytosis and is essential for *Xenopus laevis* convergent extension movements. *J. Cell Biol.* 182:1073-1082.
- Kim SH, Jen WC, De Robertis EM, Kintner C. 2000. The protocadherin P APC establishes segmental boundaries during somitogenesis in *xenopus* embryos. *Curr Biol* 10:821-830.
- Kim SH, Yamamoto A, Bouwmeester T, Agius E, Robertis EM. 1998. The role of paraxial protocadherin in selective adhesion and cell movements of the mesoderm during *Xenopus* gastrulation. *Development* 125:4681-4690.
- Klein SL. 1987. The first cleavage furrow demarcates the dorsal-ventral axis in *Xenopus* embryos. *Dev Biol* 120:299-304.
- Klein TJ, Mlodzik M. 2005. Planar cell polarization: an emerging model points in the right direction. *Annu Rev Cell Dev Biol* 21:155-176.
- Krieg M, Arboleda-Estudillo Y, Puech PH, Kafer J, Graner F, Muller DJ, Heisenberg CP. 2008. Tensile forces govern germ-layer organization in zebrafish. *Nat Cell Biol* 10:429-436.
- Kühl M. 2002. Non-canonical Wnt signaling in *Xenopus*: regulation of axis formation and gastrulation. *Seminars in Cell and Developmental Biology* 13:243-249.
- Kühl M, Wedlich D. 1996. *Xenopus* cadherins: Sorting out types and functions in embryogenesis. *Developmental Dynamics* 207:121-134.
- Kuhl M, Finnemann S, Binder O, Wedlich D. 1996. Dominant negative expression of a cytoplasmically deleted mutant of XB/U-cadherin disturbs mesoderm migration during gastrulation in *Xenopus laevis*. *Mech Dev* 54:71-82.
- Kuhl M, Sheldahl LC, Malbon CC, Moon RT. 2000. Ca<sup>2+</sup>/calmodulin-dependent protein kinase II is stimulated by Wnt and Frizzled homologs and promotes ventral cell fates in *Xenopus*. *J Biol Chem* 275:12701-12711.
- Kuroda H, Inui M, Sugimoto K, Hayata T, Asashima M. 2002. Axial protocadherin is a mediator of prenotochord cell sorting in *Xenopus*. *Dev Biol* 244:267-277.
- Laemmli UK. 1970. Cleavage of structural proteins during the assembly of the head of bacteriophage T4. *Nature* 227:680-685.
- Lawson A, Schoenwolf GC. 2001. New insights into critical events of avian gastrulation. *Anat Rec* 262:238-252.
- Lee CH, Gumbiner BM. 1995. Disruption of gastrulation movements in *Xenopus* by a dominant-negative mutant for C-cadherin. *Dev Biol* 171:363-373.
- Leptin M. 2005. Gastrulation movements: the logic and the nuts and bolts. *Dev Cell* 8:305-320.
- Levine E, Lee CH, Kintner C, Gumbiner BM. 1994. Selective disruption of E-cadherin function in early *Xenopus* embryos by a dominant negative mutant. *Development* 120:901-909.
- Lilien J, Balsamo J. 2005. The regulation of cadherin-mediated adhesion by tyrosine phosphorylation/dephosphorylation of  $\beta$ -catenin. *Current Opinion in Cell Biology* 17:459-465.
- Lu B, Usui T, Uemura T, Jan L, Jan YN. 1999. Flamingo controls the planar polarity of sensory bristles and asymmetric division of sensory organ precursors in *Drosophila*. *Curr Biol* 9:1247-1250.
- Lu X, Borchers AG, Jolicoeur C, Rayburn H, Baker JC, Tessier-Lavigne M. 2004. PTK7/CCK-4 is a novel regulator of planar cell polarity in vertebrates. *Nature* 430:93-98.
- Mahoney PA, Weber U, Onofrechuk P, Biessmann H, Bryant PJ, Goodman CS. 1991. The fat tumor suppressor gene in *Drosophila* encodes a novel member of the cadherin gene superfamily. *Cell* 67:853-868.
- Marambaud P, Shioi J, Serban G, Georgakopoulos A, Sarnier S, Nagy V, Baki L, Wen P, Efthimiopoulos S, Shao Z, Wisniewski T, Robakis NK. 2002. A presenilin-1/ $\gamma$ -secretase cleavage releases

- the E-cadherin intracellular domain and regulates disassembly of adherens junctions. *EMBO J* 21:1948-1956.
- Maretzky T, Reiss K, Ludwig A, Buchholz J, Scholz F, Proksch E, de Strooper B, Hartmann D, Saftig P. 2005. ADAM10 mediates E-cadherin shedding and regulates epithelial cell-cell adhesion, migration, and  $\beta$ -catenin translocation. *Proceedings of the National Academy of Sciences of the United States of America* 102:9182-9187.
- Marlow F, Topczewski J, Sepich D, Solnica-Krezel L. 2002. Zebrafish Rho kinase 2 acts downstream of Wnt11 to mediate cell polarity and effective convergence and extension movements. *Curr Biol* 12:876-884.
- Marsden M, DeSimone DW. 2003. Integrin-ECM interactions regulate cadherin-dependent cell adhesion and are required for convergent extension in *Xenopus*. *Curr Biol* 13:1182-1191.
- Matakatsu H, Blair SS. 2004. Interactions between Fat and Dachshous and the regulation of planar cell polarity in the *Drosophila* wing. *Development* 131:3785-3794.
- Matakatsu H, Blair SS. 2006. Separating the adhesive and signaling functions of the Fat and Dachshous protocadherins. *Development* 133:2315-2324.
- Medina A, Reintsch W, Steinbeisser H. 2000. *Xenopus* frizzled 7 can act in canonical and non-canonical Wnt signaling pathways: implications on early patterning and morphogenesis. *Mech Dev* 92:227-237.
- Medina A, Steinbeisser H. 2000. Interaction of Frizzled 7 and Dishevelled in *Xenopus*. *Dev Dyn* 218:671-680.
- Medina A, Swain RK, Kuerner KM, Steinbeisser H. 2004. *Xenopus* paraxial protocadherin has signaling functions and is involved in tissue separation. *EMBO J* 23:3249-3258.
- Miller JR, McClay DR. 1997. Characterization of the role of cadherin in regulating cell adhesion during sea urchin development. *Dev Biol* 192:323-339.
- Moon RT, Campbell RM, Christian JL, McGrew LL, Shih J, Fraser S. 1993. Xwnt-5A: a maternal Wnt that affects morphogenetic movements after overexpression in embryos of *Xenopus laevis*. *Development* 119:97-111.
- Morell M, Espargaro A, Aviles FX, Ventura S. 2008. Study and selection of in vivo protein interactions by coupling bimolecular fluorescence complementation and flow cytometry. *Nat Protoc* 3:22-33.
- Morishita H, Yagi T. 2007. Protocadherin family: diversity, structure, and function. *Curr Opin Cell Biol* 19:584-592.
- Moriyoshi K, Richards LJ, Akazawa C, O'Leary DD, Nakanishi S. 1996. Labeling neural cells using adenoviral gene transfer of membrane-targeted GFP. *Neuron* 16:255-260.
- Munro EM, Odell GM. 2002. Polarized basolateral cell motility underlies invagination and convergent extension of the ascidian notochord. *Development* 129:13-24.
- Murata Y, Hamada S, Morishita H, Mutoh T, Yagi T. 2004. Interaction with protocadherin-gamma regulates the cell surface expression of protocadherin-alpha. *J Biol Chem* 279:49508-49516.
- Murdoch JN, Henderson DJ, Doudney K, Gaston-Massuet C, Phillips HM, Paternotte C, Arkell R, Stanier P, Copp AJ. 2003. Disruption of scribble (*Scrb1*) causes severe neural tube defects in the circletail mouse. *Hum Mol Genet* 12:87-98.
- Nakatsuji N, Johnson KE. 1983. Comparative study of extracellular fibrils on the ectodermal layer in gastrulae of five amphibian species. *J Cell Sci* 59:61-70.
- Nakayama M, Nakajima D, Nagase T, Nomura N, Seki N, Ohara O. 1998. Identification of high-molecular-weight proteins with multiple EGF-like motifs by motif-trap screening. *Genomics* 51:27-34.
- Nieuwkoop P, Faber J. 1967. Normal table of *Xenopus laevis* (Daudin). Amsterdam: North Holland Publishing, Co.
- Nutt SL, Dingwell KS, Holt CE, Amaya E. 2001. *Xenopus* Sprouty2 inhibits FGF-mediated gastrulation movements but does not affect mesoderm induction and patterning. *Genes & Development* 15:1152-1166.

- Ogata S, Morokuma J, Hayata T, Kolle G, Niehrs C, Ueno N, Cho KW. 2007. TGF-beta signaling-mediated morphogenesis: modulation of cell adhesion via cadherin endocytosis. *Genes Dev* 21:1817-1831.
- Park TJ, Gray RS, Sato A, Habas R, Wallingford JB. 2005. Subcellular localization and signaling properties of dishevelled in developing vertebrate embryos. *Curr Biol* 15:1039-1044.
- Patel SD, Chen CP, Bahna F, Honig B, Shapiro L. 2003. Cadherin-mediated cell-cell adhesion: sticking together as a family. *Curr Opin Struct Biol* 13:690-698.
- Phillips GR, Tanaka H, Frank M, Elste A, Fidler L, Benson DL, Colman DR. 2003. Gamma-protocadherins are targeted to subsets of synapses and intracellular organelles in neurons. *J Neurosci* 23:5096-5104.
- Rangarajan J, Luo T, Sargent TD. 2006. PCNS: a novel protocadherin required for cranial neural crest migration and somite morphogenesis in *Xenopus*. *Dev Biol* 295:206-218.
- Reiss K, Maretzky T, Haas IG, Schulte M, Ludwig A, Frank M, Saftig P. 2006. Regulated ADAM10-dependent ectodomain shedding of gamma-protocadherin C3 modulates cell-cell adhesion. *J Biol Chem* 281:21735-21744.
- Reiss K, Maretzky T, Ludwig A, Toussey T, de Strooper B, Hartmann D, Saftig P. 2005. ADAM10 cleavage of N-cadherin and regulation of cell-cell adhesion and beta-catenin nuclear signalling. *EMBO J* 24:742-752.
- Rhee J, Takahashi Y, Saga Y, Wilson-Rawls J, Rawls A. 2003. The protocadherin papc is involved in the organization of the epithelium along the segmental border during mouse somitogenesis. *Dev Biol* 254:248-261.
- Riethmacher D, Brinkmann V, Birchmeier C. 1995. A targeted mutation in the mouse E-cadherin gene results in defective preimplantation development. *Proc Natl Acad Sci U S A* 92:855-859.
- Sausedo RA, Schoenwolf GC. 1994. Quantitative analyses of cell behaviors underlying notochord formation and extension in mouse embryos. *Anat Rec* 239:103-112.
- Schambony A, Wedlich D. 2007. Wnt-5A/Ror2 regulate expression of XPAPC through an alternative noncanonical signaling pathway. *Dev Cell* 12:779-792.
- Seifert JR, Mlodzik M. 2007. Frizzled/PCP signalling: a conserved mechanism regulating cell polarity and directed motility. *Nat Rev Genet* 8:126-138.
- Sheldahl LC, Park M, Malbon CC, Moon RT. 1999. Protein kinase C is differentially stimulated by Wnt and Frizzled homologs in a G-protein-dependent manner. *Curr Biol* 9:695-698.
- Shih J, Keller R. 1992. Cell motility driving mediolateral intercalation in explants of *Xenopus laevis*. *Development* 116:901-914.
- Shimizu T, Yabe T, Muraoka O, Yonemura S, Aramaki S, Hatta K, Bae YK, Nojima H, Hibi M. 2005. E-cadherin is required for gastrulation cell movements in zebrafish. *Mech Dev* 122:747-763.
- Shyu YJ, Liu H, Deng X, Hu CD. 2006. Identification of new fluorescent protein fragments for bimolecular fluorescence complementation analysis under physiological conditions. *Biotechniques* 40:61-66.
- Simon MA. 2004. Planar cell polarity in the *Drosophila* eye is directed by graded Four-jointed and Dachous expression. *Development* 131:6175-6184.
- Simons M, Mlodzik M. 2008. Planar cell polarity signaling: from fly development to human disease. *Annu Rev Genet* 42:517-540.
- Sivak JM, Petersen LF, Amaya E. 2005. FGF signal interpretation is directed by Sprouty and Spred proteins during mesoderm formation. *Dev Cell* 8:689-701.
- Slusarski DC, Corces VG, Moon RT. 1997. Interaction of Wnt and a Frizzled homologue triggers G-protein-linked phosphatidylinositol signalling. *Nature* 390:410-413.
- Sokol SY. 1996. Analysis of Dishevelled signalling pathways during *Xenopus* development. *Curr Biol* 6:1456-1467.
- Solnica-Krezel L. 2005. Conserved patterns of cell movements during vertebrate gastrulation. *Curr Biol* 15:R213-228.
- Solnica-Krezel L. 2006. Gastrulation in zebrafish -- all just about adhesion? *Current Opinion in Genetics & Development* 16:433-441.

- Steinbeisser H. 2007. Regulation of Tissue Separation in the Amphibian Embryo. In: Principles of developmental genetics. Amsterdam ; London: Elsevier Academic Press. pp 392-403.
- Steinberg MS. 1970. Does differential adhesion govern self-assembly processes in histogenesis? Equilibrium configurations and the emergence of a hierarchy among populations of embryonic cells. *J Exp Zool* 173:395-433.
- Strutt D. 2008. The planar polarity pathway. *Curr Biol* 18:R898-902.
- Sumanas S, Strege P, Heasman J, Ekker SC. 2000. The putative wnt receptor *Xenopus* frizzled-7 functions upstream of beta-catenin in vertebrate dorsoventral mesoderm patterning. *Development* 127:1981-1990.
- Suzuki ST. 2000. Recent progress in protocadherin research. *Exp Cell Res* 261:13-18.
- Tada M, Smith JC. 2000. *Xwnt11* is a target of *Xenopus* Brachyury: regulation of gastrulation movements via Dishevelled, but not through the canonical Wnt pathway. *Development* 127:2227-2238.
- Tahinci E, Symes K. 2003. Distinct functions of Rho and Rac are required for convergent extension during *Xenopus* gastrulation. *Dev Biol* 259:318-335.
- Tepass U, Truong K, Godt D, Ikura M, Peifer M. 2000. Cadherins in embryonic and neural morphogenesis. *Nat Rev Mol Cell Biol* 1:91-100.
- Triana-Baltzer GB, Blank M. 2006. Cytoplasmic domain of protocadherin-alpha enhances homophilic interactions and recognizes cytoskeletal elements. *J Neurobiol* 66:393-407.
- Ulrich F, Krieg M, Schotz EM, Link V, Castanon I, Schnabel V, Taubenberger A, Mueller D, Puech PH, Heisenberg CP. 2005. Wnt11 functions in gastrulation by controlling cell cohesion through Rab5c and E-cadherin. *Dev Cell* 9:555-564.
- Ungar AR, Kelly GM, Moon RT. 1995. Wnt4 affects morphogenesis when misexpressed in the zebrafish embryo. *Mech Dev* 52:153-164.
- Unterseher F, Hefele JA, Giehl K, De Robertis EM, Wedlich D, Schambony A. 2004. Paraxial protocadherin coordinates cell polarity during convergent extension via Rho A and JNK. *EMBO J* 23:3259-3269.
- Usui T, Shima Y, Shimada Y, Hirano S, Burgess RW, Schwarz TL, Takeichi M, Uemura T. 1999. Flamingo, a seven-pass transmembrane cadherin, regulates planar cell polarity under the control of Frizzled. *Cell* 98:585-595.
- Veeman MT, Axelrod JD, Moon RT. 2003. A second canon. Functions and mechanisms of beta-catenin-independent Wnt signaling. *Dev Cell* 5:367-377.
- Wacker S, Grimm K, Joos T, Winklbauer R. 2000. Development and control of tissue separation at gastrulation in *Xenopus*. *Dev Biol* 224:428-439.
- Wallingford JB, Habas R. 2005. The developmental biology of Dishevelled: an enigmatic protein governing cell fate and cell polarity. *Development* 132:4421-4436.
- Wallingford JB, Rowling BA, Vogeli KM, Rothbacher U, Fraser SE, Harland RM. 2000. Dishevelled controls cell polarity during *Xenopus* gastrulation. *Nature* 405:81-85.
- Wang Y. 2007. Identification and characterization of interacting partners of cytoplasmic domain of *Xenopus* Paraxial Protocadherin. In: Heidelberg. p 115.
- Wang Y, Janicki P, Koster I, Berger CD, Wenzl C, Grosshans J, Steinbeisser H. 2008. *Xenopus* Paraxial Protocadherin regulates morphogenesis by antagonizing Sprouty. *Genes Dev* 22:878-883.
- Wang Y, Nathans J. 2007. Tissue/planar cell polarity in vertebrates: new insights and new questions. *Development* 134:647-658.
- Wessely O, Kim JI, Geissert D, Tran U, De Robertis EM. 2004. Analysis of Spemann organizer formation in *Xenopus* embryos by cDNA macroarrays. *Dev Biol* 269:552-566.
- Wheelock MJ, Buck CA, Bechtol KB, Damsky CH. 1987. Soluble 80-kd fragment of cell-CAM 120/80 disrupts cell-cell adhesion. *J Cell Biochem* 34:187-202.
- Wilson P, Keller R. 1991. Cell rearrangement during gastrulation of *Xenopus*: direct observation of cultured explants. *Development* 112:289-300.
- Winklbauer R, Keller RE. 1996. Fibronectin, mesoderm migration, and gastrulation in *Xenopus*. *Dev Biol* 177:413-426.

- Winklbauer R, Medina A, Swain RK, Steinbeisser H. 2001. Frizzled-7 signalling controls tissue separation during *Xenopus* gastrulation. *Nature* 413:856-860.
- Winklbauer R, Selchow A, Nagel M, Angres B. 1992. Cell interaction and its role in mesoderm cell migration during *Xenopus* gastrulation. *Dev Dyn* 195:290-302.
- Winter CG, Wang B, Ballew A, Royou A, Karess R, Axelrod JD, Luo L. 2001. *Drosophila* Rho-associated kinase (Drok) links Frizzled-mediated planar cell polarity signaling to the actin cytoskeleton. *Cell* 105:81-91.
- Witzel S, Zimyanin V, Carreira-Barbosa F, Tada M, Heisenberg CP. 2006. Wnt11 controls cell contact persistence by local accumulation of Frizzled 7 at the plasma membrane. *J Cell Biol* 175:791-802.
- Wolpert L. 2006. Principles of development. Oxford: Oxford University Press. xxiii, 551 p. pp.
- Wunnenberg-Stapleton K, Blitz IL, Hashimoto C, Cho KW. 1999. Involvement of the small GTPases XRhoA and XRnd1 in cell adhesion and head formation in early *Xenopus* development. *Development* 126:5339-5351.
- Yamamoto A, Amacher SL, Kim SH, Geissert D, Kimmel CB, De Robertis EM. 1998. Zebrafish paraxial protocadherin is a downstream target of spadetail involved in morphogenesis of gastrula mesoderm. *Development* 125:3389-3397.
- Yamamoto A, Kemp C, Bachiller D, Geissert D, De Robertis EM. 2000. Mouse paraxial protocadherin is expressed in trunk mesoderm and is not essential for mouse development. *Genesis* 27:49-57.
- Yamanaka H, Moriguchi T, Masuyama N, Kusakabe M, Hanafusa H, Takada R, Takada S, Nishida E. 2002. JNK functions in the non-canonical Wnt pathway to regulate convergent extension movements in vertebrates. *EMBO Rep* 3:69-75.
- Yamanaka H, Nishida E. 2007. Wnt11 stimulation induces polarized accumulation of Dishevelled at apical adherens junctions through Frizzled7. *Genes to Cells* 12:961-967.
- Yang CH, Axelrod JD, Simon MA. 2002. Regulation of Frizzled by fat-like cadherins during planar polarity signaling in the *Drosophila* compound eye. *Cell* 108:675-688.
- Yap AS, Crampton MS, Hardin J. 2007. Making and breaking contacts: the cellular biology of cadherin regulation. *Curr Opin Cell Biol* 19:508-514.
- Yasuda S, Tanaka H, Sugiura H, Okamura K, Sakaguchi T, Tran U, Takemiya T, Mizoguchi A, Yagita Y, Sakurai T, De Robertis EM, Yamagata K. 2007. Activity-induced protocadherin arcadlin regulates dendritic spine number by triggering N-cadherin endocytosis via TAO2beta and p38 MAP kinases. *Neuron* 56:456-471.
- Yu JS, Koujak S, Nagase S, Li CM, Su T, Wang X, Keniry M, Memeo L, Rojzman A, Mansukhani M, Hibshoosh H, Tycko B, Parsons R. 2008. PCDH8, the human homolog of PAPC, is a candidate tumor suppressor of breast cancer. *Oncogene*.
- Zhong Y, Briehner WM, Gumbiner BM. 1999. Analysis of C-cadherin regulation during tissue morphogenesis with an activating antibody. *J Cell Biol* 144:351-359.

---

## Abbreviations

a	anterior
ab	antibody
Amp	ampicillin
an	animal pole
BCR	blastocoel roof
BIFC	bimolecular fluorescence complementation
CE	convergent extension
CP	cytoplasmic domain
cyt	cytoplasmic fraction
d	dorsal
DAG	diacylglycerol
DAPI	4',6-diamidino-2-phenylindole
DMZ	dorsal marginal zone
EC	extracellular calcium-binding repeats of cadherins
eGFP	enhanced green fluorescent protein
ER	endoplasmatic reticulum
h	hour(s)
H2B	histone 2B
inj	injected
IP <sub>3</sub>	inositol 1,4,5-trisphosphate
mb	membrane-bound
MEF	mouse embryonic fibroblast
min	minute(s)
Mo	morpholino oligonucleotide
mRFP	monomeric red fluorescent protein
nuc	nuclear fraction
p	posterior
Pcdh	protocadherin
PCP	planar cell polarity
Pro	prodomain
RBD	rhotekin Rho-binding-domain
rpm	rounds per minute
S	signal peptide
sec	seconds
TM	transmembrane domain
v	ventral
veg	vegetal pole
WT	wild type
YFP	yellow fluorescent protein

## Figures

<i>Fig.1. Schematic drawing of early Xenopus gastrulation.</i>	4
<i>Fig.2. Cellular behavior during gastrulation.</i>	5
<i>Fig.3. Temporal development of tissue separation during gastrulation.</i>	7
<i>Fig.4. Schematic representation of the Wnt signal transduction cascade.</i>	10
<i>Fig.5. Classification of the cadherin superfamily according to protein structure.</i>	12
<i>Fig.6. Regulation of cell adhesion during gastrulation.</i>	18
<i>Fig.7. The activation of Rho depends on PAPC in the DMZ.</i>	21
<i>Fig.8. Distribution of activated Rho in DMZ explants at gastrulation and neurulation stages.</i>	22
<i>Fig.9. bFGF-induced membrane recruitment of Spry can be inhibited by SU5402.</i>	24
<i>Fig.10. PAPC recruits Spry to the membrane independently of FGF-signaling.</i>	25
<i>Fig.11. The ability to bind Spry is independent of the cell sorting properties of PAPC.</i>	26
<i>Fig.12. PAPC does not recruit dsh-GFP to the cell membrane.</i>	27
<i>Fig.13. The intracellular domain of PAPC is cleaved and can enter the nucleus.</i>	29
<i>Fig.14. PAPCc is localized to the nucleus and to the cell membrane.</i>	30
<i>Fig.15. Loss of PAPC leads to a change in cell shape.</i>	32
<i>Fig.16. Loss of PAPC leads to a loss of cell polarity.</i>	33
<i>Fig.17. PAPC mediates cell sorting.</i>	35
<i>Fig.18. PAPCc causes cells to detach in DMZ explants.</i>	36
<i>Fig.19. PAPC increases the number of intracellular C-Cadherin-eGFP spots in animal caps.</i>	38
<i>Fig.20. C-Cadherin-eGFP and PAPC colocalize in the dot-like structures.</i>	39
<i>Fig.21. Blocking endocytosis leads to accumulation of C-Cadherin-eGFP and PAPC at the cell membrane.</i>	40
<i>Fig.22. Formation of intracellular C-Cadherin-eGFP spots depends on PAPC and Fz7 function in dorsal mesoderm.</i>	41
<i>Fig.23. The localization of C-Cadherin-eGFP and mCherry-Rab5a depend on PAPC and Fz7 in DMZs.</i>	42
<i>Fig.24. Schematic drawing of the Bimolecular Fluorescent Complementation (BIFC) principle.</i>	45
<i>Fig.25. The interaction of PAPC and Fz7-TM1 can be detected using the BIFC assay.</i>	46
<i>Fig.26. PAPC and C-Cadherin interact in vivo.</i>	47
<i>Fig.27. The interaction between PAPC and Fz7-TM1 can be modulated.</i>	48
<i>Fig.28. Example of flow cytometry analysis.</i>	49
<i>Fig.29. Frequency and intensity of BIFC signal can be measured by flow cytometry.</i>	50
<i>Fig.30. The interaction between PAPC and Fz7-TM1 can be detected in Xenopus using BIFC.</i>	51
<i>Fig.31. PAPC and Fz7 must be in the same cell to trigger tissue separation.</i>	53
<i>Fig.32. Fz7 can reverse the loss of adhesion induced by PAPC in dissociated cells.</i>	54
<i>Fig.33. Model of dynamic cell adhesion in dorsal mesoderm cells.</i>	64
<i>Fig.34. Schematic outline of the dissociation and reaggregation experiment.</i>	82

---

**Tables**

<i>Table 1. Summary of BIFC experiments.....</i>	<i>52</i>
<i>Table 2. Table of plasmids used in this work. ....</i>	<i>74</i>
<i>Table 3. PCR program used for cloning. ....</i>	<i>77</i>
<i>Table 4. PCR program used for mutagenesis. ....</i>	<i>78</i>
<i>Table 5. PCR program used for colony PCR. ....</i>	<i>78</i>
<i>Table 6. PCR program used for sequencing.....</i>	<i>79</i>

---

## Acknowledgements

*"Men wanted: for hazardous journey. Small wages, bitter cold, long months of complete darkness, constant danger, safe return doubtful. Honour and recognition in case of success."* Sir Ernest Shackleton.

This work has been carried out in the Institute of Human Genetics of the University of Heidelberg. I want to thank Prof. Herbert Steinbeisser for giving me the opportunity to embark on my own scientific journey to developmental biology. Your guidance, kindness and patience have enabled me to grow both scientifically and personally.

I also want to thank Prof. Jörg Großhans for supervising my thesis and for the stimulating discussions during seminars.

Finally I want to thank my family and especially my husband Luis Deza Tarnawiecki for supporting me throughout this time. Knowing that you are always there means a great deal to me.

### Shout-out

Thanks to Dr. Oliver Gruß from ZMBH for providing *Xenopus* oocytes.

Thanks to Dr. Emil Karaulanov and Malte Paulsen from DKFZ for suggestions and help on cadherin antibodies and FACS.

Thanks to Dr. Ulrike Engel from the Nikon Imaging Center at Heidelberg University for help and advice.

Special thanks to Isabelle Köster and Anja Kietzmann for critically reading my thesis. Last but not least thanks to all the people, past or present, of the Steinbeisser lab. Without your help, friendship and support, the past four years just wouldn't have been possible.